# The role of chemokine receptor trafficking in regulating neutrophil migration to inflammatory sites

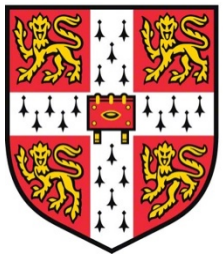

UNIVERSITY OF CAMBRIDGE

This dissertation is submitted for the degree of Doctor of Philosophy

Caroline Gisele Coombs

Sidney Sussex College

September 2019

# Declaration

This thesis is the result of my own work and includes nothing which is the outcome of work done in collaboration except as declared in the Preface and specified in the text. It is not substantially the same as any that I have submitted, or, is being concurrently submitted for a degree or diploma or other qualification at the University of Cambridge or any other University or similar institution except as declared in the Preface and specified in the text. I further state that no substantial part of my thesis has already been submitted, or, is being concurrently submitted for any such degree, diploma or other qualification at the University of Cambridge or any other University or similar institution except as declared in the Preface and specified in the text. It does not exceed the prescribed word limit for the relevant Degree Committee.

# The role of chemokine receptor trafficking in regulating neutrophil migration to inflammatory sites

Caroline Gisele Coombs

# Abstract

Neutrophils are the first immune cells to be recruited to sites of tissue injury or infection. Upon detection of an inflammatory stimulus, neutrophils exit the vasculature and migrate directionally through the interstitial tissue towards the target site. Once at the target site, neutrophils may either focalise and form clusters or may exhibit a more dispersive and exploratory behaviour. Focalisation acts to concentrate local neutrophil effector responses but excess clustering can prove detrimental, resulting in undesirable tissue damage. Neutrophil dispersal promotes the encounter of alternative signals and therefore drives resolution of the response. A fine balance between focalisation and exploration must exist to ensure that the inflammatory response is effective but also transient and self-resolving.

Neutrophils are recruited to target sites by gradients of attractant molecules, a major class of which is chemokines. Chemokines bind to G-protein coupled receptors (GPCRs) and initiate complex intracellular signalling cascades which ultimately result in directional neutrophil migration. Upon ligand binding, GPCRs can undergo multiple trafficking fates which may in turn influence sensitivity to the gradient. However, the functional significance of receptor trafficking during neutrophil responses *in vivo* remains unknown.

Here, I address this question using zebrafish Cxcl8a (a homologue of human CXCL8) which signals through two G-protein coupled receptors, Cxcr1 and Cxcr2. Through new *in vivo* biosensors, I show that Cxcr1 and Cxcr2 exhibit differential trafficking in response to endogenous gradients. Cxcr1 is extensively internalised whilst Cxcr2 is sustained on the cell membrane. Live-imaging of receptor knockout neutrophils revealed that Cxcr1 promotes neutrophil clustering at wounds, whilst Cxcr2 drives dispersal. Through receptor mutagenesis I show that neutrophil dispersal relies on Cxcr1 internalisation and membrane sustenance of Cxcr2. Thus, I show that differential trafficking of two receptors balances the rise and fall of neutrophil inflammatory responses. To my knowledge, this is the first study to functionally link receptor dynamics to neutrophil migration behaviour *in vivo.*

# Acknowledgements

Firstly, I would like to thank my supervisor Dr Milka Sarris, not only for giving me the opportunity to work in her lab, but also for her support and guidance throughout my PhD. Her door was quite literally always open and for that I am very grateful. I extend my deepest gratitude to my fellow lab members for their constant support and friendship and without whom my PhD experience would not have been the same. Thank you to Antonios Georgantzoglou for always being so happy to help me with anything and to Hugo Poplimont, who went through the PhD process alongside me. It was certainly a comfort to me knowing that I could turn to him for support along the way. My sincerest gratitude to Hazel Walker for her friendship and for always so kindly offering to listen to me whenever things weren't going well. A problem shared is a problem halved! I would like to thank Alexis Crockett for constantly supplying me with coffee, sweets, lots of laughs and for generally being such a good friend. I would also like to express my appreciation to all those who worked in the fish facility over the years, it was always a very friendly and fun atmosphere to work in. Finally, I would like to thank my family and friends for their continued support and of course my dog Hollie, who sat beside me during the thesis writing process.

# Table of Contents

# Abbreviations

| Abbreviation | Definition |
|---|---|
| ATP | Adenosine triphosphate |
| CGD | Chronic Granulomatous Disease |
| CHT | Caudal hematopoietic tissue |
| CXCLxx | C-X-C motif chemokine ligand XX |
| CXCRxx | C-X-C motif chemokine receptor XX |
| CRISPR | Clustered regularly interspaced short palindromic repeats |
| CTC | Circulating tumour cells |
| C5a | Complement component C5a |
| C3a | Complement component C3a |
| DAMPs | Damage Associated Molecular Patterns |
| DNA | Deoxyribonucleic acid |
| DMSO | Dimethyl sulfoxide |
| Dpf | Days post-fertilisation |
| F-actin | Filamentous actin |
| fMLP | N-formylmethionine-leucyl-phenylalanine |
| G-CSF | Granulocyte colony stimulating factor |
| GDP | Gaunosine diphosphate |
| GEF | Guanosine nucleotide exchange factor |
| GPCR | G-protein coupled receptor |
| GTP | Guanosine triphosphate |
| GTPase | Guanosine triphosphatase |
| Gα, Gβ, Gγ | Guanine nucleotide-binding proteins |
| HEK293T | Human embryonic kidney 293T cells |
| HL-60 cells | Human leukaemia cell line |
| HSPG | Heparin sulphate proteoglycan |
| Hpw | Hours post wound |
| $H_20_2$ | Hydrogen peroxide |
| KDa | Kilodaltons |
| KO | Knockout |
| LPS | Lipopolysaccharide |
| LTB4 | Leukotriene B4 |
| MMP9 | matrix metalloproteinase 9 |
| MO | Morpholino |
| Mpx/Mpo | Myeloperoxidase |
| NADPH oxidase | Nicotinamide adenine dinucleotide phosphate oxidase |
| NETs | Neutrophil Extracellular Traps |
| NOS | Nitric oxide synthase |
| Owa | Occupied wound area |
| PA | Photoactivation |
| PAMP | Pathogen Associated Molecular Pattern |
| PCR | Polymerase chain reaction |

| | |
|---|---|
| $PIP_3$ | Phosphatidylinositol (3,4,5)-triphosphate |
| PI3K | Phosphoionositide-3-kinase |
| RNA | Ribonucleic acid |
| ROS | Reactive oxygen species |
| rIM | Reverse interstitial migration |
| rTEM | Reverse transendothelial migration |
| RT-PCR | Reverse transcription polymerase chain reaction |
| SEM | Standard error of the mean |
| sfGFP | Superfolder green fluorescent protein |
| TNF-α | Tumour necrosis factor-α |
| VEGF | Vascular endothelial growth factor |
| WT | Wildtype |

# Transgenic and knockout lines generated during PhD

| Line Name | Description |
|---|---|
| Tg(*lyz*:Cxcr1-FT) | Transgenic line with neutrophil-specific expression of wildtype Cxcr1 receptor (fused to a fluorescent timer cassette) in a wildtype *cxcr1*$^{+/+}$ genetic background. |
| Tg(*lyz*:Cxcr2-FT) | Transgenic line with neutrophil-specific expression of wildtype Cxcr2-FT receptor (fused to a fluorescent timer cassette) in a wildtype *cxcr2*$^{+/+}$ genetic background. |
| Tg(*lyz*:mCFP) | Transgenic line with neutrophil-specific expression of membrane CFP. |
| Tg(*lyz*:Cxcr1-FT); *cxcr1*$^{-/-}$ | Transgenic rescue line with neutrophil-specific expression of Cxcr1-wildtype receptor (fused to a fluorescent timer cassette) in a *cxcr1*$^{-/-}$ genetic background. |
| Tg(*lyz*:Cxcr1_ala-FT); *cxcr1*$^{-/-}$ | Transgenic rescue line with neutrophil-specific expression of Cxcr1-alanine mutant receptor (fused to a fluorescent timer cassette) in a *cxcr1*$^{-/-}$ genetic background. |
| Tg(*lyz*:Cxcr1_chim-FT); *cxcr1*$^{-/-}$ | Transgenic rescue line with neutrophil-specific expression of Cxcr1-chimera mutant receptor (fused to a fluorescent timer cassette) in a *cxcr1*$^{-/-}$ genetic background. |
| Tg(*lyz*:Cxcr2-FT); *cxcr2*$^{-/-}$ | Transgenic rescue line with neutrophil specific expression of Cxcr2-wildtype receptor (fused to a fluorescent timer cassette) in a *cxcr2*$^{-/-}$ genetic background. |
| Tg(*lyz*:Cxcr2_ala-FT); *cxcr2*$^{-/-}$ | Rescue line with neutrophil specific expression of Cxcr2-alanine mutant receptor (fused to a fluorescent timer cassette) in a *cxcr2*$^{-/-}$ genetic background. |
| Tg(*lyz*:Cxcr2_chim-FT); *cxcr2*$^{-/-}$ | Rescue line with neutrophil specific expression of Cxcr2-chimera mutant receptor (fused to a fluorescent timer cassette) in a *cxcr2*$^{-/-}$ genetic background. |
| *cxcr1*$^{-/-}$ | Cxcr1 receptor knockout line without fluorescent neutrophils. Line used for generation of rescue transgenic lines. |
| *cxcr2*$^{-/-}$ | Cxcr2 receptor knockout line without fluorescent neutrophils. Line used for generation of rescue transgenic lines. |
| Tg(*mpx:GFP)*$^{i114}$*; cxcr1*$^{-/-}$ | Cxcr1 receptor knockout line with fluorescent neutrophils used for cell-tracking experiments. |

| | |
|---|---|
| Tg(*mpx:GFP)$^{i114}$; cxcr2$^{-/-}$* | Cxcr2 receptor knockout line with fluorescent neutrophils used for cell-tracking experiments. |

# Constructs generated during PhD

pCS2$^{+}$-Cxcl8a-CFP

pCS2$^{+}$-Cxcr1-FT

pCS2$^{+}$-Cxcr2-FT

pCS2$^{+}$-Cxcr1-trunc

pCS2$^{+}$-Cxcr1-ser

pCS2$^{+}$-Cxcr1-ala

pCS2$^{+}$-Cxcr1-chim

Tol2-Lyz-Cxcr1-FT

Tol2-Lyz-Cxcr2-FT

Tol2-Lyz-Cxcr1-ala

Tol2-Lyz-Cxcr1-chim

Tol2-Lyz-Cxcr2-ala

Tol2-Lyz-Cxcr2-chim

# Chapter 1: Introduction

## General overview of introduction

In this chapter I will begin by introducing the neutrophil and outlining its functional role at target sites. Following this, the introduction will focus on the core theme of this thesis, the regulation of neutrophil migration during inflammatory responses. For this, I will provide a general introduction into the diverse range of chemoattractant cues that guide neutrophil migration, with an emphasis on chemokines. I will then extensively discuss the role of these chemoattractants in each distinct stage of neutrophil recruitment to target sites. Finally, I will introduce the current understanding of how neutrophil responses resolve and will close by summarising the objectives of my thesis, along with justification of the zebrafish model.

# Subchapter 1.1: Introduction to neutrophils and their functions in immune responses

Neutrophils are the most abundant circulating immune cells in the human body and are typically the first to be recruited to sites of infection or injury[1]. As such, they are at the frontline of the body's defence system and form an essential part of innate immunity. Neutrophils are generated in the bone marrow where they develop from a myeloid precursor and undergo several stages of maturation from myeloblast, through to promyelocyte, myelocyte, metamylocyte, band cell and finally the neutrophil[2]. Under homeostatic conditions (i.e. in the absence of infection or injury), approximately $10^{11}$ neutrophils are released from the bone marrow and enter the circulation per day, corresponding to a neutrophil blood count in the range of 1.8-7.7 x $10^9$ cell/L[3,4]. The number of mature neutrophils released into the bloodstream must be tightly regulated and requires a delicate balance between the rate of production, rate of release from the bone marrow and the rate of clearance. Mature neutrophils released from the bone marrow form a 'circulating pool' of neutrophils in the blood and a 'marginated pool' of neutrophils that have prolonged residency in specific tissues such as the liver and spleen[4]. Importantly, during inflammatory responses, the production and release into the circulation can be significantly increased up to 10-fold in a process termed emergency granulopoiesis[4]. Upon detection of an inflammatory stimulus, circulating neutrophils migrate to the target site where they accumulate in large numbers to exert their effector function. The importance of neutrophil recruitment to target sites is reflected in cases of neutrophil

depletion from the blood (referred to as 'neutropenia'), which confers severe immunodeficiency and susceptibly to recurrent infections[5]. At the other extreme, excessive neutrophil accumulation can result in tissue damage, perpetuating inflammation and is associated with a range of chronic inflammatory disorders such as septic shock, rheumatoid arthritis, asthma, chronic obstructive pulmonary disease (COPD)[6]. Thus, it is essential that neutrophil recruitment and accumulation at the target site are finely controlled.

## 1.1.1 Neutrophil Killing Mechanisms

Neutrophils have an array of highly effective killing mechanisms at their disposal to eliminate invading pathogens at target sites including phagocytosis, generation of reactive oxygen species (ROS), degranulation and the release of neutrophil extracellular traps (NETs)[7]. Further to these well characterised roles in pathogen clearance, recent evidence points to a more diverse repertoire of neutrophil functions with, for example, roles in tissue repair and in the tumour environment[8].

### Phagocytosis and generation of Reactive Oxygen Species (ROS)

Neutrophils possess a remarkable capacity to rapidly engulf invading microbes in a process known as phagocytosis[9]. Phagocytosis is facilitated by 'opsonisation', in which pathogens are coated with complement-derived peptides or immunoglobulins. Upon recognition of opsonised pathogens, neutrophils send out membrane pseudopods that engulf and encapsulate the pathogen into an intracellular membrane bound vesicle called a phagosome[10]. Neutrophils can subsequently kill encapsulated microbes via the 'respiratory burst' (also known as the 'oxidative burst'), a sequence of biochemical reactions that result in the rapid release of highly cytotoxic reactive oxygen species (ROS)[11,12]. These reactions rely on the assembly of a multi-subunit protein complex, nicotinamide adenine dinucleotide phosphate oxidase (NADPH oxidase)[12]. Activated NADPH oxidase on the phagosome membrane reduces molecular oxygen to a superoxide anion ($O_2^-$) which spontaneously reacts with other molecules to form hydrogen peroxide ($H_2O_2$) and free radicals such as hydroxyl radicals (HO). A protein called myeloperoxidase (mpx) converts $H_20_2$ to the potent bactericidal oxidant, hypochlorite (HOCl)[12]. As well as being released intracellularly in the phagosome, ROS can also be released extracellularly into the environment to target extracellular pathogens[13]. The importance of the respiratory burst in pathogen killing is highlighted in chronic granulomatous disease (CGD) in which defects in any of the NADPH oxidase subunits results in failure to produce

enough antimicrobial oxidants[12,14]. This results in recurrent infections that, in severe cases, can be fatal.

## Degranulation

Neutrophils are classed as 'granulocytes', as their cytoplasm is rich in granules and secretory vesicles containing an arsenal of antimicrobial proteins[15]. The release of these granules, either intracellularly into the phagosome or extracellularly via exocytosis, is referred to as 'degranulation' and represents a key effector mechanism employed by neutrophils[16]. Neutrophil granules are classified as primary, secondary and tertiary granules, which along with secretory vesicles are formed sequentially during neutrophil development. Primary granules, also known as azurophilic granules, are rich in myeloperoxidase (encoded by the *mpo*/*mpx* gene) which, as mentioned above, is crucial for the 'respiratory burst'. The presence of myeloperoxidase is commonly used as a neutrophil marker during neutrophil biology investigative studies. In addition, primary granules contain a plethora of other antimicrobial proteins such as elastase, α-defensins and cathepsin C[15]. Secondary granules also known as 'specific granules' are rich in lactoferrin, an iron-binding protein that can inhibit bacterial growth through nutrient sequestration[17]. Tertiary granules, also known as 'gelatinase granules', predominantly contain matrix degrading proteins such as matrix metalloproteinase 9 (MMP9). Whilst some proteins are heavily enriched or unique to particular granules, some are more evenly represented across multiple granules. For example, the antimicrobial protein lysozyme, which cleaves bacterial cell wall peptidoglycans, is found in all granules. Degranulation also involves exocytosis/release of secretory vesicles which contain serum albumin and provide a reservoir of membrane receptors which are required during an inflammatory response e.g. Mac-1, FcγIII, fMLP receptor[18]. During degranulation, receptors are delivered to and integrated into the membrane[18,15].

## Neutrophil extracellular traps (NETs)

In addition to the well-defined roles of phagocytosis, ROS generation and degranulation, a further neutrophil killing mechanism, in the form of neutrophil extracellular traps (NETs), was identified more recently in 2004[19]. NETs are web-like structures of de-condensed chromatin mixed with histones, antimicrobial proteins and enzymes (such as neutrophil elastase, MPO, cathepsin G etc.) derived from neutrophil granules that are released into the extracellular environment[7]. NETs appear

to physically trap the pathogen and localise the antimicrobial agents to spatially restrict effector responses[19]. NETs have also been shown to trap bacteria in the circulation during sepsis[20]. However, as well as their role in defence, the presence of NETs has also been associated with autoimmune disease. For example, abnormal regulation of NETs has been linked to pathogenesis in systemic lupus erythematosus (SLE)[21]. SLE is an autoimmune disease characterised by overproduction of auto-antibodies against nuclear antigens. It has been suggested that increased NET-derived DNA acts as a self-antigen that induces development of auto-antibodies and triggers an autoimmune response[22].

## 1.1.2 Unconventional context-specific functions of neutrophils

### Neutrophils in tissue repair and regeneration

The role of neutrophils in fighting infection is well established[23]. In the case of sterile injury, the general understanding is that neutrophils are recruited to prevent infection of the damaged tissue which, being compromised, is more vulnerable to infection. Macrophages, which are typically recruited after neutrophils, are well known to play a crucial role in tissue repair and restoration of homeostasis[24,25]. However, recent evidence has shown that in some settings neutrophils can also contribute to tissue repair. For example, in a murine model of hepatic injury, neutrophils were shown to interact with, dismantle and phagocytose collapsed blood vessels[26]. This neutrophil-vessel interaction facilitated vascular regrowth whilst neutrophil depletion led to persistent lesions with delayed re-vascularisation of the tissue. These finding are in line with evidence that neutrophils can promote angiogenesis during tissue repair. In the context of pancreatic islet transplantation, transplants did not re-vascularise in neutropenic mice[27]. In another study, antibody-mediated neutrophil depletion inhibited angiogenesis in a murine corneal injury model, with a 90% reduction in the length of newly generated blood vessels and area of revascularisation at 5 days post-injury compared to control mice[28]. Here it was suggested that neutrophils mediate angiogenesis via the release of vascular endothelial growth factor (VEGF).

### Neutrophils in the tumour microenvironment

The tumour microenvironment consists not only of transformed cancer cells but also stromal cells and recruited leukocytes. The role of tumour-associated macrophages has been well studied but there is increasing evidence that neutrophils also have important and complex roles in the tumour

microenvironment[29]. Tumour associated neutrophils (TANs) can have pro- or anti- tumour roles[30,31,32,33].

***Pro-tumour***

Neutrophil presence in the tumour microenvironment often correlates with a poor prognosis for the patient[34,35]. The mechanisms by which neutrophils may promote tumour evolution is unclear but is a matter of active investigation. One mechanism by which neutrophils may favour tumour growth and dissemination is through their effects on angiogenesis. Angiogenesis, the formation of new blood vessels, can act to promote tumour growth by enhancing nutrient and oxygen supply. In a murine model, Bekes et al. showed that neutrophils in the tumour microenvironment produce proMMP-9, a latent form of the protease MMP-9[36]. MMP-9 activates VEGF which promotes angiogenesis and re-vascularisation of damaged tissue. This is consistent with a finding in mice, where infiltrating neutrophils were found to mediate an angiogenic 'switch' in pancreatic islet carcinogenesis by promoting angiogenesis through release of MMP9 and the subsequent activation of VEGF[37]. Neutrophils can also promote tumour growth through secretion of chemokines which recruit additional pro-tumour cells such as T regulatory cells to the tumour microenvironment[38]. Another recently identified mechanism by which neutrophils can promote tumour growth is through metastatic seeding[39]. In invasive human breast cancer models and murine cancer models, neutrophils were found to interact with circulating tumour cells (CTCs), forming so called CTC-neutrophil clusters[39]. This interaction supported cell cycle progression of CTC cells, accelerating CTC metastatic seeding and conferring a poor prognosis for the patient. Neutrophil extracellular traps have been reported to promote metastasis by trapping circulating tumour cells[40].

***Anti-tumour***

Neutrophils have also been shown to have anti-tumour roles. This is primarily mediated by the direct killing of tumour cells through release of ROS such as hydrogen peroxide[41]. Recently it was shown that neutrophil release of hydrogen peroxide induces a lethal influx of $Ca^{2+}$ in tumour cells via the $H_20_2$ responsive calcium channel, TRPM2[42]. Monoclonal antibodies that target tumour cells are a commonly employed therapeutic strategy used in cancer treatment. Neutrophils possess Fcγ receptors and are able to recognise tumour bound antibody and can kill tumour cells directly by antibody-dependent cell cytotoxicity[43]. Further to these anti-tumour roles, neutrophils can secrete anti-tumour mediators which facilitates recruitment of other immune cells such as T cells. Tumour-

associated neutrophils can act as antigen presentation cells and can stimulate proliferation of tumour-killing T cells[44,45].

# Subchapter 1.2 Neutrophil guidance cues and GPCRs

## 1.2.1 Neutrophil chemoattractants

To initiate their effector functions neutrophils must undergo an extensive migratory journey. This journey is guided by groups of biochemically diverse chemoattractant cues[46]. In sterile injury, in which there is no associated infection (e.g. blunt trauma, ischemia-reperfusion injury), neutrophils respond to 'damaged-self' signals known as damage-associated molecular patterns (DAMPs)[47]. DAMPs are released during necrosis, a cellular death process in which rupturing of the plasma membrane results in the release of normally intracellular molecules such as DNA, RNA, ATP, mitochondrial derived formylated peptides, heat shock proteins, mitochondrial DNA, high-mobility group box 1 protein (HMGB1) and S100 proteins[47,48]. During infection, neutrophils can recognise DAMPs produced through pathogen-induced damage of host cells. Furthermore, neutrophils can recognise pathogen-associated molecular patterns (PAMPs), such as lipopolysaccharide (LPS) and N-formylmethionine-leucyl-phenylalanine (fMLP). Some DAMPs and PAMPs are directly chemotactic and recruit neutrophils by signalling through corresponding neutrophil receptors. For example, N-formylated peptides which are derived from degraded bacterial or mitochondrial proteins are highly chemotactic and directly recruit neutrophils to target sites. Other DAMPs and PAMPs recruit neutrophils indirectly by activating the production of further attractants. As such, chemoattractants can be broadly categorised as 'primary' and 'secondary' attractants. Primary attractants are released directly, either from damaged endogenous cells or invading pathogens, whilst secondary attractants are produced indirectly by local host cells in response to tissue injury or infection. Potent neutrophil secondary attractants include the complement-activated protein products, C5a and C3a[49], as well as eicosanoids such as the lipid leukotriene B4 (LTB4)[50]. A major class of secondary chemoattractants that play a crucial role in neutrophil migration is the family of small secreted chemoattractant proteins (8-12 KDa) called chemokines[51].

### Chemokines

Chemokines are classed into sub-families according to their amino acid sequence, or more specifically by the positioning of the first two N-terminal conserved cysteine residues[52]. Accordingly, there are 4 subfamilies: C, CC, CXC and CX3C chemokines. In the CC family, the

first two cysteine residues are immediately adjacent whilst in the CXC and CX3C the N-terminal cysteine residues are separated by one or three amino acids respectively, where X represents any other amino acid residue. Chemokines have a highly conserved tertiary structure consisting of three anti-parallel β-sheets and a C-terminal α-helix[52]. The CXC chemokines are further categorised as being $ELR^+$ or $ELR^-$, meaning they either contain or lack the glutamic acid-leucine-arginine (ELR) amino acid motif before the first cysteine at the N- terminus. Chemokines can be broadly categorised as homeostatic chemokines (expressed constitutively) or inflammatory chemokines (expression induced by infection/injury).

## 1.2.2 Chemokines signal through G-protein coupled receptors (GPCRs)

### G-protein coupled-receptor structure

Chemokines signal through G protein coupled receptors (GPCRs). GPCRs are the largest family of receptors in eukaryotes with over 800 encoded in the human genome[53]. All GPCRs share a distinctive overall structure consisting of an extracellular N-terminus followed by 7 transmembrane α-helices and an intracellular C-terminus[54,55]. GPCRs transduce external signals to intracellular effectors via activation of the membrane-associated guanine nucleotide-binding proteins (G proteins) to which they are coupled[56,54].

### G-protein activation cycle

GPCR-associated G proteins are heterotrimeric complexes consisting of a Gα subunit and a Gβγ dimer[54]. The Gα and Gβ subunits are membrane-bound by lipid anchors. Importantly, the Gα subunit acts as molecular switch, existing reversibly in either an inactive GDP-bound state or an active GTP-bound state. In unstimulated cells, whilst the GPCR is not bound to its cognate ligand, Gα is GDP-bound and the G protein heterotrimer is inactive. The binding of an extracellular ligand to a GPCR induces a conformational change in the tertiary structure of the receptor such that the cytoplasmic region can bind and activate the Gα subunit by facilitating the exchange of GDP for GTP [54,57]. The binding of GTP causes a conformational change in the Gα subunit such that it dissociates from the Gβγ dimer. The Gα and Gβγ moieties are released and can diffuse laterally in the plasma membrane to initiate independent signalling cascades through interaction with different

downstream proteins. Owing to its intrinsic GTPase activity, Gα hydrolyses GTP to GDP and Gα re-associates with Gβγ to its inactive state, thus concluding the cycle.

## Signalling pathways activated by chemoattractant receptors

The Gα and Gβγ subunits can initiate independent signalling cascades which drive different cellular responses[57,58]. The current understanding is that the Gβγ subunits are responsible for initiating signalling cascades that result in chemotaxis. The main signalling pathway involved in neutrophil chemotaxis is the PI3K signalling pathway in which Gβγ subunits activate phosphoinositide-3 kinases (PI3Kγ) leading to the generation of phosphatidylinositol-3,4,5 trisphosphate ($PIP_3$)[58,59,60]. Accumulation of $PIP_3$ at the front of migrating cells is a hallmark of cell polarisation in neutrophils[61]. This has been visualised *in vivo* where neutrophil specific expression of a $PIP_3$ probe (Pleckstrin homology (PH) domain of protein kinase B (AKT) fused to EGFP) revealed that $PIP_3$ distribution was polarised towards the front of the migrating cell[61]. Interestingly, this study found that $PIP_3$ accumulated at the cell front of the cell when neutrophils migrated towards and away from the inflammatory loci. Thus, accumulation of $PIP_3$ at the anterior of the cell occurs during both random and directed migration of neutrophils. $PIP_3$ activates the small GTPase Rac which leads to polymerisation of dynamic filamentous actin (F-actin) to drive protrusions at the leading edge, facilitating directed motility. In zebrafish, local photoactivation of a genetically encoded photoactivatable small GTPase Rac at the leading edge generated protrusions and could induce directed migration. Through photoactivation the neutrophil could be guided and redirected at will, as seen in experiments where the migration path of the cell could be manipulated to spell out the word 'RAC'[61]. Interestingly, when PI3K was inhibited, photo-activation of Rac did not lead to directed migration. Instead, protrusions were rescued while anteroposterior polarity was not, suggesting that PI3K regulates anteroposterior polarity of stable F-actin. As well as the PI3K pathway, the Gβγ subunit can activate the phospholipase CB (PLCB2/3) pathway leading to the generation of diacylglycerol (DAG), inositol triphosphate ($IP_3$), release of calcium and activation of protein kinase C (PKC), though this is not believed to contribute to chemotaxis[62]. As is true for Gα proteins, there are multiple Gβ and Gγ proteins, though the role of different dimers remains unclear. There are many different combinations of each subunit that can combine to form a wide range of different heterodimers which can activate different downstream proteins. The role of the Gα subunit is unclear and is discussed more extensively in chapter 5.

# Subchapter 1.3: Neutrophil trafficking during inflammatory responses

Neutrophil recruitment to target sites relies heavily on chemokine signalling and involves multiple trafficking steps which can be broadly broken down into: mobilisation from the bone marrow, extravasation and migration through the interstitial tissue (Fig. 1.1)[1].

## 1.3.1. Mobilisation from the bone marrow

The bone marrow provides a large reservoir of neutrophils that can be readily mobilised and released into the circulation in response to an inflammatory stimulus. Under homeostatic conditions (i.e. in the absence of inflammation), neutrophil release from the bone marrow is regulated by the chemokine CXCL12, also known as stromal cell derived factor 1a (SDF1a), which is expressed constitutively by bone marrow stromal cells and signals through its cognate receptor CXCR4. The binding of CXCL12 to CXCR4 expressed on neutrophils promotes their retention in the bone marrow whilst CXCR4 down-regulation facilitates release from the bone marrow [63,64,65]. Retention mediated by the CXCL12/CXCR4 signalling axis is antagonised by CXCR2 which is upregulated during maturation[66]. During inflammatory responses, this balance of signals is shifted to promote release from the bone marrow into the circulation. This can result in a rapid and significant increase in the number of circulating neutrophils and thus represents an important trafficking step in neutrophil recruitment to inflammatory sites.

## 1.3.2 Extravasation

Circulating neutrophils must traverse the blood vessel to enter target tissues. This process, termed extravasation, involves several well characterised steps which include: tethering, rolling, adhesion, crawling and finally, transmigration[67,68]. The presence of an infection/injury leads to increased expression of adhesion molecules such as P-selectin and E-selectin on the blood vessel endothelium. Circulating neutrophils bind to these adhesion molecules using surface receptors such as P-selectin glycoprotein ligand-1 (PSGL1), which binds endothelial P-selectin. This binding leads to tethering of the neutrophil. Tethered neutrophils roll in the direction of the blood flow and this rolling increases contact with the endothelium and endothelial-bound chemokines. These endothelial chemokines are generated by inflammatory sentinel cells or the endothelium directly

and are presented on the luminal side of endothelium. Presented chemokines are immobilised on the endothelium by binding negatively charged heparin substrates, which serve as anchors preventing chemokine washing away in blood flow and facilitates the formation of intravascular gradients. Neutrophil binding of endothelial-bound chemokines (e.g. CXCR2 binding the chemokine CXCL8) plays an important role in promoting further adhesion to the endothelium through the activation of integrins. Activation of GPCRs results in a conformational change in neutrophil integrin receptors which bind extracellular matrix proteins. This conformational change increases affinity for ligand (switch from low to high affinity) and facilitates tight adhesion to the endothelium e.g. Lymphocyte function-associated antigen 1 (LFA-1) increasing affinity for its ligands endothelial intercellular adhesion molecule 1 (ICAM1) and ICAM2. Adherent neutrophils crawl to sites of transmigration and can cross the vessel via two routes, migrating either through the endothelial cell (transcellularly) or more commonly between endothelial cells (paracellularly)[69,70,1].

## 1.3.3 Neutrophil interstitial migration

Whilst the process of extravasation has been extensively studied and is well characterised, the cues and mechanisms governing the subsequent stages of neutrophil migration remain far less understood. Following transmigration from the circulation into the interstitial tissue, neutrophils adopt a polarised morphology and migrate directionally, following gradients of chemotactic cues, towards the target site[71]. This process, in which cells migrate towards higher concentrations of chemoattractant, is broadly termed chemotaxis.

### Establishing cell polarity

Establishment of the initial polarity of a neutrophil can be triggered by an external gradient or can be randomly acquired. For example, exposure to an external gradient triggers symmetry breaking, typically directed towards the increasing attractant concentration. On the other hand, exposure to a uniform attractant triggers symmetry breaking in an arbitrary direction leading to random motion (Brownian random walk)[72]. To migrate, whether directionally or randomly, a cell must establish an axis of polarity by forming a distinct cell front (leading edge) and a cell back (uropod). Establishment of polarity is important because different cytoskeletal regulators are required to generate forward protrusions and contraction at the sides and rear. For example, $PIP_3$, Rac (a Rho

GTPase) and dynamic F-actin are characteristically localised at the cell front and promote protrusions whilst asymmetric rearward localisation of RhoA (a Rho GTPase), Rho-associated coiled-coil containing protein kinase 1 (ROCK), myosin II and stable F-actin promote contraction[73].

## Directional sensing

A key step in directed migration is the ability of a cell to sense the external chemotactic gradient and adjust its axis of polarity accordingly. There are two mechanisms proposed to play a role in directional sensing: spatial and temporal sensing[74,75]. In spatial sensing, a cell compares the number of ligand bound receptors across its membrane and polarises in the direction in which this number is greatest. In temporal sensing, the cell compares the chemoattractant concentration at different time points, i.e. comparing the concentration at position and time X to the concentration at position and time Y. Thus, by definition, spatial sensing implies that cells do not need to move to resolve a gradient whereas temporal sensing requires them to move to sample the environment. Temporal sensing is the directional sensing utilised by bacterial cells which are significantly smaller than eukaryotic cells and as such cannot spatially discern gradients across their cell surface[76].

### *Spatial sensing*

Spatial sensing as a directional sensing mechanism is supported by the observation that stationary neutrophils extend protrusions when exposed to a gradient[77]. Furthermore, rounded, latrunculin-treated neutrophil-like HL-60 cells, show asymmetric PI3K distribution towards an applied fMLP gradient[78], again suggesting that a spatial sensing mechanism independent of cell movement plays a role in directional sensing. However, spatial sensing is complex given sensitivity is not uniform across polarised cells (i.e. cells that are already migrating). Instead polarised cells exhibit asymmetric sensitivity with the front being more sensitive to attractant than the rear. Therefore, polarised cells are more likely to maintain their original direction and gradually turn their leading edge towards the gradient. This was shown in HL-60 neutrophil-like cells where placing a micropipette releasing chemoattractant at the back of the cell was more likely to trigger a U-turn than a 180° reversal in polarity[79]. Asymmetric sensitivity was also shown in zebrafish neutrophils, where photoactivation of Rac was more successful in steering polarised neutrophils when light was targeted to the leading edge[61]. This polarised sensitivity has been shown to depend on cytoskeletal

architecture[80]. Wang et al. used a pharmacological cocktail (JLY) consisting of Jasplakinolide (J), Latrunculin B (L) and ROCK inhibitor Y27632 (Y) to block actin dynamics (actin assembly/polymerisation and disassembly/depolymerisation) but preserve existing actin cytoskeleton architecture[80]. This pharmacological cocktail acted to 'stall' HL-60 neutrophils. Interestingly, 'stalled' polarised cells responded to uniform low concentrations of fMLP with an asymmetric accumulation of $PIP_3$ at the front of the cell. Thus, the directional response of the cell depends on both the external gradient and the polarised architecture of the cytoskeleton. Although the established leading edge is relatively more sensitive to chemoattractants, cells can be forced to re-polarise by increasing the steepness of the reverse gradient, showing that at least some sensitivity is maintained around the entire perimeter[80].

***Temporal sensing***

Evidence for temporal sensing has been obtained in human neutrophils which were found to adjust their direction in response to temporal decreases of uniform chemoattractant (fMLP)[81]. This is further supported by more recent *in vitro* evidence showing that stable gradients of the chemoattractant CXCL12 failed to drive persistent directional migration in neutrophils[82]. Only when the absolute concentration of chemoattractant was constantly rising did cells show persistent migration. These results suggest that persistent directed migration depends on sensing a temporal increase in absolute concentration of chemoattractant. This suggests that neutrophils can sense they are going the 'wrong' way when they sense a temporally decreasing uniform chemoattractant.

Thus, compelling evidence exists for both spatial and temporal sensing and it is likely that there is a complex interplay between the two sensing mechanisms. Given that it is not trivial to decouple temporal and spatial cues, as movement of a cell in a heterogeneous environment also confers a temporal difference, the sensing mechanisms driving eukaryotic directed migration are yet to be fully deciphered.

## Mechanism of interstitial movement

As is typical for eukaryotic cells, motility in leukocytes is mediated by the cytoskeleton, the coordinated movement of which drives motility. Forward protrusions are generated by actin polymerisation at the leading edge whilst myosin facilitates tail contraction at the rear[83,73]. Like all

leukocytes, neutrophils exhibit an 'ameboid' mode of migration characterised by rapid, adhesion- and protease-independent motility[83]. This contrasts with the 'mesenchymal' migration mechanism displayed by other eukaryotic cells such as fibroblasts, where migration is slower and is adhesion- and protease-dependent[84]. Furthermore, in fibroblasts, protrusion, adhesion and contraction appear to be intricately linked, with leading-edge protrusions generating pulling forces towards the cell body[83]. In contrast, neutrophils protrude without rearward pulling forces and during non-contractile phases the cell rear appears to be passively dragged by the protruding cell front suggesting that in neutrophils, protrusion and contraction are de-coupled[83]. As such, neutrophils are said to migrate using a 'flowing and squeezing' model of migration where protrusive flow of F-actin at the front is sufficient to drive forward migration and actomyosin contraction at the rear (uropod) serves to squeeze and propel the rigid nucleus through confined regions of the 3D environment[83]. Interestingly, neutrophil interstitial migration does not appear to require integrin-mediated traction forces[83]. Integrins are transmembrane receptors which couple the force of the cytoskeleton to the extracellular environment. Whilst integrins have been shown to be indispensable for 2D migration *in vitro*, they are not required for 3D migration *in vitro* or *in vivo*[83]. This discrepancy between *in vitro* and *in vivo* findings highlights the importance of physiologically relevant systems to study neutrophil migration behaviour.

## Amplification/swarming

At the target site neutrophils accumulate and can exhibit a highly co-ordinated, self-organised clustering behaviour known as 'swarming', named as such due to similarities with the behaviour of swarming insects [85,86,87]. Swarming is often described in stages, beginning with the arrival of a small number of 'pioneer neutrophils' which are recruited by the initial signals generated at the site[88]. These pioneer cells then further amplify the response through recruitment of additional neutrophils from distal sites in what is called a 'second wave' of recruitment[88]. Neutrophil swarms have been observed *in vivo* in response to both infection and sterile injury[85,89]. In a murine lymph node infection model, neutrophils were shown to form both persistent and transient swarms. Transient swarms formed and dispersed over 10-40 minutes and remained small (about 150 neutrophils) whilst persistent swarms were longer lasting and larger comprising over 300 neutrophils[90]. Whilst the signals governing swarming remain largely unknown, Lammerman et al. have reported a prominent role for the chemoattractant LTB4 in the recruitment additional cells

and the swarming response. Here, in murine ear skin, neutrophils lacking the LTB4 receptor displayed normal chemotaxis to a laser-induced focal wound but impaired amplified recruitment at later stages and an impaired swarming response[86]. The physiological role of swarming is not yet fully understood. Swarming may act to concentrate cytotoxic function and/or to form a physical seal, isolating damaged/infected tissue from healthy tissue and preventing the spread of pathogens. For example, in a murine *Leishmania* infection model, neutrophil swarms appeared to form an epidermal 'plug' in the hole left by the sand fly proboscis following biting[85]. However, here swarming was also suggested to facilitate dissesmination of infection as neutrophils were found to harbour viable parasites and neutrophil depletion promoted productive *Leishmania* infections.

## 1.3.4 Resolution of neutrophil recruitment

Whilst neutrophil recruitment is required for the clearance of pathogens and the repair of injured tissue, it is essential that neutrophils are cleared from the site after having completed their effector function. Excess neutrophil accumulation can be detrimental to the host and is associated with a range of chronic inflammatory diseases such as chronic obstructive pulmonary disease, asthma and rheumatoid arthritis[91,92]. Targeting neutrophil recruitment in the context of inflammatory diseases is a double-edged sword as it also compromises host defence. For this reason, targeting the resolution phase of the neutrophil response is envisaged as a more promising and viable approach for therapy of chronic inflammatory disorders. However, this phase of the neutrophil response is less understood, in part because of the difficulty in long-term tracking of neutrophils after they reach inflammatory loci.

### Apoptosis and resolution of inflammation

Neutrophil apoptosis and subsequent removal by macrophage phagocytosis is thought to play a key role in the clearance of neutrophils from the target site[93]. Apoptosis is a regulated mechanism of programmed cell death in which cells undergo characteristic morphological changes, such as rounding up, condensation of chromatin, nucleus fragmentation, cytoplasmic vacuolisation, and blebbing of the cell membrane leading to so-called 'apoptotic bodies'[94]. Importantly, the cell membrane remains intact throughout, protecting the host from the release of potentially damaging intracellular contents. Thus, apoptosis is distinct from necrosis, another form of cell death in which the cell membrane ruptures, releasing intracellular contents. Evidence for apoptosis as a mechanism

of neutrophil clearance was first put forward by Newman et al[95]. In these experiments, they showed that macrophages phagocytosed aged human neutrophils but did not phagocytose freshly isolated neutrophils, suggesting that neutrophils become susceptible to phagocytosis with increasing age. A subsequent study by Savill et al. identified the mechanism underlying this increased susceptibility to phagocytosis[93]. In this study, imaging revealed that aged neutrophils showed morphological signs of apoptosis including condensation of chromatin and cytoplasmic vacuolisation. Acquisition of apoptotic morphology was temporally correlated with the recognition of neutrophils by macrophages, suggesting that apoptosis facilitated their recognition and phagocytosis by macrophages. As well as these *in vitro* studies, there is also evidence of the presence of apoptotic neutrophils at inflammatory sites *in vivo*. For example, macrophage engulfment of apoptotic neutrophils was found to contribute to the resolution of inflammation in an *in vivo* rat model of acute pulmonary inflammation[96]. Here, intra-tracheal administration of LPS induced neutrophil recruitment to the lung, with recruitment peaking at 18hrs and decreasing after 24hrs. The number of apoptotic neutrophils at the site gradually increased, peaking at 24hrs and subsequently declined with resolution of the neutrophil response. This temporal correlation suggested a role for macrophage clearance of apoptotic cells at inflammatory tissue sites. Whilst these studies provide evidence for apoptosis occurring at inflamed sites, the extent to which this contributes to the overall resolution of the response remains somewhat unclear.

## Reverse migration

The detection of apoptotic neutrophil corpses at inflammatory sites led to the idea that apoptosis is the main mechanism of neutrophil clearance at target sites. However, recently numerous studies have provided evidence that neutrophils actively migrate away from the target in a process that has been termed ‘reverse migration’. More specifically, this general term can be sub-divided into two processes, ‘reverse interstitial migration’ (rIM) in which neutrophils migrate through the interstitial tissue away from the target site, and ‘reverse transendothelial migration’ (rTEM) in which neutrophils re-enter the vasculature in an abluminal-to-luminal direction.

The idea that neutrophils may be cleared from inflammatory sites via a mechanism other than apoptosis was first put forward by Hughes et al. in 1997[97]. Here, in a rat inflamed kidney model, apoptosis was shown to be responsible for the clearance of only a small percentage of recruited neutrophils (10%) with most neutrophils (over 70%) appearing to leave the glomerulus/inflamed

kidney. However, owing to limitations of the models and tracking tools available at the time, the destination of these non-apoptotic neutrophils remained unknown. Reverse transendothelial transmigration (rTEM) was first observed in human neutrophils *in vitro*[98]. In this study, neutrophils that had transmigrated through a TNF-α stimulated endothelial monolayer were found to reappear on the top of the monolayer. When compared to naïve circulating neutrophils, these reverse transmigrated neutrophils showed a distinct CXCR1$^{low}$ and intercellular adhesion molecule-1$^{high}$ (ICAM-1$^{high}$) surface expression profile. This was not purely a result of activation, as fMLP exposed neutrophils did not display this phenotype. Interestingly, the number of neutrophils with a reverse transmigrated surface expression phenotype was found to be increased in patients suffering from inflammatory disorders such as Atherosclerosis.

More recent studies have been able to go a step further and have tracked the fate of the cells post-arrival at target sites *in vivo*. Indeed, both reverse interstitial migration (rIM) and reverse transmigration (rTEM) have now been visualised in both the zebrafish and murine model, supporting the idea that reverse migration is a conserved mechanism in the resolution of inflammation[99]. Neutrophil rIM was first directly visualised *in vivo* in the zebrafish, a model particularly amenable to imaging/tracking of cells across the whole organism. Here, generation of a zebrafish transgenic line in which neutrophils express the fluorescent protein GFP under the neutrophil-specific myeloperoxidase promoter, facilitated live-tracking of cells during inflammatory responses. Live-imaging revealed that most recruited neutrophils (over 80%) migrated away from the site towards the vasculature[100]. Interestingly, no apoptotic events were observed in this study, again supporting the idea that other mechanisms can drive resolution. Subsequent studies in zebrafish tracked the fate of neutrophils post-arrival at the wound by utilising a genetically encoded photolabelling system in which the photoconvertable protein 'dendra' is expressed specifically in neutrophils[73]. Following exposure to 405nm light, Dendra changes from emitting green fluorescence to emitting red fluorescence. Thus, photoconversion enables individual cells to be tracked throughout the organism over a long period of time. Tracking of photoconverted cells revealed that neutrophils display bidirectional migration at the target site, repeatedly migrating back and forth between the wound and blood vessel. Furthermore, long-term tracking over the period of days revealed that photoconverted neutrophils dispersed to distal non-specific sites. High-resolution confocal imaging in a murine inflamed cremaster muscle model provided direct evidence for the ability of neutrophils to perform reverse transendothelial migration (rTEM)

and re-enter the vasculature[69]. *In vivo* evidence for reverse interstitial migration (rIM) in the mouse came from a model of sterile hepatic injury, where neutrophils were shown to depart from the injury site by migrating through the interstitial tissue to healthy tissue and/or re-entering the vasculature[26]. Here, consistent with other studies, only 10% of recruited cells were found to be apoptotic, again supporting the idea that resolution occurs by another/additional mechanism[26]. Furthermore, depleting macrophage recruitment had no effect on the rate of neutrophil clearance, suggesting that mechanisms other than macrophage clearance of apoptotic neutrophil corpses play a prominent role in neutrophil clearance from target sites[26].

## Fate and role of reverse migrated neutrophils

The fate and role of reverse migrated neutrophils is not well understood. Buckley et al.[98] found that rTEM neutrophils could not cross a second tumour necrosis factor-α (TNF-α) stimulated EC monolayer suggesting that rTEM neutrophils may be unable to re-enter inflamed tissue following reverse transmigration. Reverse transmigrated neutrophils were more adherent, with reduced filtration rates compared to freshly isolated cells further supporting the idea that rTEM neutrophils may not be able to enter secondary tissue sites. In this study, reverse transmigrated neutrophils showed an enhanced ability to generate ROS when activated with fMLP, indicating that they are primed. Studies *in vivo* have shown that rTEM neutrophils can be detected in distal organs and that the presence of these cells is associated with tissue inflammation/damage at secondary sites[69]. Another *in vivo* study tested the ability of rTEM neutrophils to mount an effective response to a secondary inflammatory stimulus[101]. Here, following a tail injury, photoconverted neutrophils (wound experienced) and naïve (non-wound experienced) neutrophils were tracked responding to a secondary *Staphylococcus aureus* infection. Interestingly, reverse-migrated and naïve neutrophils showed no difference in directionality or velocity. Furthermore, reverse migrated cells mounted an effective anti-microbial effector response with phagocytosis and ROS production being comparable to that of naïve recruited cells. Thus, the responses of reverse-migrated and naïve cells to a secondary insult were indistinguishable. In the mouse, long-term tracking of cell fate revealed that reverse migrated neutrophils were found in two other main sites, the lung and the bone marrow[26].

## Mechanisms driving reverse interstitial migration

Reverse migration is still a relatively new concept in the field of neutrophil migration and the underlying mechanisms are unclear. Whilst there is evidence that cells can migrate directionally away from attractants, e.g. via fugetaxis (meaning 'to flee' from) or chemorepulsion (analogous to the reverse of chemotaxis)[102], the more supported view is that reverse migration occurs via random dispersal. Mathematical modelling of neutrophil responses in tail transections has shown that reverse migration lacks directionality and instead is achieved via random dispersal[103,101,104]. Thus, random dispersal from the target site seems to be an important mechanism but how cells decide to disperse or stay at the target site is unclear but remains an important question.

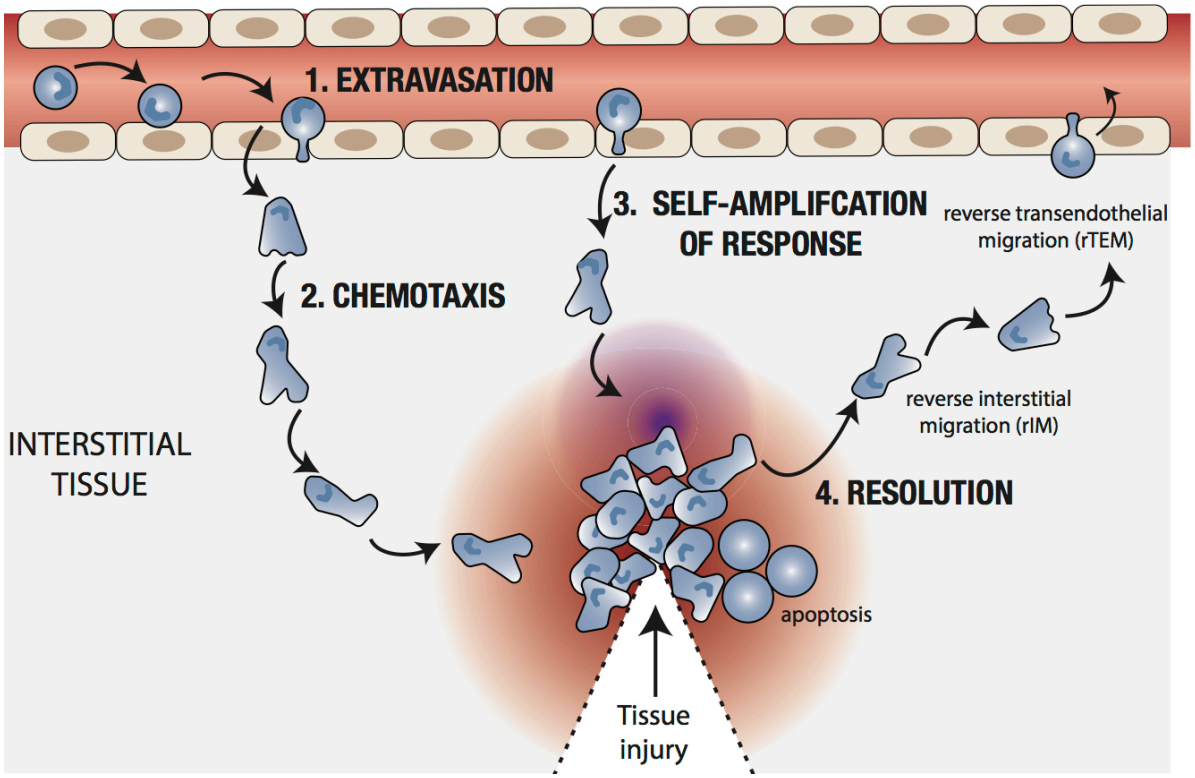


**Figure 1.1. Schematic showing neutrophil recruitment and behaviour post-arrival at a tissue wound.** 1) Neutrophils circulating around the body in the blood stream adhere to the blood vessel endothelium and extravasate into the interstitial tissue. 2) Once in the interstitial tissue neutrophils follow gradients of chemoattractants and migrate directionally towards the wound. 3) Neutrophils can self-amplify their response through secretion of secondary attractants which recruit further cells. 4) Neutrophils may perform apoptosis or may actively migrate away from the target site via reverse migration.

# Subchapter 1.4 Model systems to study neutrophil interstitial migration

The overarching aim of this thesis is to understand how chemoattractant interpretation within inflammatory sites might change over time to both drive recruitment but enable effective dispersal. This question is best addressed *in vivo*, as it requires the ability to visualize and manipulate the behaviour of both neutrophils and their interpretation machinery, i.e. the relevant cell surface receptors. Monitoring neutrophil migration in interstitial tissue is difficult owing to experimental limitations of available model systems and commonly employed methods lack the required spatiotemporal resolution as I will discuss below.

## 1.4.1 *In vitro* model systems to study neutrophil migration

### Primary human neutrophils

There are a range of *in vitro* and *in vivo* systems and tools commonly used to study neutrophil migration. Arguably, primary human neutrophils represent the ideal model when it comes to translating findings to human biology. However, *in vitro* studies in this system are severely restricted due to technical limitations in the manipulation of primary cells. These cells are inherently short-lived and spontaneously undergo apoptosis *in vitro* making them difficult to work with. Furthermore, human-derived neutrophils are terminally differentiated and cannot be transfected, making genetic manipulation of these cells difficult. Tracking of primary neutrophils *in vitro* is commonly performed using migration chambers and applied chemokine gradients. However, migration chambers cannot fully recapitulate the *in vivo* physiological environment. This is particularly limiting when studying reverse migration as the physiological determinants of this process are still unclear. Receptor expression in primary cells is usually monitored via antibody staining and flow cytometry. Whilst this offers the benefit of directly reflecting endogenous receptor levels, it is not compatible with dynamic live imaging and therefore offers very limited temporal resolution.

### Neutrophil-like cell lines

Neutrophil-like differentiated cells (such as HL-60 and PBL-985) overcome many of the above caveats and therefore represent another popular *in vitro* model used to study neutrophil

biology[105,106]. A commonly used model is the HL-60 cell line, an immortal human-leukaemia line. Neutrophil-like HL-60 cells can be differentiated from HL-60 cells as and when required through use of dimethyl sulfoxide (DMSO) or retinoic acid[107]. Differentiated HL-60 cells share many characteristics of primary human neutrophils and respond to chemotactic stimuli. Furthermore, unlike primary human cells, these cells can be transfected and can thus be genetically manipulated[108].

### Human cell lines

The study of receptor dynamics in response to ligand often involves expression in other cells such as HEK293T cells (Human embryonic kidney 293T cells). Such studies are particularly useful for understanding receptor biochemistry but in terms of understanding how receptors behave in neutrophils, they can be poorly predictive. For example, CXCR1 internalisation was shown to require co-expression of G protein-coupled receptor kinases 2 (GRK2) and β-arrestin in HEK293T cells[109].

## 1.4.2 *In vivo* model systems to study neutrophil migration

### The murine model

As discussed above, a limitation of *in vitro* studies is that they are unable to fully recapitulate the complex endogenous environment. *In vivo* animal models overcome this caveat. The murine model is a popular immunological model system used to study neutrophil biology and, being a mammalian model, shares a high degree of homology with human biology. There are knockout lines and fluorescent reporter lines readily available in the mouse. For example, LyzM-eGFP mice which express eGFP under the neutrophil specific promotor Lyzozyme M have facilitated real-time visualisation of neutrophil migration *in vivo*[86]. However, *in vivo* imaging and thus live tracking of cell behaviour and dynamics can be limited in the mouse as fluorescent reporters cannot be visualised due to the depth of the tissue. As such, imaging and tracking are usually restricted to superficial regions such as the ear pinnae or alternatively invasive surgery is employed to access the area for imaging[86]. *Ex vivo* imaging is also a popular technique e.g. studying migration in excised lymph nodes. Recently, advances in imaging techniques such as 2-photon intravital microscopy has enabled imaging of neutrophils in deeper tissues in live mice such as in peripheral lymphoid organs, though imaging range is undoubtedly still limited[86].

## The zebrafish as a model of vertebrate immunity

The zebrafish is an ever increasingly popular immunological model system and is ideally suited to the study of neutrophil migration[110,111]. The zebrafish vertebrate immune system draws many parallels to the mammalian vertebrate immune system with all major immune cells and molecules represented, including neutrophils which develop at 48 hours post fertilisation (hpf)[112]. Zebrafish neutrophils are morphologically and functionally similar to mammalian neutrophils possessing a segmented nucleus, a granule rich cytoplasm and are fully competent in effector mechanisms such as phagocytosis, the generation of ROS and the release of NETs[113,114]. This model is particularly well suited to studying innate immune processes given that the zebrafish adaptive immune system (i.e. T and B cells) does not mature until approximately 4-6 weeks post-fertilisation. Zebrafish are genetically tractable enabling the generation of transgenic and mutant lines and their many progeny allows for quick genetic screening. Arguably, the primary advantage of the zebrafish as a model is that zebrafish larvae are optically transparent and as such are highly amenable to non-invasive live-imaging. This enables genetically labelled cells and sub-cellular molecules to be tracked in real time during inflammatory responses, providing better temporal resolution. Thus, the zebrafish provides the ideal model system to study neutrophil migration and receptor dynamics in response to *in vivo* gradients.

# Subchapter 1.5 The zebrafish Cxcl8/Cxcr1/Cxcr2 axis as a model system to study neutrophil interstitial migration

## 1.5.1 Zebrafish Cxcl8 homologues as a model system

### Zebrafish have two Cxcl8 lineages, Cxcl8a and Cxcl8b

In humans, a major chemokine involved in neutrophil recruitment to inflammatory sites is CXCL8[115]. Whilst the murine model lacks a CXCL8 homologue, two orthologues referred to as Cxcl8a and Cxcl8b, have been characterised in the zebrafish [116,117]. The *Cxcl8a* gene is located on zebrafish chromosome 1 and encodes an open reading frame of 288bp, corresponding to a protein of 98 amino acids. Cxcl8a is found in all teleosts whilst Cxcl8b is specific to zebrafish and carp. The *Cxcl8b* gene is located on chromosome 7 and encodes a protein of 118 amino acids. Both Cxcl8a and Cxcl8b have the four cysteines characteristic of CXC chemokines. However, unlike human CXCL8, they both lack the angiogenic ELR motif. Cxcl8a and Cxcl8b show 41.4% similarity in protein sequence (Fig. 1.2). Zebrafish Cxcl8a and human CXCL8 show 55% similarity in protein sequence (Fig. 1.3a). Zebrafish Cxcl8b and human CXCL8 shows 46% similarity in protein sequence (Fig. 1.3b).

```
Cxcl8a              1 -----MTSKIISVCVIVFLAFLTIIEGMSLRGLAVDP--RCRCIETESR-     42
                            :::.:::.:|....|.        :..|.|:.|  ||:||:|.|:
Cxcl8b              1 MMKLSVSAFMLLICTTALLC--------ANEGEALPPPQRCQCIKTHSKP     42

Cxcl8a             43 RIGK-HIKSVELFPPSPHCKDLEIIATLMTTGQEICLDPSAPWVKKIIDR     91
                      .|.| .:..:::.|...||::.|||||| ..|| |||:|:..||..:.::
Cxcl8b             43 PIPKRQVLGLKVTPAGSHCRNEEIIATL-KKGQ-ICLNPTETWVISLKEK     90

Cxcl8a             92 IIVNRKP----------------------     98
                      ...:...
Cxcl8b             91 FAASATKLAATAAPAQTTTTFSTIMTTN    118
```

**Figure 1.2. Cxcl8a and Cxcl8b protein alignment.** Pairwise Sequence Alignment using EMBOSS needle[118].

**a**

```
zCxcl8a            1 MTSKIISVCVIVFLAFLTIIEGMSLRGLAVDPRCRCIETESRRI-GKHIK     49
                     ||||:....:..||....:.||..|...|.:.||:||:|.|:.. .|.||
hCXCL8             1 MTSKLAVALLAAFLISAALCEGAVLPRSAKELRCQCIKTYSKPFHPKFIK     50

zCxcl8a           50 SVELFPPSPHCKDLEIIATLMTTGQEICLDPSAPWVKKIIDRIIVNRKP-     98
                     .:.:....|||.:.|||..| :.|:|:||||...||::::::.:...:.
hCXCL8            51 ELRVIESGPHCANTEIIVKL-SDGRELCLDPKENWVQRVVEKFLKRAENS     99
```

**b**

```
zCxcl8b            1 -MMKLSV---SAFMLLICTTALLCANEGEALP---PPQRCQCIKTHSKPP     43
                      ..||:|   :||::    :|.||  ||..||   ...|||||||:|||.
hCXCL8             1 MTSKLAVALLAAFLI----SAALC--EGAVLPRSAKELRCQCIKTYSKPF     44

zCxcl8b           44 IPKRQVLGLKVTPAGSHCRNEEIIATLKKG-QICLNPTETWVISLKEKFA     92
                     .|| .:..|:|..:|.||.|.|||..|..| ::||:|.|.||..:.|||.
hCXCL8            45 HPK-FIKELRVIESGPHCANTEIIVKLSDGRELCLDPKENWVQRVVEKFL     93

zCxcl8b           93 ASATKLAATAAPAQTTTTFSTIMTTN    118
                     ..|...
hCXCL8            94 KRAENS--------------------     99
```

**Figure 1.3. Zebrafish Cxcl8 and human CXCL8 protein alignments.** a) zCxcl8a and human CXCL8 protein alignment. b) zCxcl8b and human CXCL8 protein alignment. Pairwise Sequence Alignment using EMBOSS needle[118].

## Upregulation of Cxcl8a and Cxcl8b expression following inflammatory insult

Both Cxcl8a and Cxcl8b have been shown to be up-regulated during inflammatory responses, including during injury[117,119], infection [120] and in the tumour initiating environment[121]. In a caudal fin wound injury model, both chemokines were found to be upregulated[119]. Interestingly, the number of neutrophils recruited to the injury site was significantly reduced following knockdown (via morpholino injections) of either Cxcl8a or Cxcl8b, suggesting that the absence of just one of the chemokines is sufficient to significantly reduce neutrophil recruitment to caudal tail fin transections[119]. However, it is worth noting that injection of Cxcl8b morpholino (MO) was shown to affect Cxcl8a expression, thus a specific role for Cxcl8b versus an indirect role through Cxcl8a cannot be ruled out. Both chemokines were also found to be upregulated in response to *S.*

*Typhimorium* infection. Here, neutrophil accumulation and pathogen clearance were reduced in both Cxcl8a and Cxcl8b morpholino injected larvae, suggesting that both chemokines are important in this infection setting[122]. However, in certain contexts, differences in expression of the two chemokine lineages have been reported. For example, a study investigating whether the degree of wounding differentially affects expression of Cxcl8a and Cxcl8b found that Cxcl8a is upregulated in response to both 'mild' and 'severe' damage whilst Cxcl8b expression is upregulated in response to 'severe' damage only. Here, 'mild' damage refers an injury model in which the tip of caudal tail fin (excluding muscle) is transected, whilst the 'severe' damage refers to model in which a more extensive region (including muscle) is transected. In this study, injection of a Cxcl8a targeting MO significantly reduced neutrophil recruitment to both severe and mild wounds providing evidence that this chemokine plays an important role in neutrophil recruitment in both settings. In contrast, injection of a Cxcl8b targeting MO decreased recruitment to severe wounds but had no effect on recruitment to mild wounds[123]. Differential expression of the two chemokines has also been reported in certain infection settings. Sarris et al. found only Cxcl8a to be induced after non–pathogenic Escherichia coli (*E. coli*) infection[120]. Thus, Cxcl8a appears to be expressed in all inflammatory contexts whereas cxcl8b is only expressed under certain conditions. Accordingly, studies of neutrophil migration in zebrafish have focused on Cxcl8a.

## Cxcl8a forms hypotactic gradients *in vivo*

*In vivo* studies by Sarris et al. revealed that Cxcl8a establishes tissue-bound or 'haptotactic' gradients by binding extracellular components called heparan sulphate proteoglycans (HSPGs)[120]. This binding was shown to be important for gradient function as neutrophil recruitment was severely compromised upon inhibition of chemokine-HSPG binding, as assessed either through use of mutant chemokine that did not bind HSPGs or by local HSPG degradation (via heparinase treatment). Mutant Cxcl8a defective in binding HSPGs was not detected as a local gradient nor at the distal caudal vein plexus, providing further evidence that this chemokine is tissue bound *in vivo*.

## Cxcl8a biases neutrophil directional speed

Cxcl8a imposes a directional bias on the neutrophil random walk[120]. Analysis of neutrophil trajectories revealed that Cxcl8a does not influence neutrophil turning or persistence but instead biases directional speed such that cells move faster when migrating up-gradient (<45° approach

angles) and slower movement when migrating down-gradient. The net result of this migration response is directionally biased motion towards the source. Furthermore, once at the target source, Cxcl8a acts as a 'break' on neutrophil movement by triggering local deceleration, further enhancing local retention at the site of infection. The molecular mechanisms that influence directional speed and thus govern these dynamic migration behaviours remain unknown.

### A distinct role for Cxcl8b in mobilising neutrophils into the bloodstream

Recent work has reported differential roles for Cxcl8a and Cxcl8b in influencing neutrophil migration, with Cxcl8b regulating neutrophils entry into circulation. Whilst Cxcl8a MO-injected larvae had comparable neutrophils in the circulation to control, Cxcl8b MO had a significantly decreased number of neutrophils in the circulation[123].

## 1.5.2 Zebrafish Cxcr1 and Cxcr2

CXCL8 signals through two receptors, CXCR1 and CXCR2. Orthologues of both receptors have been characterised in zebrafish and have been shown to be expressed in zebrafish neutrophils[124]. Zebrafish Cxcr1 and Cxcr2 are located, in tandem, on chromosome 9[117]. Zebrafish Cxcr1 and Cxcr2 show 57% similarity in protein sequence (Fig 1.4). Zebrafish Cxcr1 shares approximately 58% sequence similarity to human CXCR1 (Fig. 1.5) and zebrafish Cxcr2 shares approximately 63% sequence similarity to human CXCR2 (EMBOSS needle) (Fig 1.6). Phylogenetic comparison of Cxcr1 and Cxcr2 to their mammalian counterparts showed that Cxcr2 is more closely related to the mammalian receptors than Cxcr1[117].

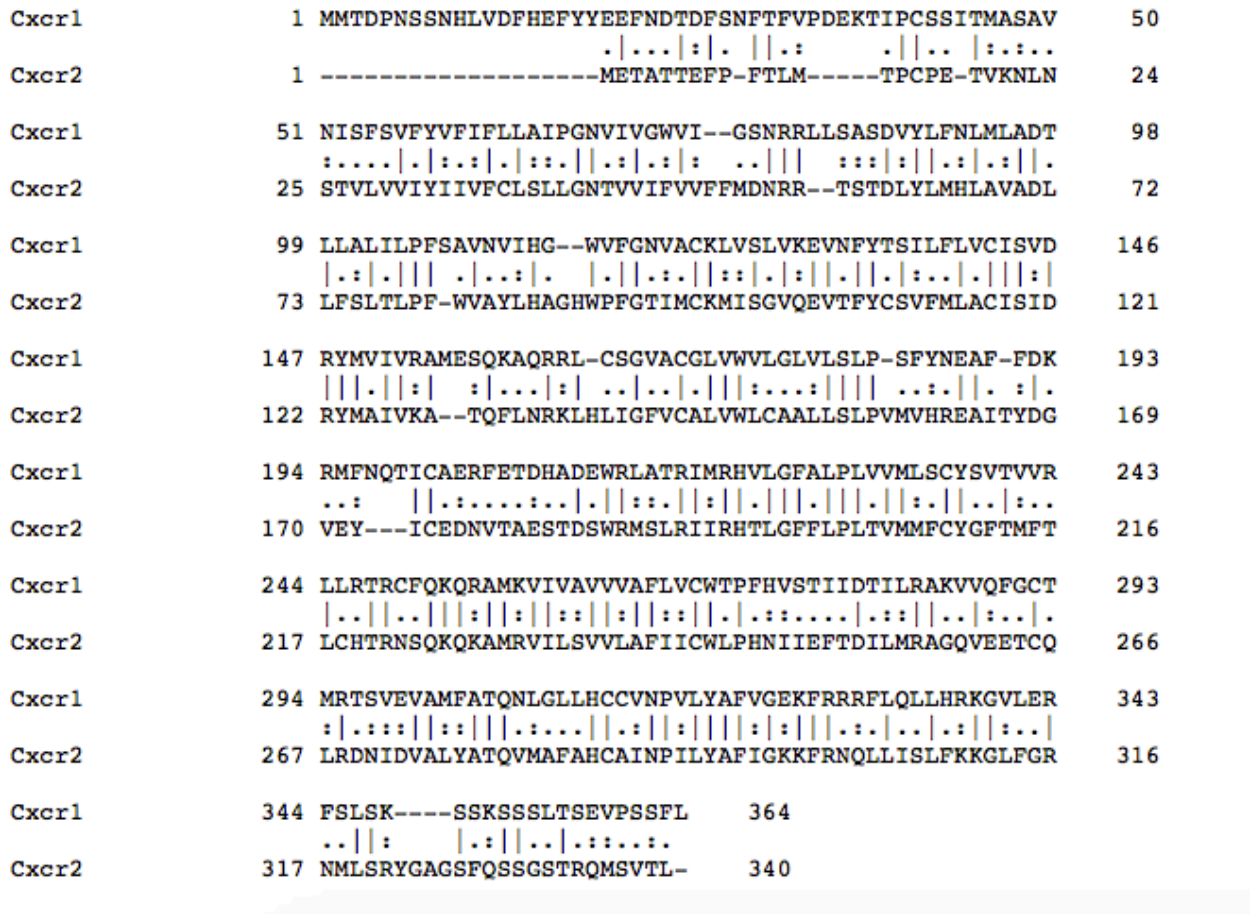


**Figure 1.4. Cxcr1 and Cxcr2 protein alignment.** Pairwise Sequence Alignment using EMBOSS needle[118].


**Figure 1.5. Human CXCR1 and zebrafish Cxcr1 protein alignment.** Pairwise Sequence Alignment using EMBOSS needle[118].

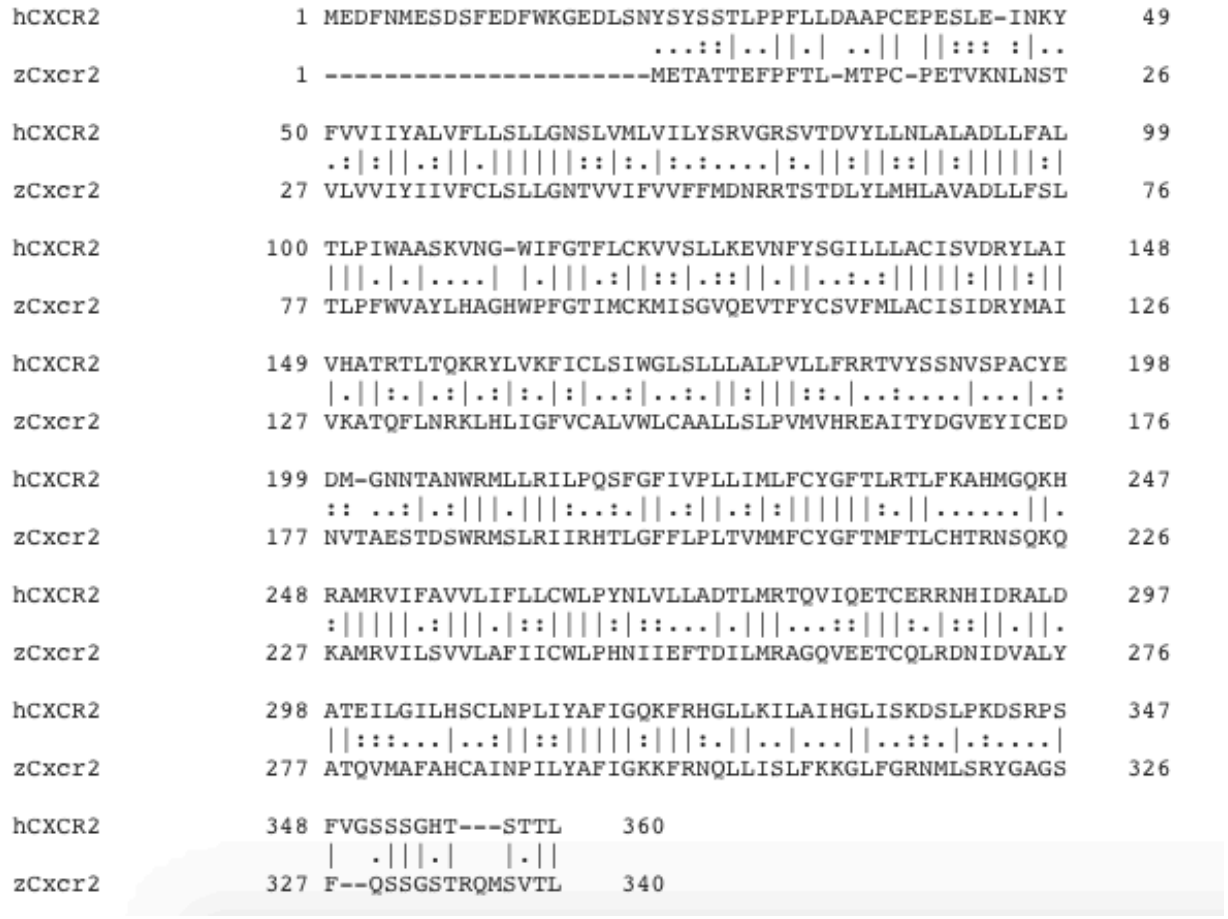


**Figure 1.6. Human CXCR2 and zebrafish Cxcr2 protein alignment.** Pairwise Sequence Alignment using EMBOSS needle[118].

## Functional role of Cxcr1 and Cxcr2 signalling

To date, studies investigating the functional role of Cxcr1 and Cxcr2 in zebrafish have primarily utilised morpholino knockdown or pharmacological inhibition approaches. Morpholino knockdown of Cxcr2, but not Cxcr1, reduced the number of neutrophils recruited to a *P. aeruginosa* PAK strain otic infection[124] and to Cxcl8a that was injected into the otic cavity of zebrafish larvae, suggesting that Cxcr2 specifically promotes neutrophil recruitment in these settings. Treatment with SB22005, an inhibitor of human CXCR2, suppressed neutrophil accumulation around Cxcl8a-secreting transplants[72] and to PAK otic infections[124]. This could provide evidence that recruitment to Cxcl8a depends on Cxcr2 signalling, assuming the SB22005 specifically inhibits Cxcr2. Interestingly, in the same model Cxcr2 signalling was shown to promote long range recruitment of cells from the CHT to distal infection sites[124]. Here, using neutrophils labelled with photo-convertible Dendra2 protein, CHT-resident neutrophils were photo-converted and the number of converted cells that reached a PAK ear infection quantified. SB225002 treatment and injection of Cxcr2 targeting MO reduced the number of photo-converted neutrophils recruited to the PAK-infected ear. Such long-distance effects of Cxcl8a/Cxcr2 signalling are supported by data by Sarris et al. 2012, showing that a fluorescently labelled Cxcl8a-mCherry secreted in the head is visible on the vasculature as far as the CHT. This suggests Cxcl8a enters the blood and is presented on endothelial cells, enabling systemic responses.

# Subchapter 1.6: Thesis aim

The aim of this thesis is to investigate how receptor trafficking influences chemoattractant interpretation at inflammatory sites to generate specific migration behaviours. The chemoattractant CXCL8, which signals through CXCR1 and CXCR2, plays an important role in neutrophil recruitment to target sites and thus represents an attractive model to address this question. Importantly, homologues of CXCL8, CXCR1 and CXCR2 have been identified in the zebrafish. This, together with the transparency of the zebrafish model and its amenability to genetic manipulation, makes the zebrafish an ideal model system to investigate how chemokine receptor dynamics act to influence interstitial migration behaviour *in vivo.*

# Chapter 2: Methods

## Zebrafish maintenance and husbandry

Zebrafish were maintained in accordance with UK Home Office regulations, UK Animals (Scientific Procedures) Act 1986. At the Wellcome Sanger Institute, zebrafish were maintained under project licence 70/7606, which was reviewed by the Wellcome Trust Sanger Institute Ethical Review Committee. At the University of Cambridge (Department of Physiology, Development and Neuroscience) zebrafish were maintained under project licence 70/8255, which was reviewed by the University Biomedical Services Committee. Zebrafish were bred and maintained under standard conditions at 28.5 ±0.5 °C on a 14 hr light: 10 hr dark cycle. Embryos were collected from natural spawnings at 4-5 hours post-fertilisation (hpf) and thereafter kept in a temperature controlled incubator at 28 °C. Embryos were grown at 28 °C in E3 medium (5mM NaCl, 0.17mM KCl, 0.33 mM $CaCl_2$, 0.33mM $Mg_2SO_4$, 5 mM HEPES), bleached as described in the Zebrafish Book[125] and then kept in E3 medium supplemented with 0.3 µg/ml of methylene blue and 0.003% 1-phenyl-2-thiourea (Sigma-Aldrich) to prevent melanin synthesis. For live-imaging of neutrophils expressing fluorescent receptors, methylene blue was omitted from E3 medium to minimise tissue autofluorescence.

## Generation and screening of *cxcr1* and *cxcr2* knockout zebrafish lines

Zebrafish carrying the mutant alleles *cxcr1*$^{sa14414}$ (*cxcr1* is otherwise annotated as *si:ch73-54b5.2)* and *cxcr2*$^{sa6118}$ were generated in the Zebrafish Mutation Project and subsequently maintained at the Wellcome Trust Sanger Institute through natural matings and *in vitro* fertilisation using frozen sperm as previously published[126]. Heterozygous *cxcr1*$^{sa14414}$ (*cxcr1*$^{+/-}$) and *cxcr2*$^{sa6118}$ (*cxcr2*$^{+/-}$) embryos were transferred to University of Cambridge (PDN) for further screening and maintenance. For genotyping, *cxcr1*$^{sa14414}$ and *cxcr2*$^{sa6118}$ fish were anaesthetised in fish water containing 200 µg/ml tricaine and tissue samples were obtained via fin clipping. DNA was extracted using a ThermoScientific Phire Tissue Direct PCR Master Mix. Fish were genotyped using KASP genotyping chemistry[126], using two allele-specific primers and a common reverse primer synthesised by LGC. For *cxcr1*$^{sa14414}$ primers were as follows, primer_alleleFAM: AGTGAGAGCACTAAACCCAAAACC, primer_alleleHEX: CAGTGAGAGCACTAAACCCAAAACT, primer_common:

GTGGAGTCGCKTGCGGATTAGTTT. For *cxcr2*$^{sa6118}$, primers were as follows, primer_alleleFAM: ATCTGATTGGGTTTGTGTGTGCGTT, primer_alleleHEX: ATCTGATTGGGTTTGTGTGTGCGTA, primer_common: GGTGCACCATAACCGGAAGAGATAA. KASP genotyping assays were conducted according to the manufacturer's instructions (https://www.lgcgroup.com/products/kasp-genotyping-chemistry/#.W036CxjMzXQ). Briefly, 100 ng samples of extracted DNA were loaded onto a 384-well PCR plate and left to dry overnight. KASP assays were assembled as follows: 2.5 µl, 0.07 µl primer mix and 2.43 µl water. Plates were read on a Roche LC480 LightCycler VII and genotypes were assigned to samples using cluster analysis. Fish screened positive for the desired mutation were outcrossed to a Tg(*mpx:GFP)*$^{i114}$ transgenic line[127] in order to visualize neutrophils during microscopy. Outcrosses were repeated to progressively remove additional mutations carried by the *cxcr1* and *cxcr2* mutant fish, followed by incrosses to generate 'clean' Tg(*mpx*:GFP)$^{i114}$; *cxcr1*$^{sa14414/sa14414}$ and Tg(*mpx:GFP)*$^{i114}$; *cxcr2*$^{sa6118/sa6118}$ homozygous knockout lines. Homozygous *cxcr1*$^{-/-}$ and *cxcr2*$^{-/-}$ mutant fish lines with non-fluorescent neutrophils (screened negative for GFP during the crossing process) were used for generating rescue lines.

## DNA constructs

cDNA for zebrafish Cxcr1 (Entrez ID: 797181; Ensembl gene: ENSDARG00000052088) and Cxcr2 (Entrez ID: 796724; Ensembl gene: ENSDARG00000054975) was fused to a fluorescent timer cassette as described in Dona et al. 2013[128] and cloned into a pCS2+ vector for mRNA production or a Tol2 backbone vector carrying a Lysozyme C promoter[129] using KpnI-MfeI sites. pCS2$^{+}$-ECFP was made by overlapping PCR. pCMV-Cxcl8a-mCherry was cloned previously by overlapping PCR[120]. mCFP (membrane ECFP) was amplified by PCR from the Clontech vector 'p-ECFP-Mem' (cat no: 6918-1) and cloned into the Tol2-lyz vector using KpnI-MfeI sites. For generation of mutant receptors, the Cxcr1 or Cxcr2 ORF was inputted into TMpred. a programme which predicts membrane-spanning regions of proteins based on statistical analysis of the TMbase database of naturally occurring transmembrane proteins. The C-terminus was taken as the sequence following the final of the seven predicted transmembrane domains. The Cxcr1 C-terminus was thus assigned as the final 42 amino acid region (324→ 364 inclusive) (see C-terminus sequence). The C-terminus of Cxcr2 was assigned as the 45 amino acid region (297→340). All mutant receptors (excluding Cxcr2-ala) were generated by overlapping PCR. Overlapping primers used for Cxcr1-

trunc mutant: Fw: GGAGAGAAGTTCAGACGGAGGGACCCAGCTTTCTTGTACAAAGTGG and Rv: CCACTTTGTACAAGAAAGCTGGGTCCCTCCGTCTGAACTTCTCTCC. Overlapping primers used for Cxcr1-ser mutant: Fw: AGTTGCTCCACAGGAAGGGAGTTCTGGAGCGGTTCGACCCAGCTTTCTTGTACAAAG TGG and Rv: CCACTTTGTACAAGAAAGCTGGGTCGAACCGCTCCAGAACTCCCTT. Overlapping primers used for Cxcr1-ala mutant: Fw: CGCAGAGGTCCCTGCGGCGTTTCTGGACCCAGCTTTCTTGTACAAAGTGG and Rv: CAGAAACGCCGCAGGGACCTCTGCGGTCAGAGCAGCTGCCTTGGCGGCTTTAGCAA GCGCGAACCGCTCCAGAACTCCCTT. Overlapping primers used for Cxcr1-chim-FT mutant: Fw: CGTCGGAGAGAAGTTCAGACGGAGGCGTAACCAGTTGCTGATTTCTCTC and Rv: GAGAGAAATCAGCAACTGGTTACGCCTCCGTCTGAACTTCTCTCC. Overlapping primers used for Cxcr2-chim mutant: Fw: CCATCCTGTACGCCTTCATCGGGAAGAAATTTTTTCTGCAGTTGCTCCACAGGAAGG GAG and Rv: CTCCCTTCCTGTGGAGCAACTGCAGAAAAAATTTCTTCCCGATGAAGGCGTACAGGA TGG. The Cxcr2-ala mutant was made by synthesis of the segment carrying the mutations (Genewiz) and this segment was cloned into the pCS2$^{+}$-Cxcr2-FT construct using NheI and Bsu36I and further subcloned into the Tol2-lyz vector using Kpn-Bsu36I. Some of the mutant constructs were cloned into pCS2$^{+}$ vector for mRNA production and all mutant constructs were cloned into the Tol2-Lyz backbone vector for transgenesis using the Fw GGGGGGGGGTACCGCCACCATGATGACTGATCCAAACAGCTCTAA and Rv GGGGGGGCAATTGTCTAGAGGCTCGAGTTAACCGGTGCTGCCCTTG. A pCS2$^{+}$ plasmid containing Cxcl8a cDNA (XM_001342570)[120] was used for *in vitro* transcription.

## Chemokine and chemokine receptor internalisation assays in early embryos

For mRNA production, the pCS2$^{+}$ plasmids containing the Cxcr1/2-wt, Cxcr1-trunc, Cxcr1-ser, Cxcr1-ala, mCFP and Cxcl8a constructs were linearised and transcribed with an SP6 message machine kit (Ambion) followed by polyA addition (Ambion). 100 pg of receptor-FT or mCFP was injected into the cell body of one-cell stage embryos. In some cases, 150 pg (or 30 pg for Cxcr1-ala) Cxcl8a mRNA or 30 pg Cxcl8-ECFP mRNA was co-injected. Injected embryos were stored in petri dishes at 28 °C and imaged at about 8 hpf. For imaging, embryos were de-chorionated

using forceps and mounted on glass bottomed microwell dishes (MatTek) in 0.8% low melting point agarose covered with 2 ml E3. Embryos were imaged on an inverted Olympus Fluoview FV1000 confocal microscope and z-stacks were acquired using a 40x/1.25 NA silicon objective (Olympus). The mCFP, sfGFP and tagRFP were visualised using 480 nm, 488 nm and 559 nm excitation wavelengths respectively. Temperature was maintained at 28 °C throughout experiments using a digital temperature regulator (Biotronix Temperature Controller). Internalisation of receptors in gastrulating embryos was quantified in Fiji. For analysis, a binary membrane mask was made using the cyan channel of the mCFP control by thresholding. This mask was then applied to all three channels (sfGFP, tagRFP and mCFP) using the image calculator. Ratios of masked images were normalised to the corresponding ratios of the unmasked images. This normalised variation in expression levels across different embryos and allowed pooling of ratios from different samples.

## Generation of transgenic zebrafish lines

1 nl solution containing 12.5 ng/µl Tol2 DNA construct and 17.5 ng/µl transposase mRNA was injected into the cell body of one-cell stage embryos (either in wild type AB embryos or *cxcr1*$^{-/-}$ or *cxcr2*$^{-/-}$ (GFP-negative) embryos for rescue lines). Transposase mRNA was synthesised from pCS2-TP[130] by in vitro transcription (SP6 message machine, Ambion). Injected embryos were stored at 28 °C until 5 dpf and thereafter were raised in the fish nursery according to standard rearing protocols. At 3 months old, G0 Tg(*lyz*:Cxcr1-FT) and Tg(*lyz*:Cxcr2-FT) fish were outcrossed to a wildtype (TL) line in order to screen for germline transgenesis. G0 Tg(*lyz*:Cxcr1-FT) and Tg(*lyz*:Cxcr2-FT) and all mutant lines were outcrossed to knockout lines. Offspring were kept as separate sub-strains due to differences in expression of the transgenic cassette used. F0 to F3 embryos were used for live imaging.

## Ventral fin wounds

Larvae at 3 dpf were anaesthetised with 200 µg/ml tricaine and wounded in the ventral fin using a sterile surgical scalpel blade[124] (Swann-Morton, 23). In some cases, 30 nM of LTB4 (Sigma) was added in E3 for 30 minutes, transferred to E3 medium (supplemented with tricaine) and wounded using a sterile blade as previously described[124]. In some cases, 1-2 nl of 1 mM solution of YM-

254890 (Wako Chemicals) or FR900359 (prepared as previously described[131]) or equivalent DMSO dilution was injected in the duct of Cuvier 10 min prior to wounding

## Bacterial ear infections

5 µl of CFP-or Crimson-expressing fluorescent K12 E.coli were cultured overnight in 2 ml of LB broth (Sigma-Aldrich) supplemented with 100µg/ml ampicillin at 37 °C. 100 µl of the overnight bacterial culture was pelleted by centrifugation (5000 rpm for 7 minutes). The pellet was re-suspended in 40 µl sterile PBS and 10 µl phenol red and kept on ice. 3 dpf larvae were anaesthetised by immersion in 200 µg/ml tricaine (Sigma) and positioned with their ventral side against the vertical walls of an injection plate. Larvae were then injected into the left otic cavity with CFP- or crimson- marked E.coli at a pressure of 20 p.s.i and an injection time of 20 ms.

## Morpholino knockdown

A previously validated morpholino targeting the ATG region of cxcr2 (ACTCTGTAGTAGCAGTTTCCATGTT) was injected into the yolk of *cxcr1*$^{-/-}$/ Tg(*mpx:GFP)*$^{i114}$ embryos (3nl of 100 µM solution). For Cxcl8a knockdown, morpholino oligonucleotides (Gene Tools) were injected in the yolk of one-cell stage embryos. A *cxcl8a* splice-blocking morpholino 5'-ATTTATGCTTACTTGACAATGATC-3' (12 ng) was used in combination with a *cxcl8a* translation-blocking morpholino 5'-TTTGCTGGTCATTTTGCCTAAGTGA-3' (9 ng)[72]. For genotyping the splice-blocking morpholinos (genotyping conducted by Hazel Walker), RNA was prepared from pools of 10 injected or non-injected 3 dpf larvae using the RNeasy Mini Kit (Qiagen). cDNA was prepared using M-MLV reverse transcriptase (Invitrogen) and used for RT-PCR. The following primers were used: *cxcl8a* forward: 5'-GCCACCTTGATGACAACTGGA-3', *cxcl8a* reverse: 5'-TGTCTGACGTATGAACATCATCAAAC–3'. The following primers were used for the housekeeping gene: *ef1a* forward: 5- GCTGATCGTTGGAGTCAACA-3', *ef1a* reverse: 5'-ACAGACTTGACCTCAGTGGT-3'. For comparison of *cxcl8a* expression levels in wounded versus unwounded larvae, 3dpf larvae were wounded in the ventral fin and RNA was extracted from pools of 10 larvae at 30 minutes and 1.5 hours post wound. The following primers were used for RT-PCR: *cxcl8a* forward: 5'- ATGAGCTTGAGAGGTCTGGC-3' *cxcl8a* reverse: 5'- GTGATCCGGGCATTCATGG.

## Live imaging of zebrafish neutrophils

Wounded fish were mounted immediately after ventral fin wound onto a glass-bottom plate in 1% low melting agarose (Invitrogen) or a custom-built coverslip chamber (for when using an upright scope). Agarose-embedded embryos were covered with 2 ml E3 medium (supplemented with tricaine) and imaged either on i) an inverted PerkinElmer Spinning Disk UltraVIEW ERS, Olympus IX81 spinning disk confocal microscope with a 20x/0.45 NA air objective (Olympus), or 30x/ NA silicon (Olympus) or 40x/1.25 NA silicon objective (Olympus) and 405nm for CFP excitation, 488 nm for GFP excitation and 561 nm for tagRFP or mCherry excitation, or ii) an upright Nikon E1000 microscope coupled to a Yokogawa CSU10 spinning disc confocal scanner unit with a 20x/0.75 NA air objective (Nikon) or 10x/0.5 NA air objective (Nikon) and illuminated using a Spectral Applied Research LMM5 laser module (491 nm for GFP excitation; 561 nm for tagRFP or mCherry excitation). Confocal stacks using a 2 μm z spacing were acquired every 30 sec. Laser wounding of parabiotic fish and live imaging was performed on a two-photon scanning microscope (LaVision Biotec TriM Scope II). A tunable ultrafast laser (Insight DeepSee, SpectraPhysics) was tuned to 930 nm and the laser power adjusted to approximately 500 mW. A square region of interest (ROI) of ~40 μm in width was defined in one focal plane followed by single laser scan across the ROI at a pixel spacing of 240 nm and dwell time of 13 μs. Confocal stacks were acquired using a 25x/1.05 NA water-dipping lens. GFP was imaged with 930 nm and DsRed was imaged with a 1040 nm line.

## *In vivo* Cxcl8a response assay

HEK293T cells were cultured in DMEM (Invitrogen) containing 10% FBS (Gibco ThermoFisher Scientific) and 1% Penicillin/Streptomycin (Sigma). HEK293T cells were transfected with Cxcl8a-mcherry using Lipofectamine-2000 (Invitrogen). Transfected cells were incubated at 37 $^0$C (with 5% $CO_2$) overnight, harvested the following morning and re-suspended in DPBS (Invitrogen) at a density of 30x10$^6$/ml. Cells were transplanted above the yolk as previously described[8] into 48 hpf *wildtype*/Tg(*mpx:GFP)*$^{i114}$, *cxcr1*$^{-/-}$/ Tg(*mpx:GFP)*$^{i114}$ or *cxcr2*$^{-/-}$/ Tg(*mpx:GFP)*$^{i114}$ larave. Transplanted larvae were incubated in E3 medium containing PTU (1-phenyl-2-thiouria) at 34 $^0$C overnight. 18-24 hr post-transplantation, larvae were used for imaging and temperature was maintained at 32-35 $^0$C using a built heated chamber (for the upright scope) or a heated stage (for the inverted scope). The on/off analysis was done by measuring the number of neutrophils in

contact with a Cxcl8a-secreting HEK293 cell and divided by the total number of cells in the field of view averaged across three time points.

## Optogenetic chemokine release assay

HEK293T cells were transfected with Cxcl8a-YFP-2xUVR8 and were incubated at 37 $^{0}$C (with 5% C02) overnight, harvested and transplanted into 2 dpf larvae as described above. Transplanted larvae were kept overnight at 32 $^{0}$C in E3 medium. Larvae were mounted on 35 mm dishes in 1% low melting point agarose covered with E3 medium supplemented with 0.16 mg/mL tricaine (sigma) and imaged at approximately 15 hours post-transplantation. For UVR8 photo-activation larvae were exposed to a UVB source at a distance of 7 cm for 60 seconds.

## Generation of parabiotic larvae

Tg(*lyz*:Dsred)$^{nz50}$ were crossed to an Tg(*Ath5*:gapGFP)[132] transgenic line in which GFP is expressed in the retina. This enabled identification of wild type fish in the parabiosis embryos. Tg(*mpx*:gfp)/*cxcr1*$^{-/-}$ embryos were fused to Tg(*lyz*:Dsred)$^{nz50}$ as previously described[133]. Briefly, embryos were manually dechorionated at the 256-cell stage using forceps and transferred to 4% methylcellulose covered with high-calcium Ringers' containing antibiotics (50 U/ml penicillin-streptomycin, 50 U/ml ampicillin, 0.5 ug/ml kanamycin and 0.5 ug/ml gentamicin). Two embryos of different genetic background were fused by mechanically detaching some cells of the blastulae using the tip of a glass pipette and the wounds were pressed together to promote successful joining. Fusions were performed between the 512-cell-30% epiboly stage. Fused embryos were incubated overnight at 28 $^{0}$C. The following morning the medium was replaced with embryo water containing PTU. 3 dpf parabiotic larvae that shared the circulation were mounted for laser wounding and imaging (see live-imaging methods section).

## Sudan black staining

*Wildtype*/Tg(*mpx*:GFP), *cxcr1*$^{-/-}$/Tg(*mpx*:GFP) and *cxcr2*$^{-/-}$/Tg(*mpx*:GFP) 3 dpf larvae were wounded in the ventral fin with a scalpel blade and fixed 20-24 hours later in 1ml of 4% ethanol-free formaldehyde (Thermoscientific) in phosphate-buffered saline (PBS; Sigma-Aldrich) overnight at 4 $^{o}$C with agitation. Fixed larvae were rinsed in PBT (PBS with 0.1% Tween-20; Sigma-Aldrich) twice for 5 minutes and incubated in 1 ml Sudan Black (Sigma-Aldrich) for 15

minutes. Following staining, larvae were washed in 70% ethanol for several hours and passaged into 30% ethanol overnight at 4 $^{o}$C with agitation. Larvae were washed in PBT for ten minutes, passaged into increasing concentrations of glycerol and stored in 80% glycerol at 4 $^{o}$C.

## Statistics

All error bars indicate S.E.M (Standard Error of the Mean). All *p* values were calculated with two-tailed statistical tests and 95% confidence intervals. *t*-test (pairwise comparisons) and one-way ANOVA (multiple group comparisons) with Dunnet's post-test were performed after distribution was tested for normality, otherwise non-parametric tests were performed (Mann-Whitney for two-way comparisons and Kruskal-Wallis with Dunn's post-test for multiple comparisons). Statistical tests were performed in Prism v8.0.2 (GraphPad Software Inc., La Jolla, CA). The statistical test and the *n* number are indicated in the figure legends. The error bars show S.E.M. either across individual embryos (i.e. analysis of neutrophil recruitment, cluster size, net reverse traffic) or individual neutrophils pooled from different embryos (i.e. track straightness, which is a track-based analysis, or speed versus distance or orientation, which are step-based analyses). Live imaging experiments were acquired in minimum two independent imaging sessions unless otherwise indicated.

## Automated image analysis (methods written and conducted by Antonios Georgantzoglou)

Please note that the 'Automated Image analysis' methods below were both written and conducted by Anotonios Georgantzoglou. These methods are included for clarity.

### *Extraction of Neutrophil Trajectories*

Analysis of neutrophil trajectories was performed in Imaris v8.2 (Bitplane AG, Zürich, Switzerland) on 2D maximum intensity projections of the 4D time-lapse movies. Unless otherwise indicated, analysed trajectories were extracted from the whole fin area to account for interstitial movement (movement in the CHT was excluded). A track duration threshold of 3 time-points was defined to exclude short-lived tracks. Manual track corrections were also applied where needed. Instantaneous neutrophil coordinates over time (*x,y,t*) were exported into Microsoft Excel 2016 spreadsheets files (Microsoft Corporation, Redmond, WA).

***Definition of Occupied Wound Area, Forward and Reverse Trajectories***

Exported Excel files were imported into MATLAB R2018b (The MathWorks, Inc., Natick, MA) using a custom-written script, for neutrophil trajectory analysis. For each experimental image dataset, the area of the wound occupied by the neutrophil cluster (owa; occupied wound area) was defined by a set of manually selected points ($x,y$). To define the owa, we used a maximum intensity time projection of the movies, in which high-density neutrophil areas could be distinguished based on intensity levels. Separation of trajectories into forward and reverse segments was done as follows: for forward trajectory segments, the first time point of the trajectory segment was defined as the first time point the neutrophil was detected in the fin and the last time point of the trajectory was defined as the time point before entering the owa. For reverse trajectory segments, the first time-point was defined as the last time-point the neutrophil was detected within the owa, whereas the last time-point was taken as the last time-point it was detected in the fin. In speed-distance and speed-cosine plots, forward tracks also included tracks that did not intersect with the owa, but whose direction of movement could be defined as forward, based on the end position of the track being located closer to the owa than the start position. In the 'net reverse traffic' plots, cells not intersecting the owa were not included, to exclude contribution of tracks that did not pass by the owa. For track straightness plots, no classification on forward/reverse tracks was performed. Data were binned using custom-written scripts.

***Calculation of speed in relation to distance from owa***

For analysis of speed versus distance from the owa, custom MATLAB scripts were modified from previously used scripts[72]. The instantaneous speed was calculated based on the distance travelled by a neutrophil between two successive time-points The distance from owa was defined as the distance between the position of a neutrophil centroid (x,y coordinates) and the nearest point of the owa perimeter.

***Calculation of speed in relation to orientation from the owa***

For analysis of speed versus orientation in relation to the owa, instantaneous speed was calculated as above. The angle $\theta$ was calculated as the angle between the vector of the neutrophil instantaneous speed and the vector that connects the neutrophil initial position with the nearest point in the owa perimeter. The migration orientation effect was calculated using the cosine of angle $\theta$ within a

range of 50 μm from the owa perimeter. A value of cosine $\theta$ closer to +1 shows directed migration towards the wound whereas a value closer to -1 shows migration away from the wound.

***Calculation of track straightness***

The track straightness was calculated as the distance that a neutrophil travelled between the first and last time-point of its trajectory, divided by the cumulative distance travelled in the same time-window, using a MATLAB custom-written script. A track straightness value closer to 1 showed a direct migration while a track straightness value closer to 0 showed an arbitrary motion. For each track, data from neutrophil coordinates corresponding to positions inside a range of 50μm were included. Tracks of total length of less than 10 μm were eliminated to exclude neutrophils that did not show sufficient movement to calculate representative straightness. Data were binned using custom-written scripts.

***Calculation of Net Reverse Traffic***

The net traffic was calculated as the number of reverse neutrophil tracks, divided by the number of forward migrating neutrophil tracks. The higher the value the higher the net reverse traffic.

***Segmentation of neutrophils for receptor internalisation analysis***

Analysis of Cxcr1 or Cxcr2 receptor internalisation was performed in MATLAB using custom-written scripts. Neutrophil or cluster outline definition was achieved with active contours using MATLAB's built-in function for the Chan-Vese method[134]. To define the core of the neutrophil, a 2D point *(x,y)* inside each neutrophil was selected manually and expanded for 5-15 pixels in each direction (*-x,+x,-y,+y*). The active contour algorithm expanded this core until the neutrophil boundary. For surface segmentation, all pixels inside the contour were included to define a binary surface mask that was applied on the sfGFP channel. In this segmentation process, a threshold on the size of objects (50 pixels) was applied to eliminate small false detected objects. For contour-based membrane segmentation, the pixels comprising the outline of each neutrophil or cluster were used to define a binary membrane mask that was applied on the mCFP and sfGFP channels. Segmentation was carried out in a representative snapshot of neutrophil migration at around 1-1.5 hpw, indicating the overall internalisation level after neutrophils clustered. Only cells that were entirely visible (and not partially) were segmented. Overly dim (not enough signal) or overly bright

cells (saturated) with unreliable intracellular signal distribution were not segmented for these analyses.

***Computation of contrast as a measure of receptor internalisation***

Neutrophil contrast, reflecting intracellular heterogeneity in signal distribution, was calculated in segmented neutrophils, using MATLAB's built-in functions. The intensity matrix of each surface-segmented neutrophil was transformed into a grey-level co-occurrence matrix[135]. The latter represents the intensity difference between neighbouring pixels. Contrast was calculated as the difference in intensity-relationships, based on the following equation (https://uk.mathworks.com/help/ images/ref/graycoprops.html ):

$$C = \sum_{i,j=0}^{N-1} |i-j|^2 \, p(i,j)$$

where *p(i,j)* is the image co-occurrence matrix *and i, j* are the co-occurrence matrix coordinates.

Contrast values of neutrophils at the wound were normalised to the contrast values of neutrophils in the CHT of the same time-point to account for image intensity fluctuations across embryos acquired with independent imaging settings. For datasets in Fig. 3.14, normalisation with the contrast of cells in the CHT was not applicable as neutrophils were induced to exit the CHT prior to imaging. In this case, the contrast of neutrophils was normalised to the maximum contrast value per individual embryo. For plotting the contrast over distance in Fig 3.14, the distance of the neutrophil centroid from the nearest point of the wound margin was calculated.

***Quantification of Cxcl8a chemokine uptake***

For calculation of Cxcl8a uptake, GFP-positive neutrophils were segmented based on active contours, as described above. The resulting GFP binary mask was applied on the mCherry images to obtain the intracellular mCherry signal. Neutrophil mean intensity was calculated per cell and normalised with the mean intensity of a 150×150 pixels of the transplant. This was to account for variation in levels of mCherry expression in the transplanted cells across independent embryos.

***Calculation of Neutrophil Cluster Size***

Neutrophil cluster size at wound was calculated in Imaris. Neutrophils were tracked as a surface, rather than as neutrophil centroids, within a square area approximating the owa. The area of segmented objects (neutrophils) was computed in Imaris and imported in MATLAB for plotting. Surfaces with area below $60\mu m^2$ were excluded to minimise artefacts from erroneous surface detection. Cluster size per embryo was calculated as an average across an indicated time-window.

# Chapter 3: Cxcr1 and Cxcr2 show differential trafficking dynamics in response to endogenous gradients *in vivo*

## 3. Introduction

Neutrophils are the first immune cells to be recruited to inflammatory sites, where they accumulate in large numbers to execute their effector function[1]. To reach target sites, neutrophils undertake an extensive migratory journey, a process which involves crossing multiple endothelial barriers and navigating through the complex 3D environment of the interstitial tissue. Neutrophil recruitment to inflammatory sites is guided by gradients of chemoattractants, often in the form of secreted molecules that are recognised by G-protein coupled receptors (GPCRs). GPCR signaling activates effectors of cytoskeletal dynamics that drive directed migration (chemotaxis). Whilst the early stages of neutrophil migration to target sites are well characterised, the mechanisms governing interstitial migration remain far less understood. Following arrival at the target site, neutrophils may stop and form focalised clusters of accumulated cells. On the other hand, neutrophils may remain motile displaying a more exploratory-like, bi-directional migration behaviour[100]. Recently, neutrophils have been shown to actively migrate through the interstitial tissue away from the target site in a process termed reverse interstitial migration (rIM)[26,73]. These differential post-arrival behaviours play an important role in dictating the outcome of an immune response. For example, focalised accumulation can act to concentrate local effector responses, but in excess can be detrimental leading to chronic inflammation (e.g. through release of toxic molecules such as ROS, granule contents or recruitment of additional immune cells)[1]. Focalised accumulation occurs at the expense of exploration and can thus limit detection of alternative ligands, compromising immunosurveillance and resolution via reverse migration. Thus, there is an important trade-off between focalisation and bi-directional exploration. However, the mechanisms that drive these opposing migration behaviours remain unknown.

A potential mechanism that could drive these opposing migration behaviours is the duration of GPCR signalling which is influenced by receptor residency time at the plasma membrane. Following ligand binding, GPCRs have several possible trafficking fates that can influence

residency time and thus sensitivity to ligand. For example, phosphorylated receptors can be sustained at the cell surface, promoting re-sensitisation to ligand[136]. On the other hand, phosphorylated receptors can be internalised and may be targeted to lysosomes and degraded. This reduces receptor availability at the cell surface and de-sensitizes the cell to subsequent signalling events. Alternatively, following internalisation, receptors may be recycled back to the surface. Receptor recycling acts to replenish receptor levels at the cell surface and re-sensitises the membrane. Thus, by dictating the number of receptors available for signalling events, receptor trafficking dynamics play an important role in modulating the amplitude and duration of signal. This can have important behavioural consequences on cell migration. For example, *in vitro* evidence suggests receptor down-regulation may act to limit signal range and prevent continued neutrophil migration along a gradient[82]. The trafficking patterns of chemoattractant receptors have not been characterised *in vivo* and thus how they influence neutrophil migration in the complex milieu of the interstitial tissue remains unclear.

My aim in this chapter was to dissect the trafficking dynamics of Cxcr1 and Cxcr2 in response to Cxcl8a and endogenous gradients at inflammatory sites.

# 3. Objectives

- To visualise Cxcr1 and Cxcr2 via generation of fluorescent timer (FT) constructs of each receptor
- Assess Cxcr1-FT and Cxcr2-FT responses to Cxcl8a in gastrulating zebrafish embryos
- Generate new zebrafish transgenic lines in which neutrophils express Cxcr1-FT and Cxcr2-FT
- Assess Cxcr1-FT and Cxcr2-FT dynamics during neutrophil migration to endogenous gradients generated at infection and wound sites.

**Notes on contributions:**

Antonios Georgantzoglou (A.G) conducted most of the image analysis presented in the results section of this chapter. His contribution is noted throughout the text and figure legends. Any experimental and/or analysis contributions that were made by Hazel Walker (H.W) or Milka Sarris (M.S) are also referred to in the text and figure legends.

# 3. Results

### Generation of fluorescent timer construct to visualise Cxcr1 and Cxcr2

To visualise Cxcr1 and Cxcr2 receptor trafficking, I first fluorescently labelled both receptors. Here, instead of using a single fluorophore, I used a fluorescent timer (FT) approach[128] (Fig. 3.1). I tagged each receptor with a fast maturing (<10 minutes) superfolderGFP (sfGFP) in tandem with a slower maturing (>1.5hours), and therefore slower to fluoresce, tagRFP[137]. Owing to the different fluorescent properties of these two fluorescent proteins, newly synthesised receptors first fluoresce green and become progressively red with time. Using a fluorescent timer approach therefore not only visually labels the receptor, but also provides an additional layer of information relating to protein age. Thus, this approach can provide further insight into the rate of turnover and receptor trafficking. For example, the level of green ('new') or red ('old') receptor at the surface would be indicative of the receptor residency time at the membrane. Furthermore, given that sfGFP is quenched in acidic environments and tagRFP remains stable, this approach allows monitoring of a broad range of receptor fates.

### Cxcr1 is internalised in response to Cxcl8a

As a preliminary experiment, to test receptor responses to Cxcl8a, I first expressed the fluorescent timer receptors in gastrulating zebrafish embryos. These early stage embryos provide an ideal sample to visualise the membrane distribution of the receptors and as experiments can be conducted in a single day offer a relatively quick method to gain a first insight into receptor responses. I first assessed the response of Cxcr1-FT to Cxcl8a. For this, I injected one-cell stage zebrafish embryos with Cxcr1-FT mRNA alongside mRNA for a membrane marker (mCFP). I imaged receptor distributions via confocal microscopy at approximately 8 hours post-injection. In the absence of Cxcl8a, both green ('new') and red ('old') Cxcr1-FT receptors were visible on the membrane, showing a comparable distribution to that of the mCFP membrane marker (Fig. 3.2, upper panels). However, when I co-injected Cxcl8a mRNA, Cxcr1-FT showed extensive internalisation with virtually no green or red receptor visible on the membrane (Fig. 3.2, lower panels). Instead, both green and red receptors accumulated in intracellular vesicles. As expected, the mCFP membrane marker remained on the membrane regardless of whether Cxcl8a was expressed. Subsequent quantification of Cxcr1-FT receptor levels normalised to the membrane marker confirmed significant levels of internalisation for Cxcr1-FT in the presence of Cxcl8a (Fig. 3.3).

**Cxcr2 is not internalised in response to Cxcl8a**

I next assessed Cxcr2-FT responses to Cxcl8a using the same above experimental approach. I injected one-cell stage embryos with Cxcr2-FT mRNA alongside mRNA for the membrane marker (membrane ECFP, hereafter referred to as mCFP). In the absence of Cxcl8a, Cxcr2-FT showed a membranous distribution with both green (new) and red (old) receptors visible on the membrane (Fig. 3.4, upper panels). When Cxcl8a mRNA was co-injected, Cxcr2-FT remained membranous, showing a similar distribution to the membrane marker (Fig. 3.4, lower panels). Subsequent quantification of receptor levels normalised to the membrane marker confirmed that Cxcr2 remains membranous in response to Cxcl8a (Fig. 3.5).

**Cxcr1 and Cxcr2 show rapid constitutive turnover in unchallenged neutrophils**

Having gained an insight into receptor responses in gastrulating embryos, the next step was to characterise receptor responses during neutrophil migration by expressing Cxcr1-FT and Cxcr2-FT constructs in zebrafish neutrophils. To this end, I utilised the Tol2 transposon system[130,138,139,140] to generate Tg(*lyz:*Cxcr1-FT) and Tg(*lyz:*Cxcr2-FT) transgenic zebrafish lines in which the FT-receptors are expressed under the neutrophil-specific Lyzozyme C promotor (Fig. 3.6a). As a control, I assessed 'steady state' receptor distributions in neutrophils of unchallenged Tg(*lyz*:Cxcr1-FT) and Tg(*lyz*:Cxcr2-FT) larvae. For this I conducted live-imaging of neutrophils randomly patrolling the interstitial tissue in the head (Fig. 3.6b). Interestingly, under steady state conditions neutrophils showed a relatively high constitutive turnover of both Cxcr1-FT and Cxcr2-FT, as reflected by predominantly green fluorescence at the plasma membrane (Fig. 3.6c). Although very little red receptor was visible on the membrane, red receptors, presumably targeted for degradation, accumulated in intracellular compartments. Given these results, for future experiments I explored ligand-induced receptor trafficking based on the rapid dynamics of the sfGFP-labelled receptor molecules.

**Cxcr1, but not Cxcr2, internalises in response to endogenous gradients at wound sites**

Having assessed receptor distributions under steady state conditions, I next investigated Cxcr1 and Cxcr2 receptor dynamics in neutrophils responding to endogenous gradients. I first assessed neutrophil receptor dynamics in a wound setting. To this end, I utilised a ventral fin wound assay in which an incision is made in the larval ventral fin at a site adjacent to the caudal hematopoietic

tissue (CHT)[124]. The CHT is a vascularised region that lies between the caudal artery and the caudal vein plexus and is the first site of definitive haematopoiesis in zebrafish (equivalent to the fetal liver in mammals). As such, the region is rich in neutrophils, providing a pool of neutrophils readily available for mobilisation[141]. The proximity of the CHT and ventral fin wound site confers the advantage of being able to image all stages of the inflammatory response (i.e. mobilisation, chemotaxis and post-arrival at the wound) in the same field of view. I wounded the ventral fin of Tg(*lyz:*cxcr1-FT) and Tg(*lyz:*cxcr2-FT) 3dpf larvae and imaged neutrophil and receptor responses at each stage of the migratory response via spinning disk microscopy (Fig. 3.7a). Cxcr1 underwent internalisation upon neutrophil mobilisation from the CHT (Fig 3.7b upper panels). Once in the ventral fin, neutrophils underwent chemotaxis and progressively further internalised Cxcr1 as they migrated to the wound (Fig 3.7b, lower panels). At the wound site, Cxcr1 displayed extensive internalisation (Fig. 3.8b-c, left panels). In contrast, Cxcr2 remained sustained at the cell membrane throughout the migratory response and as such only images taken at the wound site are shown (Fig. 3.8b-c right panels).

To facilitate quantification of receptor internalisation at wound sites, my aim was to utilise a neutrophil membrane marker to which Cxcr1-FT or Cxcr2-FT receptor levels on the membrane could be compared. For this, I generated a new Tg(*lyz:*mCFP) transgenic line in which neutrophils express membrane CFP under the lysozyme C promoter. I crossed Tg(*lyz:*Cxcr1-FT) to Tg(*lyz:*mCFP) fish and imaged neutrophils responding to a ventral fin wound. Quantification of receptor levels relative to the membrane marker were conducted by A.G. Using this method, neutrophil membranes were segmented based on the mCFP channel. As expected, cells in which Cxcr1-FT is down-regulated showed a lower ratio of sfGFP/mCFP. However, it was not always possible to segment the membrane of neutrophils in clustering cells. Thus, whilst mCFP is a useful for quantification of receptor internalisation in non-clustered regions this method of quantification does not facilitate measurement of internalisation in clustered regions. To overcome this, Cxcr1-FT internalisation was instead quantified by measuring differences in intensity of sfGFP across neighbouring pixels of surface-segmented neutrophils (analysis conducted by A.G). In this method, vesicular areas in which high intensity regions are next to low intensity background regions in cytosol would have ‘high contrast’. On the hand, non-vesicular regions of segmented neutrophils (i.e. with a membranous receptor distribution) would have ‘low contrast’. As an internal reference, the contrast was computed relative to cells in the CHT, that do not internalise receptor. This enabled

comparison across embryos with different intensity levels. Quantification of 'contrast' of sfGFP signal in neutrophils that had accumulated at the wound site confirmed that Cxcr1 but not Cxcr2 is internalised at wound sites (Fig. 3.8d).

**Cxcr1 internalisation is not due to unspecific membrane dynamics**

Whilst the membrane marker was not useful for quantification of internalisation in clustered cells it was able to confirm that the vesicles quantified in the previous 'contrast' analysis were not due to unspecific membrane dynamics as Cxcr1-FT sfGFP was visible as distinct green vesicles within the cell whilst the CFP marker remained membranous (Fig. 3.09).

**Cxcr2 can show some internalisation in response to endogenous gradients**

It is worth noting that a degree of Cxcr2 internalisation was observed in some neutrophils when using a higher magnification (60x instead of 30x) (Fig. 3.10). This suggests that Cxcr2 can demonstrate a level of internalisation and thus its distribution is referred to as 'relatively sustained' throughout this thesis.

**Cxcr1, but not Cxcr2, internalises in response to endogenous gradients at infection sites**

I also assessed receptor responses during neutrophil responses to endogenous gradients formed during infection. For this, I conducted a bacterial infection assay by injecting non-pathogenic *E.coli* into the otic cavity of Tg(*lyz*:Cxcr1-FT) and Tg(*lyz*:Cxcr2-FT) 3dpf transgenic larvae (Fig. 3.11a). Using live-imaging I monitored the receptor distributions in neutrophils recruited to the infection site. Cxcr1-FT was extensively internalised at the infection site as seen by reduced membrane sfGFP fluorescence and increased intracellular sfGFP vesicularity (Fig. 3.11b left). In contrast, Cxcr2-FT remained predominantly membranous at the infection site (Fig. 3.11b right). Thus, similar receptor trafficking patterns were observed at both wound and infection sites.

**Cxcr1 is internalised in the presence of 'pure' Cxcl8a gradients**

In my experiments to this point, I had used infection and wound assays to test neutrophil receptor responses to endogenous gradients. During inflammatory responses many chemoattractants are generated (eg. damage-associated molecular patterns (DAMPs), pathogen-associated molecular patterns (PAMPs), leukotrienes)[47]. To confirm that Cxcr1 internalisation observed at wounds was due to Cxcl8a and not any other chemoattractant, I generated 'pure' Cxcl8a gradients. For this, I

transfected HEK293T cells with Cxcl8a-mcherry and transplanted the chemokine-secreting cells into Tg(*lyz:*Cxcr1-FT) 2dpf larvae into a region above the yolk sac (Fig. 3.12a). Zebrafish larvae tolerate transplants as they do not develop adaptive immunity until a later development stage (4-6 weeks post-fertilisation). Transplanted larvae were imaged the following day to allow for resolution of any inflammatory response to the process of transplantation itself. Live-imaging revealed that all neutrophils in the same visual field as the transplant, corresponding to approximately 50-100 μm, had internalised Cxcr1-FT with no sfGFP receptor visible on the cell surface (Fig. 3.12b). This provided further evidence that Cxcr1 internalises in response to Cxcl8a.

**Optogenetic release of chemokine did not assist in capturing the initiation of Cxcr1 internalisation**

Cxcl8a-secreting transplants offer the benefit of observing neutrophil and receptor responses to 'pure' Cxcl8a gradients. However, the levels of Cxcl8a in transplanted larvae are presumably much higher and more chronic compared to physiological gradients. In the transplant with constitutive cxcl8a secretion, Cxcr1-FT was already fully internalised by the time neutrophils arrived at the transplant. This suggested that systemic levels of cxcl8a in this assay are high and/or that the cells might have already passed by the transplant in the interim between transplantation and imaging (approximately 24hours). To better establish the ability of local cxcl8a gradients to trigger cxcr1 internalisation and capture initiation of internalisation in the cells as they migrate I trialled a technique for acute release of Cxcl8a that enables temporal control over the initial secretion of chemokine[142]. This approach would enable neutrophils and receptor dynamics to be imaged immediately prior to and immediately following the secretion of a 'pure' gradient. To this end, I used an optogenetic approach that exploits the photo-responsive protein UVR8, to enable light-triggered release of chemokine from transplanted cells in situ. UVR8 is a plant photoreceptor protein that constitutively forms homodimers. However, when exposed to UV-B light, UVR8 homodimers dissociate into monomers. Tandems of UVR8 protein fused to a membrane resident protein such as VSVG have been shown to spontaneously form clusters that are unable to traffic from the ER to the golgi. Upon photo-activation (PA) with UV-B light these clusters dissociate, and the UVR8-fusion protein can successfully traffic to the golgi[109]. This optogenetic trafficking technique has been further developed in our lab to enable photo-dependent secretion of proteins such as chemokines[142]. Here, tandems of UVR8 are fused to VSVG which is fluorescently tagged to enable visualisation of the protein's trafficking fate. The secreted protein, in this case Cxcl8a, is

fused to the N-terminal (luminal part) of VSVG via a furin recognition sequence. Following photoactivation (PA), the membrane bound UVR8-fusion protein dissociates and successfully traffics to the Golgi. This trafficking is visible as a more diffuse fluorescent signal. The furin enzyme, which is resident to the golgi, can then cleave the recognition sequence releasing Cxcl8a which is subsequently secreted into the extracellular milieu without the UVR8 fusion protein. I transplanted UVR8-Cxcl8a transfected HEK293 cells into Tg(*lyz:*Cxcr1-FT) transgenic fish (Fig. 3.13a). I imaged the transplanted region the following day, pre- and post-PA via spinning disk microscopy. However live-imaging revealed that, neutrophils in proximity to the transplant had already internalised Cxcr1-FT prior to photo-activation (Fig. 3.13c). This suggests that the transplant is itself 'leaky' or eliciting an inflammatory response and/or that the Cxcr1 receptor may be highly sensitive to even low levels of Cxcl8a.

**Cxcr1 down-regulation reports endogenous gradients at wound sites**

Endogenous Cxcl8a gradients cannot easily be measured given that there are no currently available antibodies. Even in the mouse, where antibodies are available, the detection is not sensitive enough to detect extracellular chemokine gradients. The only exception to this is the detection of gradients driving dendritic cell migration to lymph nodes[143]. As a result, chemokine gradients have not yet been measured in an inflammatory setting in any model system. I therefore used Cxcr1 internalisation as a reporter, to indirectly measure the gradient. To enhance neutrophil presence in the fin prior to wounding and obtain more statistically powerful data, I forced their mobilisation from the CHT by applying an alternative chemoattractant to the water bath prior to wounding (Fig. 3.14a). Leukotriene B4 is a potent neutrophil chemoattractant and when exogenously applied to the bath, causes neutrophils to migrate into the ventral fin[124]. As expected, following the addition of LTB4, neutrophils migrated outwards into the ventral fin (Fig. 3.14b top panel). Importantly, migrating neutrophils did not show any internalisation of Cxcr1-FT, the distribution of which remained membranous and directly comparable to resting cells in the CHT. Following a mechanical ventral fin wound, neutrophils present in the ventral fin migrated through the interstitial tissue towards the damaged region and progressively internalised Cxcr1-FT (Fig. 3.14b lower panel). Again, internalisation was quantified by the degree of vesicular receptor, as measured by contrast in sfGFP fluorescence intensity. Quantification of Cxcr1 internalisation over distance from the wound was used to obtain information regarding the endogenous interstitial Cxcl8a gradient. Here,

values were binned and plotted against distance from the wound (quantification performed by A.G) revealing a decaying gradient of Cxcl8a signalling in the range of 200 μm (Fig. 3.14c-d).

**Cxcr1 internalisation is specific to Cxcl8a**

As a further test to determine whether Cxcr1 internalisation was specific to Cxcl8a and not another ligand, I used knockdown of Cxcl8a and assessed Cxcr1-FT receptor responses at wound sites. To this end, I injected a previously validated *cxcl8a*-targeting morpholino into Tg(*lyz*:Cxcr1-FT) one cell stage embryos (Fig 3.15a)[119,123,120]. I wounded 3dpf morpholino-injected larvae in the ventral fin and assessed Cxcr1-FT receptor internalisation levels in recruited neutrophils. I found that *cxcl8a* knockdown markedly reduced Cxcr1-FT internalisation in neutrophils at the wound (Fig 3.15b). Quantification of internalisation, as measured by 'contrast' of the sfGFP signal (conducted by A.G), confirmed significantly reduced Cxcr1 internalisation upon *cxcl8a* knockdown (Fig. 3.16).

# 3. Discussion

**Summary of results**

In this chapter, I utilised a fluorescent timer approach to visualise Cxcr1 and Cxcr2 trafficking dynamics. When expressed in early embryos Cxcr1-FT showed extensive internalisation in the presence of co-expressed Cxcl8a, whilst Cxcr2-FT remained sustained on the membrane. I generated new zebrafish transgenic lines in which neutrophils express Cxcr1-FT or Cxcr2-FT, enabling visualisation of receptor dynamics in response to endogenous gradients *in vivo*. Neutrophil specific expression of the fluorescent timer constructs revealed that under steady state conditions neutrophils show rapid constitutive turnover of both receptors. Interestingly, the two receptors showed differential trafficking patterns in response to endogenous gradients at wound sites. Cxcr1-FT was extensively internalised whilst Cxcr2-FT remained relatively sustained at the membrane. Quantification of Cxcr1-FT internalisation revealed a decaying endogenous gradient in the range of 200 μm.

**Neutrophils show rapid constitutive turnover of Cxcr1 and Cxcr2**

Imaging of unchallenged neutrophils randomly patrolling in the head mesenchyme revealed rapid constitutive turnover of Cxcr1-FT and Cxcr2-FT even in the absence of inflammatory stimuli. Owing to this high rate of turnover, the fluorescent timer approach was not able to provide additional information relating to receptor dynamics as was originally intended. This is because the rate of turnover was faster than the maturation time of tagRFP. Therefore, green ('new') receptors are removed from the membrane before having the chance to fluoresce red. This contrasts with what I observed when expressing Cxcr1-FT and Cxcr2-FT in gastrulating embryos, where both green ('new') and red ('old') were visible on the membrane, reflecting a lower rate of turnover. This is also different to what was observed in zebrafish primordial germ cells where again both green and red receptors were visible at the cell membrane due to a lower rate of constitutive turnover[128]. Therefore, from previous studies utilising this tool and early gastrulating embryo work presented in this chapter the high rate of turnover in neutrophils could not have been predicted. However, the FT-approach did enable monitoring of fast receptor dynamics through the fast maturation of sfGFP. This enabled receptor fates to be followed from approximately 5 minutes after synthesis which is important when the turnover rate is so high. It is useful to know for any future studies in this cell type that using a slow maturing fluorescent protein would not resolve

chemokine receptor dynamics due to the rapid constitutive turnover. It remains unclear as to why neutrophils show such rapid receptor turnover relative to other cells. Indeed, constitutive non-ligand induced trafficking of chemokine receptors has not been well studied. A possibility is that rapid constitutive turnover of chemokine receptors may act to counter ligand-induced down-regulation and promote re-sensitisation to ligand.

**Cxcr1 is internalised in response to Cxcl8a generated at wound sites**

Co-expression of Cxcr1-FT and Cxcl8a in gastrulating embryos revealed that Cxcr1 shows extensive internalisation in response to Cxcl8a, providing evidence that Cxcr1 binds and signals through this chemokine. Live-imaging in wounded Tg(*lyz:*Cxcr1-FT) larvae revealed that neutrophils internalise Cxcr1 in response to endogenous gradients generated at wound sites, providing evidence for Cxcl8a being present at wound sites. Further evidence for the specificity of Cxcr1 for Cxcl8a came from Cxcl8a-secreting transplant experiments in which Cxcr1 was extensively internalised. However, a complete dataset would include a mock transplant that does not express chemokine. It is worth noting that in the absence of any transplant neutrophils in the same area (head region) showed a membranous distribution of Cxcr1. Finally, specificity of Cxcr1 for Cxcl8a was tested via injection of a Cxcl8a-targeting morpholino into Tg(*lyz*:Cxcr1-FT) larvae. Cxcr1 internalisation was reduced in neutrophils of morpholino injected larvae. Thus, taken together, the data presented in this chapter provide strong evidence that Cxcr1 is internalised in response to Cxcl8a generated at wound sites.

**Cxcr2 is sustained in response to gradients present at infection and wound sites**

Co-expression of Cxcr2-FT and Cxcl8a in gastrulating embryos revealed that Cxcr2 is sustained in response to Cxcl8a. Live-imaging in wounded Tg(*lyz:*Cxcr2-FT) larvae revealed that Cxcr2 is relatively sustained at the cell membrane of neutrophils in response to endogenous gradients. From the data presented here, it remains unclear whether Cxcr2 remains membranous due to a lack of cognate ligand at the wound site or whether Cxcr2 remains membranous because it does not internalise in response to cognate ligand. Interestingly, when using a higher magnification during imaging, a degree of Cxcr2 internalisation was visible in some neutrophils. This could suggest that Cxcr2 binds to an alternative ligand at wound sites. This point is addressed and discussed further in the following chapter and in the final discussion of this thesis. Regardless of ligand preference, Cxcr2 is relatively sustained in response endogenous gradients generated at wound sites.

**Cxcr1 internalisation provides a read-out for endogenous gradients**

It is not possible to directly measure endogenous Cxcl8a via staining given that there are currently no available antibodies for zebrafish Cxcl8a. In this study, I instead measured the chemokine gradient indirectly via measuring the degree of internalisation of Cxcr1. The gradient range reported here is longer than those previously published for ectopically expressed Cxcl8a gradients[120] and endogenous gradients of CCL21 in mouse ear skin[144,143] and mouse lymph nodes[145]. This could be due to differences in ligand distribution in the different settings or due to higher sensitivity of the readout for chemokine levels used in this study.

**Zebrafish Cxcr1 and Cxcr2 show similarities and differences with CXCR1 and CXCR2 with respect to trafficking**

This thesis focuses on understanding the role of GPCR trafficking in generating specific cell migration behaviours. The aim was that the findings would have broad relevance given that many human GPCRs have been shown to have differential ligand induced trafficking *in vitro*[146,147]. To address this, I used zebrafish Cxcr1 and Cxcr2 receptors as a model system. Owing to the evolutionary distance between zebrafish and human receptors, it was not the intention of this study to draw functional comparisons to human CXCR1 and CXCR2. Nonetheless, I will briefly discuss how the results presented in this chapter relate to the human receptors. Based on *in vitro* evidence, human CXCR1 and CXCR2 display differential trafficking dynamics in response to CXCL8. CXCR1 is partially internalised (50% after 30 min) whilst CXCR2 is internalised more rapidly and thoroughly (95% after 5-10 mins) in response to CXCL8[148]. Thus, both human and zebrafish CXCL8 receptors show differential trafficking but their trafficking patterns appear inversed, with CXCR1 being more resistant to internalisation than CXCR2. This difference is perhaps not surprising given the evolutionary distance between the two species. Indeed, mice which are more closely related to humans, do not have an orthologue of human CXCL8. Seemingly, there is no perfect animal model and it is arguable that functional convergence is more meaningful for translating findings across species.

# 3. Figures

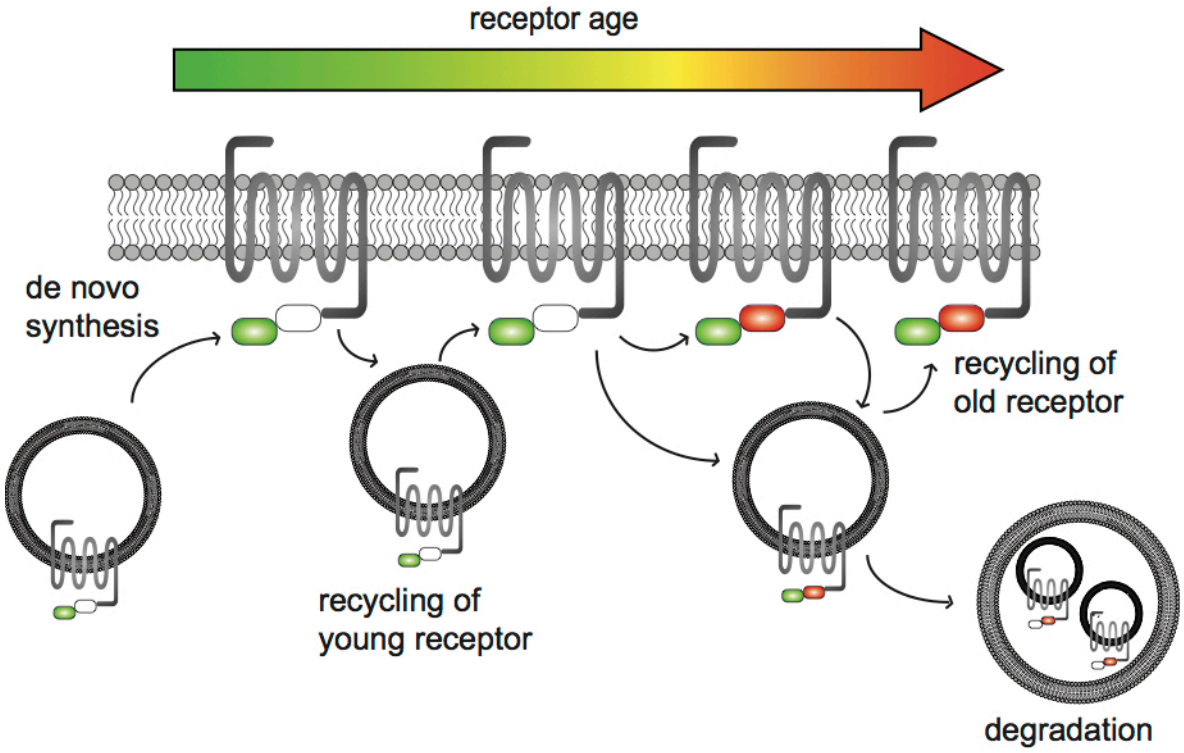


**Figure 3.1. Fluorescent timer constructs reveal information regarding protein age.** Schematic depicting the fluorescent timer (FT) approach. Newly synthesised and rapidly recycling 'young' receptors fluoresce in green. 'Old' receptors fluoresce in red and green whilst lysosomal receptors targeted for degradation fluoresce in red only.

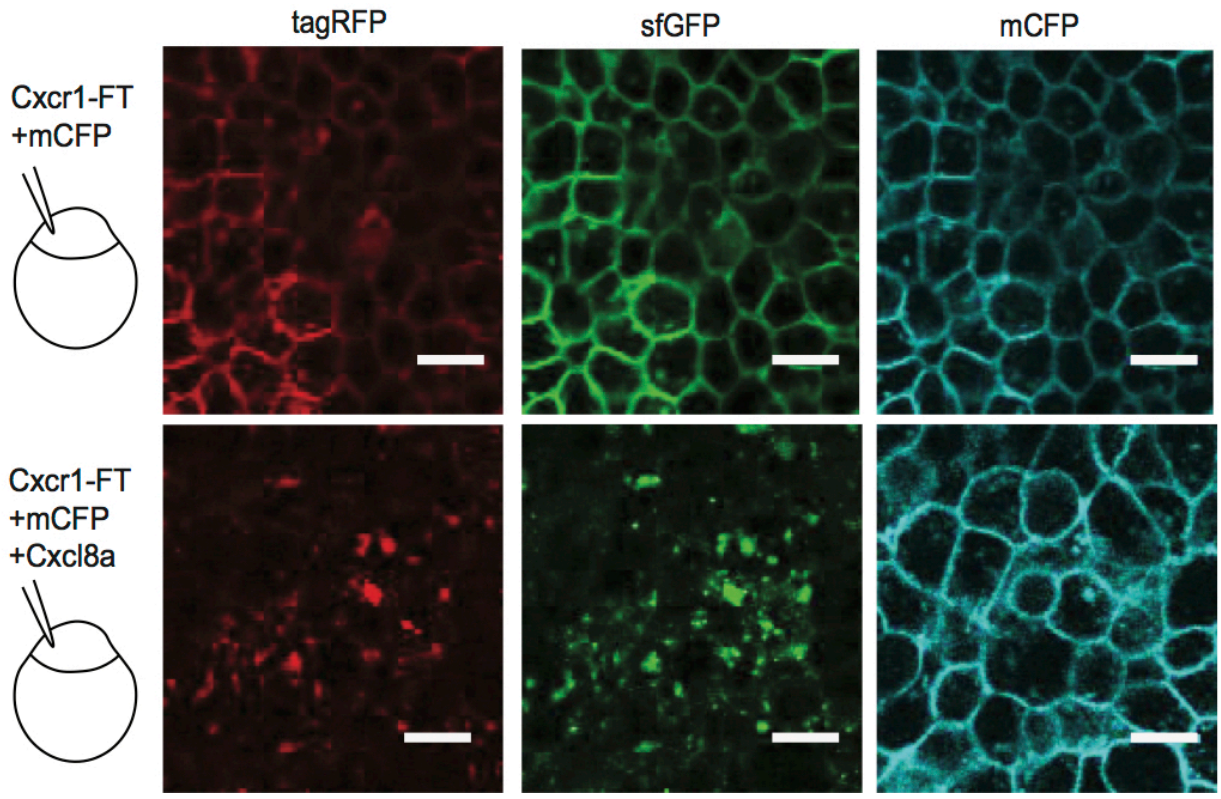


**Figure 3.2. Cxcr1 is extensively internalised in response to Cxcl8a.** 100pg of Cxcr1-FT mRNA was injected with or without 150 pg Cxcl8a mRNA into one-cell stage zebrafish embryos. 100pg of a control membrane marker mCFP mRNA was co-injected in all cases. Representative laser-scanning confocal images showing distribution of Cxcr1-FT (sfGFP and tagRFP receptors shown in separate channels) in gastrulating embryos (at approximately 6-8hpf). Control membrane marker mCFP is shown in the blue channel. Scale bar = 20μm.

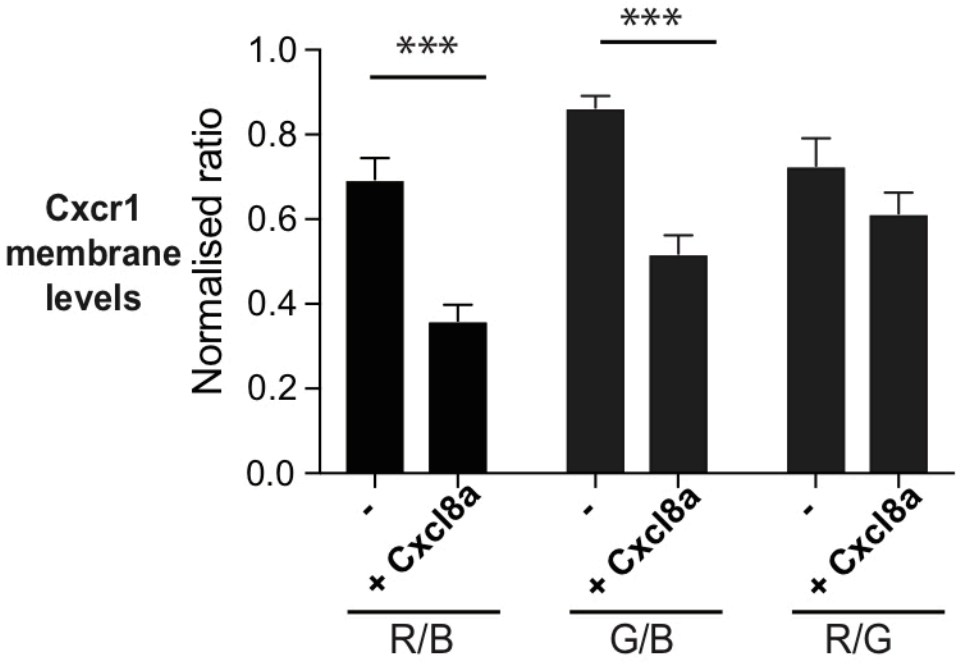


**Figure 3.3 Quantification of Cxcr1 membrane distribution compared to distribution of memCFP**. Ratio of red over blue (R/B), green over blue (G/B) and red over green (R/G) fluorescence at the cell membrane is shown. Mean ratios at the cell membrane were calculated from ratiometic images after global membrane segmentation. The membrane ratios were normalised to mean ratios of non-segmented ratiometic images of the corresponding source samples. n=10 embryos for Cxcr1 from four imaging sessions, n=6 embryos for Cxcr1+Cxcl8a from three imaging sessions, n=3 embryo. Mann-Whitney test. Quantification by myself and M.S.

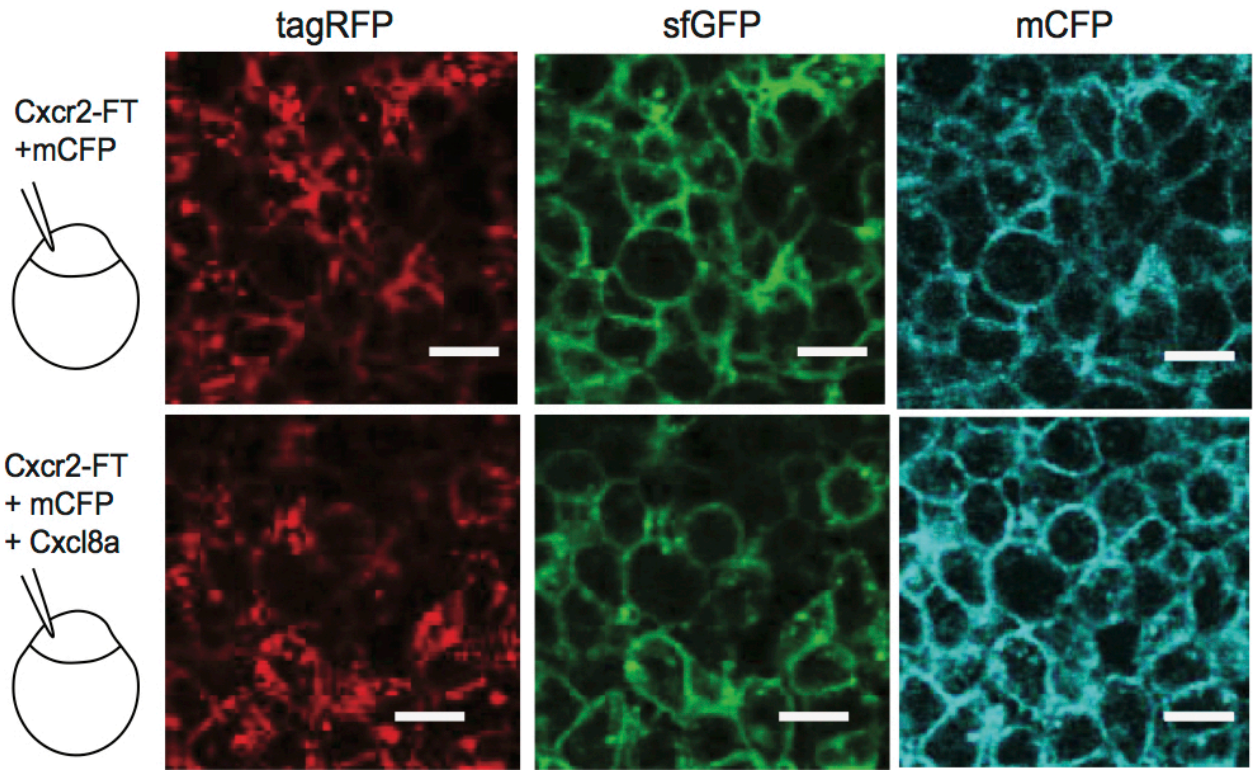


**Figure 3.4. Cxcr2 is sustained at the membrane in response to Cxcl8a** a) 100pg of Cxcr2-FT mRNA was injected with or without 150pg Cxcl8a mRNA into one-cell stage zebrafish embryos. 100pg of a control membrane marker mCFP mRNA was co-injected in all cases. Representative laser-scanning confocal images showing Cxcr2-FT receptor distribution (sfGFP and tagRFP receptors shown in separate channels) in gastrulating embryos (at approximately 6-8hpf). Control membrane marker mCFP is shown in the blue channel. Scale bar, 20um.

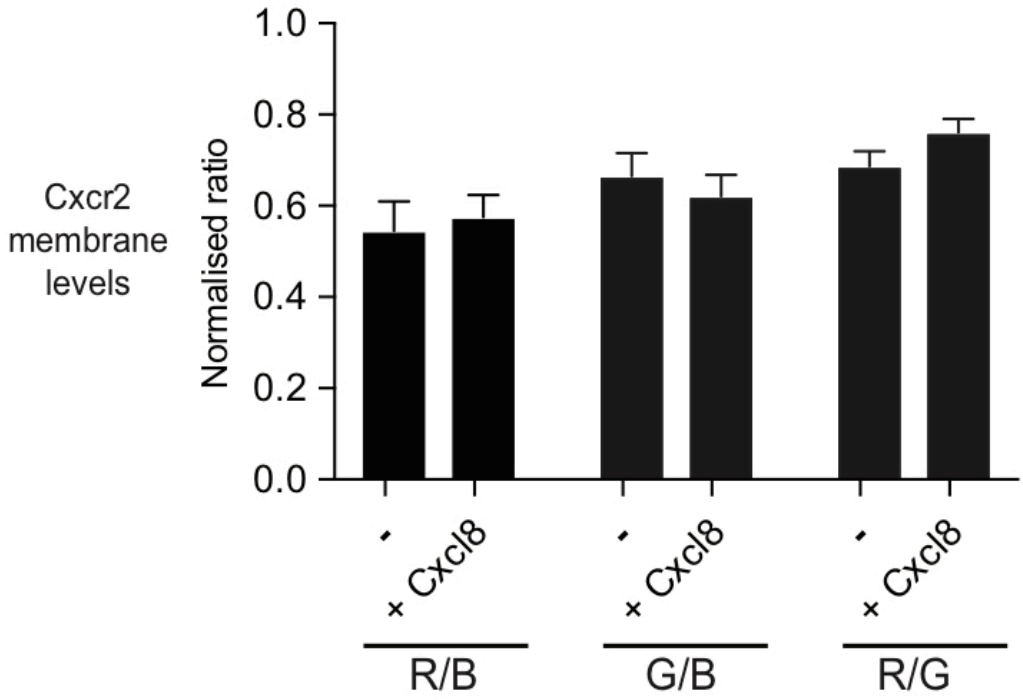


**Figure 3.5. Quantification of Cxcr2 membrane distribution compared to distribution of the control membrane marker.** Ratio of red over blue (R/B), green over blue (G/B) and red over green (R/G) fluorescence at the cell membrane is shown. Mean ratios at the cell membrane were calculated from ratiometric images after global membrane segmentation. The membrane ratios were normalised to mean ratios of non-segmented ratiometric images of the corresponding source samples. n=4 for Cxcr2 and n=3 for Cxcr2+Cxcl8a. Mann-Whitney test. Quantification by myself and M.S.

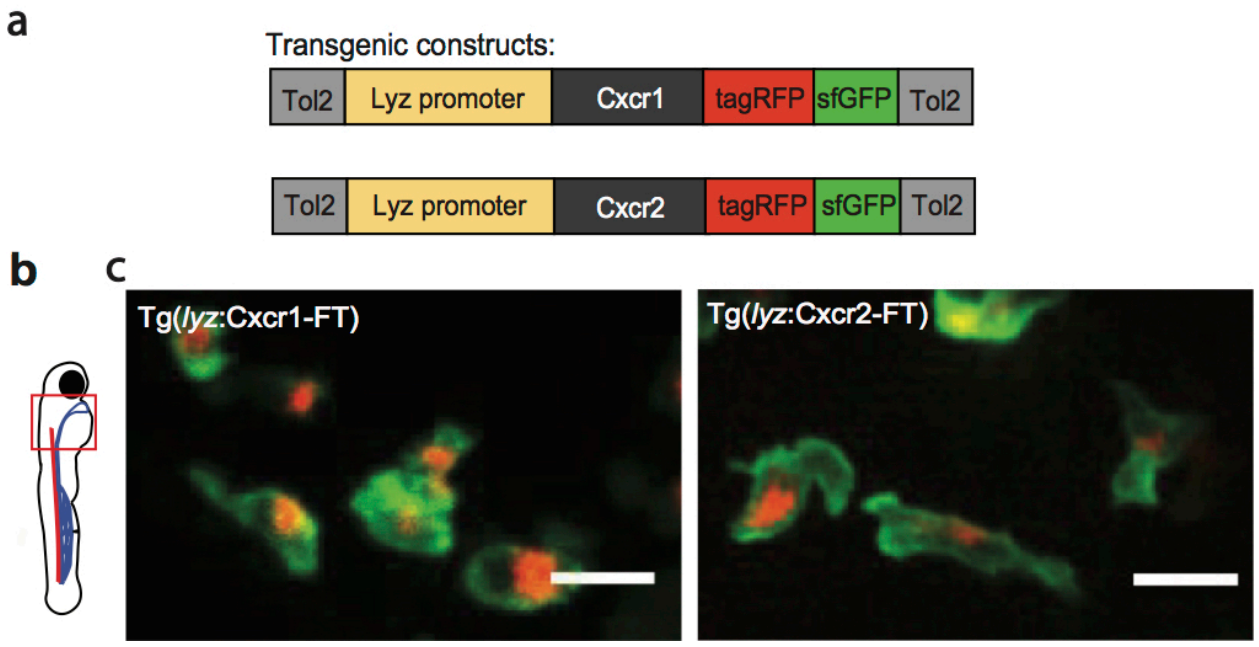


**Figure 3.6. FT-constructs reveal constitutive turnover of Cxcr1 and Cxcr2** a) Schematic of constructs used for expression of Cxcr1-FT or Cxcr2-FT in neutrophils. b) Schematic showing region of larvae imaged (red box) c) Confocal images of neutrophils randomly patrolling in the head region of 3dpf Tg(*lyz:*Cxcr1-FT) (left) and Tg(*lyz:*Cxcr2-FT) (right) transgenic larvae. Scale bar, 20 μm**.**

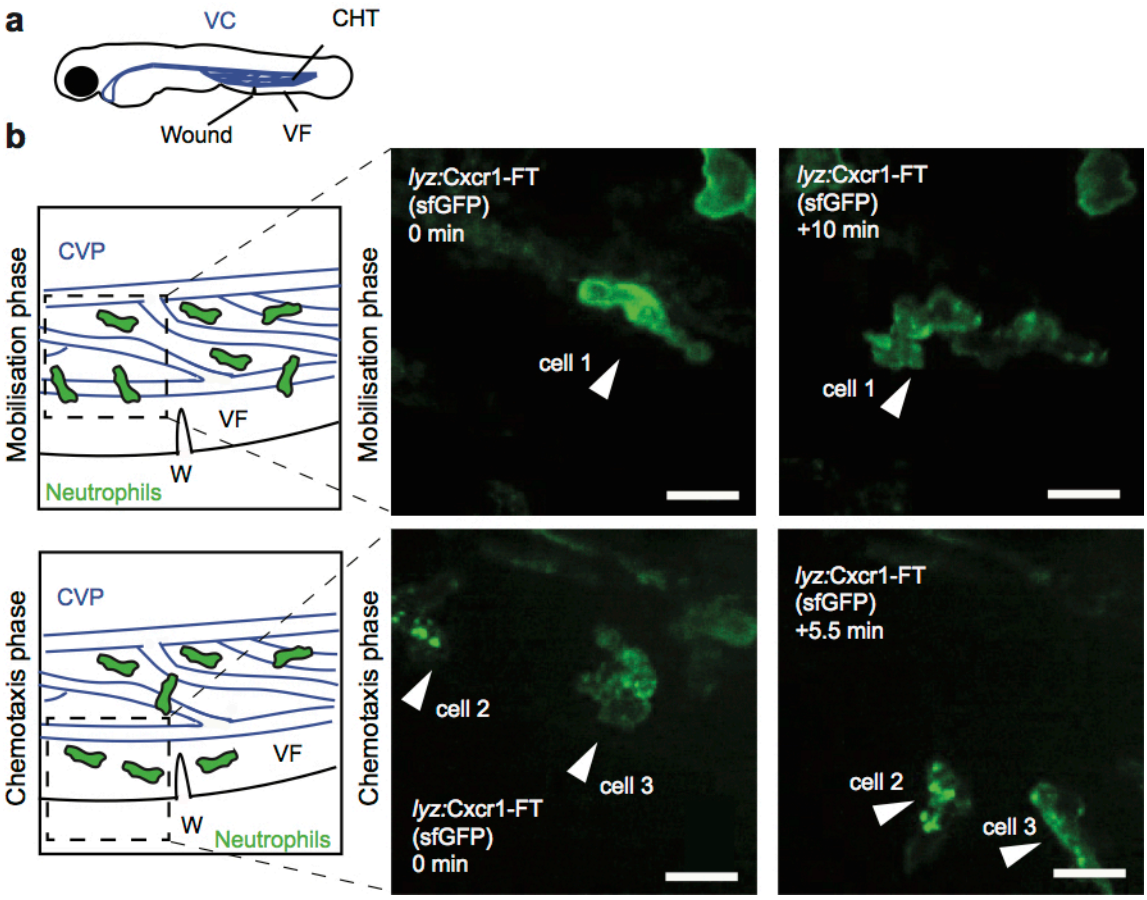


**Figure 3.7. Cxcr1 is progressively internalised during neutrophil migration to wound sites** a) Schematic of 3 dpf larva showing the location of the caudal hematopoietic tissue (CHT), the venus circulation (VC, blue), the ventral fin (VF) and the wound site. b) Schemes (left) depicting the area of the wound with neutrophils getting mobilized from the CHT (top) or performing chemotaxis upon entering the ventral fin (bottom). Caudal Vein plexus (CVP) of the CHT tissue is drawn in blue. Dashed square indicates area imaged in confocal snapshots on the right. Neutrophils in Tg(*lyz*:Cxcr1-FT) larvae (sfGFP is shown) upon mobilization from the CHT (top panels) or chemotaxis towards the wound (bottom panels). Arrows show the same cells over time. Time points on the right image are minutes elapsed after image on the left. Scale bar, 10µm.

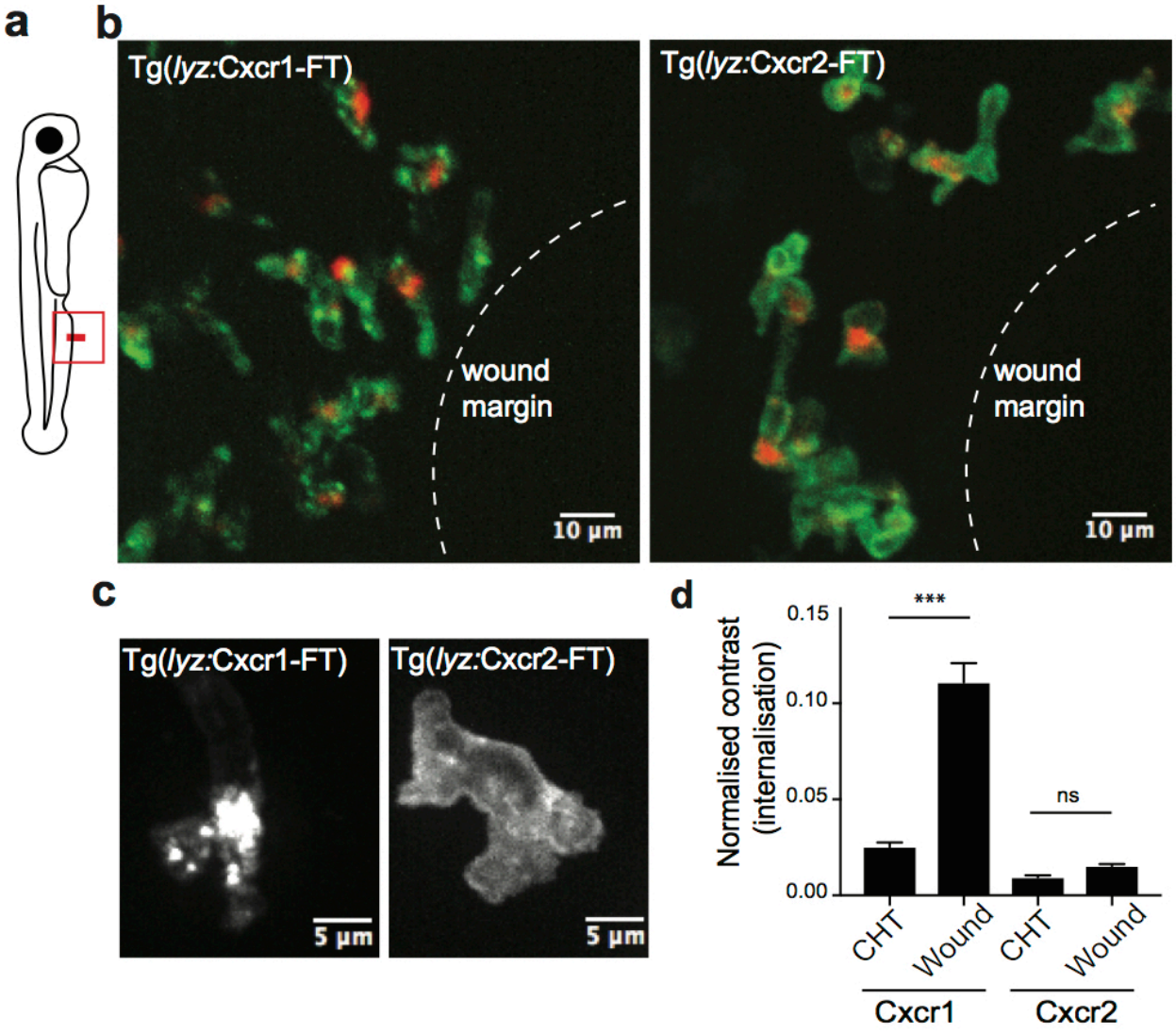


**Figure 3.8. Cxcr1, but not Cxcr2, is internalised at wound sites.** a) Schematic depicting area of larvae wounded (red line) and imaged (red box). b) Confocal images of Cxcr1-FT neutrophils (left) and Cxcr2-FT neutrophils (right) responding to a ventral fin wound Scale, 10µm c) Magnified Cxcr1-FT neutrophil (left) and Cxcr2-FT neutrophil (right) at the wound. Green receptor is shown in grey. Scale, 5µm. d) Quantification of degree of internalisation per cell as measured by contrast normalised to mean intensity of green receptor per cell. Cells were measured at the wound and at the CHT (Kruskall-Wallis wih Dunn's multiple comparison test, n=39 cells for Cxcr1-CHT, n=30 cells for Cxcr1-wound cells, n=25 for Cxr2-CHT, n=24 for Cxcr2-wound. Quantification (d) by A.G.

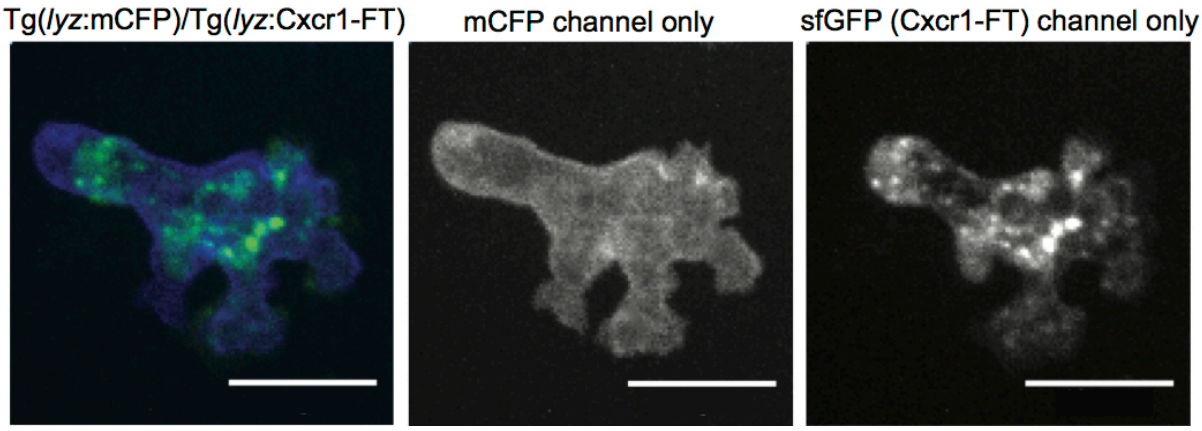


**Figure 3.9. Cxcr1-FT internalisation shows vesicular distribution compared to membrane marker.** Left panel shows confocal image of a neutrophil expressing membrane CFP (shown in blue) and Cxcr1-FT (sfGFP fluorophore shown only, in green). Middle panel shows mCFP channel only (shown in grey). Right panel shows Cxcr1-FT sfGFP channel only (shown in grey). Scale, 10μm.

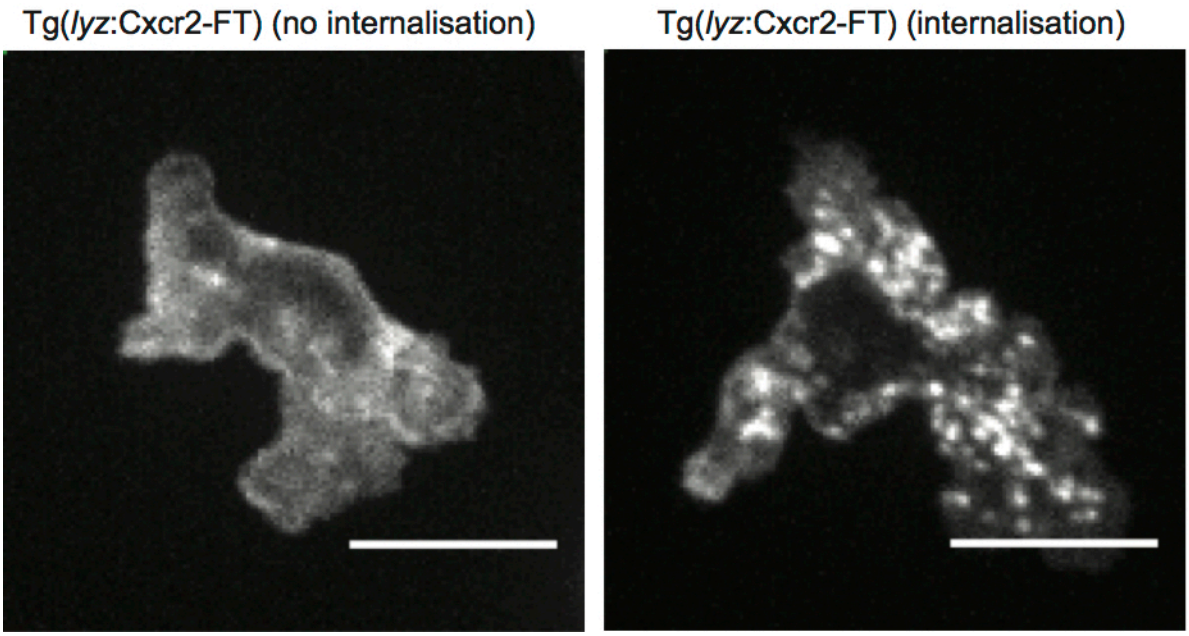


**Figure 3.10. Cxcr2 can show internalisation in response to endogenous gradients at wounds.** Confocal images of Cxcr2-FT neutrophils responding to a ventral fin wound. Left panel shows a typical Cxcr2-FT neutrophil with no internalisation of the receptor. Right panel shows a Cxcr2-FT neutrophil displaying internalisation. Scale bar, 10μm.

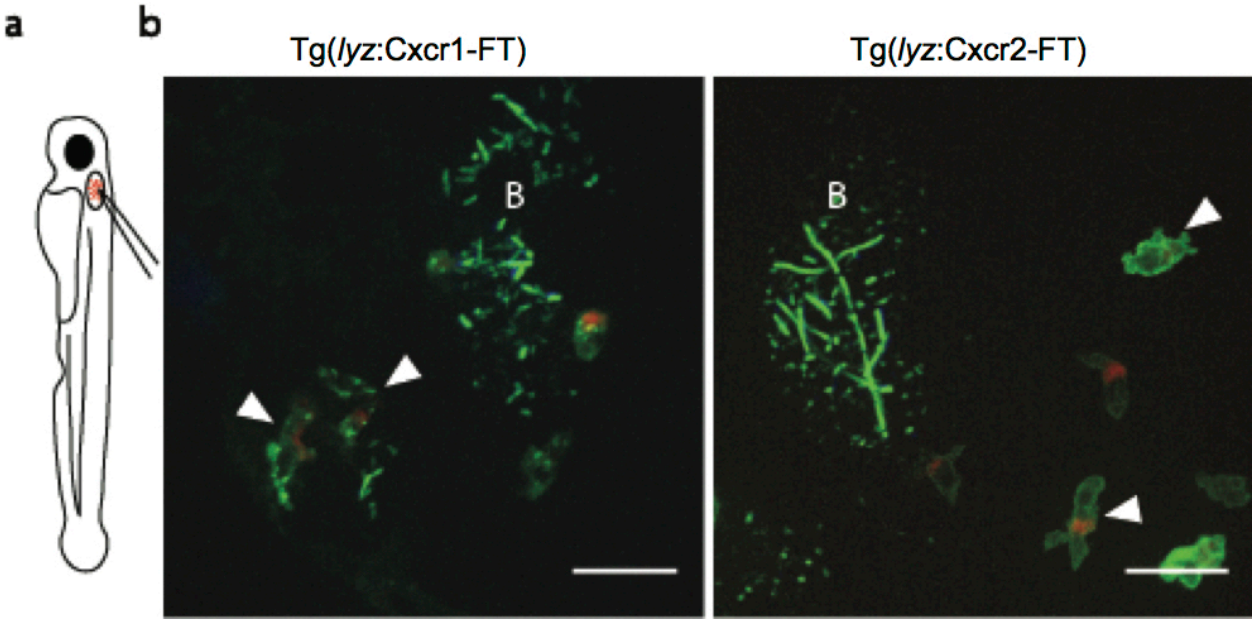


**Figure 3.11. Cxcr1, but not Cxcr2, is internalised at infection sites.** a) Schematic showing injection of bacteria into the otic cavity b) Confocal images of Cxcr1-FT neutrophils (left) and Cxcr2-FT neutrophils (right) responding to an otic infection (non-pathogenic *E.coli*). Arrows point to representative neutrophils, B=bacteria. Scale bar, 20µm

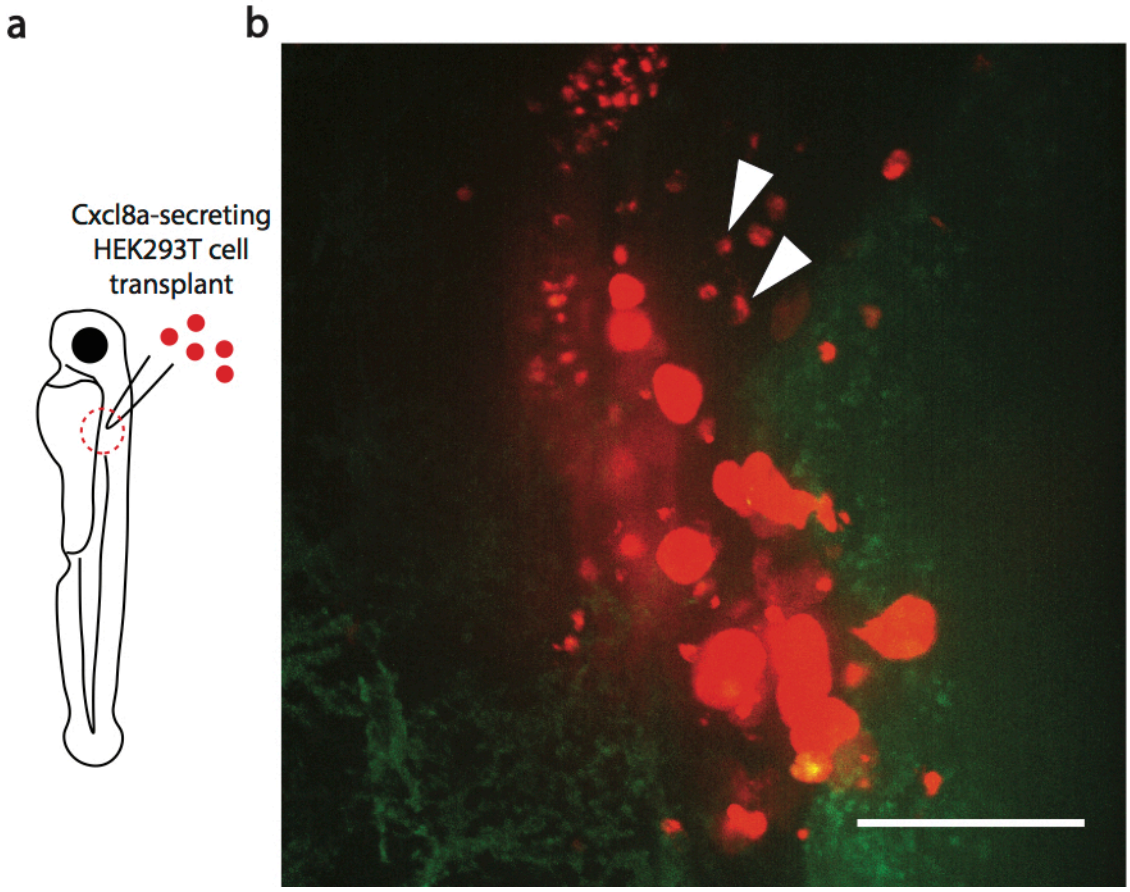


**Figure 3.12. Cxcr1 internalises in response to pure Cxcl8a gradients.** a) Schematic showing transplanted region (red dashed circle). b) Confocal image showing Cxcr1-FT neutrophils responding to a Cxcl8a-secreting HEK cell transplant (large red cells). Arrows point to example neutrophils. Scale bar, 50µm.

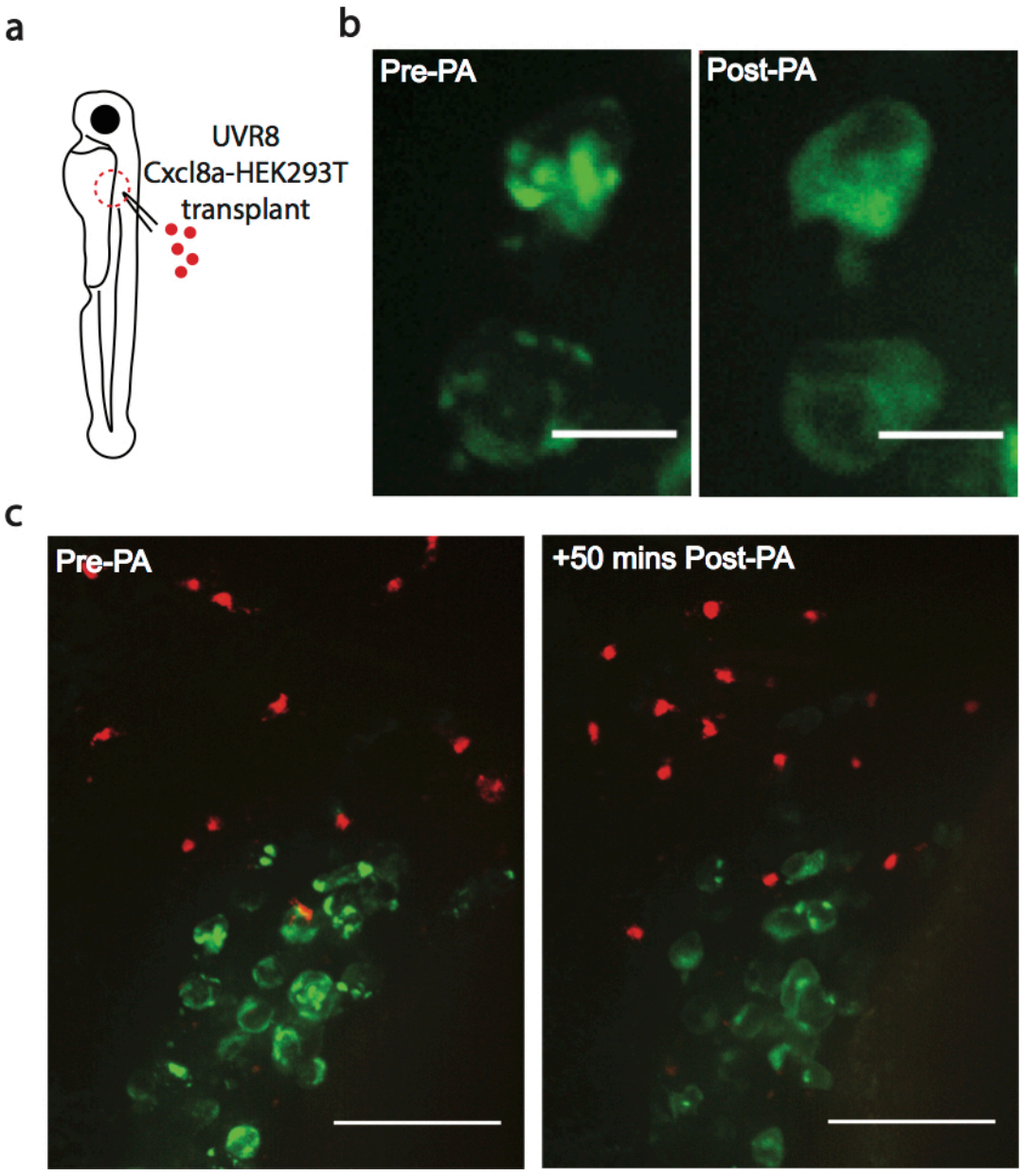


**Figure 3.13. Using light-triggered Cxcl8a release to assess Cxcr1 receptor responses** a) Schematic depicting optogenetic transplant approach b) Confocal images of transplanted UVR8 and Cxcl8a transfected HEK293 cells pre-PA and post-PA (left and right panel respectively) Scale,10µm c) Confocal projections of Cxcr1-FT neutrophils responding to a UVR8 and Cxcl8a transfected transplant, pre-PA and 50 mins post-PA (left and right panel respectively). Scale, 50µm

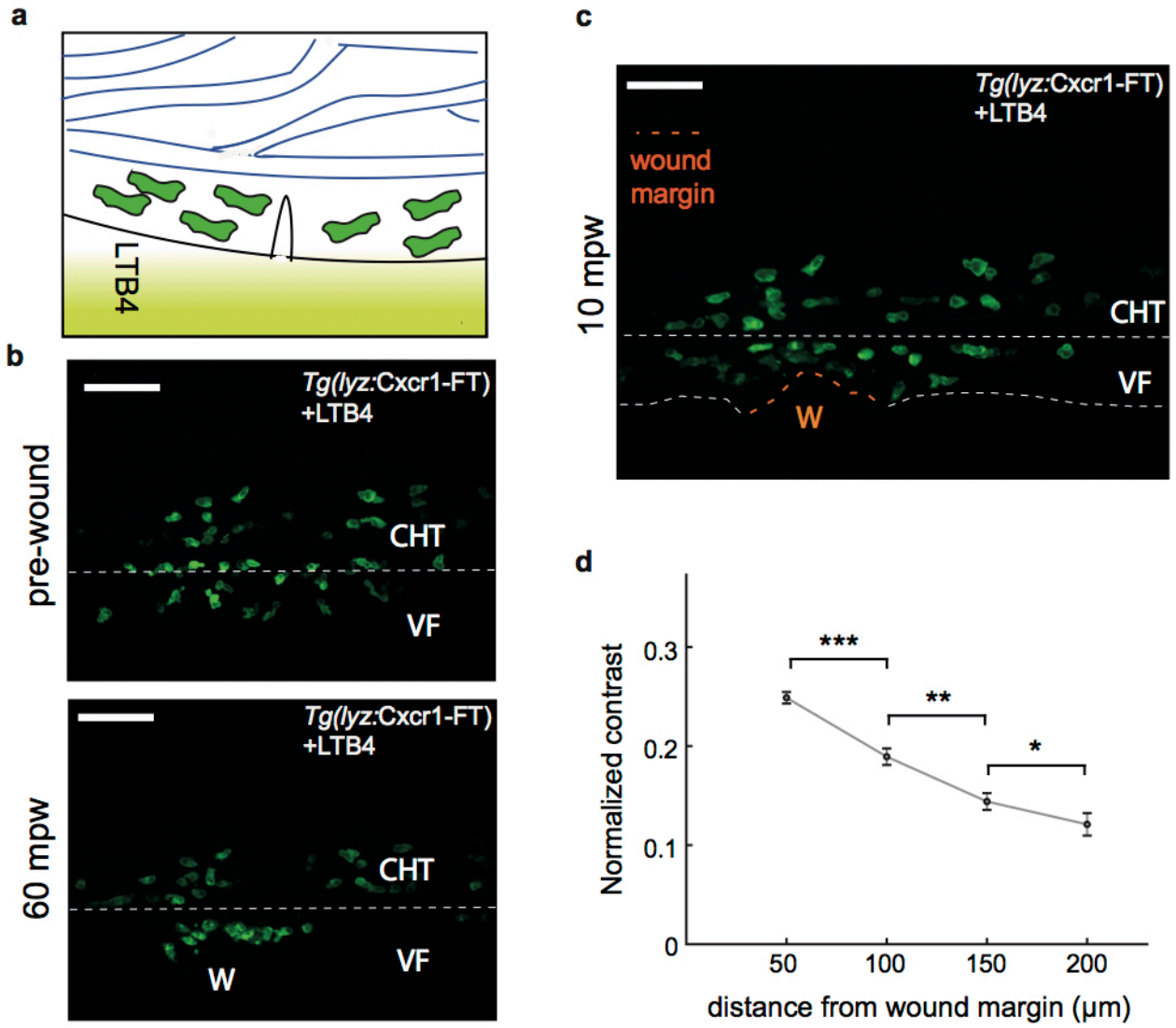


**Figure 3.14 Cxcr1 internalisation reports endogenous gradients** a) Schematic depicting neutrophils mobilised from the CHT into the ventral fin in response to an exogenously applied LTB4 gradient. b) Confocal projections of Cxcr1-FT neutrophils 30 min after LTB4 addition, immediately prior to- and 1h post- wounding. Scale bar, 50µm. c) Same larva as in b, at 10 mpw. Orange dashed line shows the wound margin. d) Graph shows normalised contrast as a function of distance from the center x. n=4 embryos in four imaging sessions. Orange dashed line denotes an area of radius 80 µm from a chosen center x of the wound area. Quantification (d) by A.G.

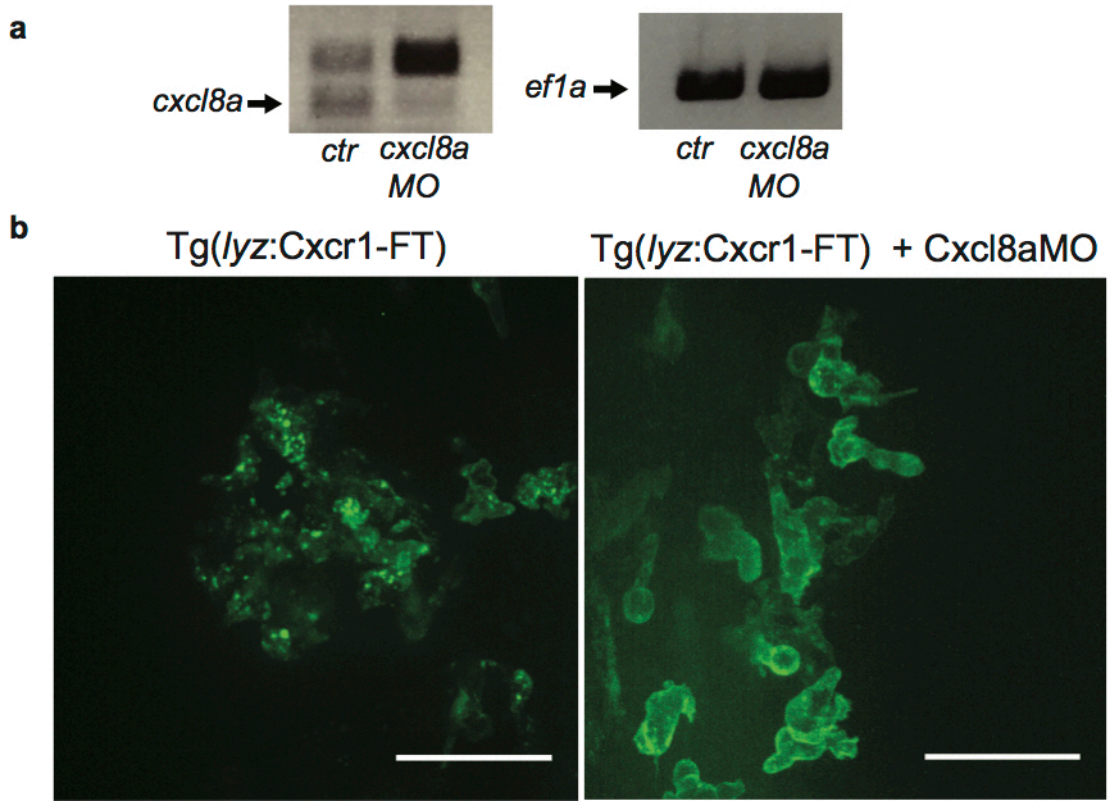


**Figure 3.15. Cxcr1 internalisation at wound sites is specific to Cxcl8a**. a) RT-PCR results showing detection of *cxcl8a* levels in the presence or absence of Cxcl8a targeting morpholino (splice blocking and translation-blocking) treatment in 3 dpf larvae. Results from *ef1a* expression-detection are shown for comparison. Conducted by H.W. b) Confocal images of neutrophils in non-injected (left) and Cxcl8a morpholino injected (right) Tg(*lyz:*Cxcr1-FT) larvae responding to a ventral fin wound. sfGFP shown only. Images taken at 2hpw. Scale bar, 30um.

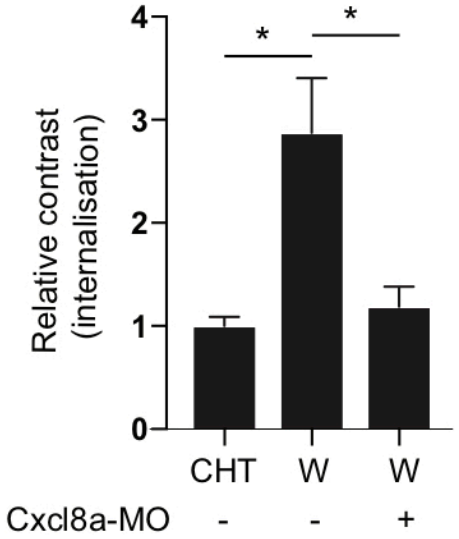


**Figure 3.16 Quantification of Cxcl8a-specific Cxcr1 internalisation**. Normalised contrast (contrast per individual neutrophil normalised to the mean contrast of non-mobilised cells in the CHT). For Tg(*lyz*:Cxcr1-FT): n=24 cells (CHT), n=47 cells (wound) from 8 larvae. For Tg(*lyz*:Cxcr1-FT) with morpholinos: n=28 cells (Cxcl8a-MO) from 5 larvae. Data were pooled from independent larvae acquired in 1-5 imaging sessions. Kruskal-Wallis test with Dunn's multiple comparisons test for Tg(*lyz*:Cxcr1-FT). Quantification by A.G.

# Chapter 4: Cxcr1 and Cxcr2 make distinct functional contributions to neutrophil interstitial migration

## 4. Introduction

In the previous chapter I investigated the receptor trafficking dynamics of Cxcr1 and Cxcr2 and showed that the two receptors show differential trafficking in response to endogenous gradients generated at wound sites. Cxcr1 is progressively internalised whilst Cxcr2 is relatively sustained at the neutrophil cell membrane throughout the response. My next aim, and the focus of this chapter, was to determine how Cxcr1 and Cxcr2 functionally contribute to neutrophil migration at wound sites, with a view to linking receptor trafficking behaviour with receptor function. To this end, my aim was to generate zebrafish knockout receptor lines and assess forward and reverse traffic defects in real-time trajectory data. Please note that a detailed background of previous work on these receptors is given together with my result discussion at the end of this chapter.

## 4. Objectives

- Generate *cxcr1*$^{-/-}$ and *cxcr2*$^{-/-}$ lines to investigate the function of Cxcr1 and Cxcr2 in gradient sensing.
- Determine *cxcr1*$^{-/-}$ and *cxcr2*$^{-/-}$ migration phenotypes
- Conduct detailed trajectory analyses to determine mechanism underlying any phenotypic differences

**Notes on contributions:**

Antonios Georgantzoglou (A.G) conducted most of the analysis presented in the results section of chapter. His contribution is noted throughout the text and figure legends. Any experimental or analysis contributions made by Hazel Walker (H.W), Milka Sarris (M.S) or Christina Kotsi (C.K) are also referred to in the text and figure legends.

# 4. Results

**Generating *cxcr1*$^{-/-}$ and *cxcr2*$^{-/-}$ knockout mutants**

To investigate the functional contribution of Cxcr1 and Cxcr2 in gradient sensing, I obtained mutant receptor zebrafish lines from the Zebrafish Mutation Project, a large-scale mutagenesis screen in which mutations are induced via exposure to the mutagenic chemical ENU (N-ethyl-N-nitrosourea)[149]. The mutant fish I received carried a single nucleotide polymorphism (SNP) heterozygous nonsense mutation in the *cxcr1* or *cxcr2* gene resulting in a premature STOP codon. In the case of *cxcr1* mutants, the point mutation (G>A) introduces a stop codon after amino acid 173 (full length WT protein is 364 amino acids) (Fig. 4.1). This mutation is predicted (TMpred) to lie in the 4$^{th}$ transmembrane domain of the receptor[150]. In the case of *cxcr2* mutants, the point mutation (T >A) introduces a stop codon after amino acid 145 (full length WT protein is 340 amino acids) (Fig.4.2). Again, this mutation is predicted (TMpred) to lie in the 4$^{th}$ transmembrane domain of the receptor[150]. As founder fish carried multiple additional mutations, I first carried out outcrosses for three generations to progressively eliminate the unwanted mutations whilst selecting for the desired Cxcr1 or Cxcr2 mutations via KASP genotyping. In the outcrossing process, fish were crossed to a Tg(*mpx*:GFP)$^{i114}$ transgenic line in which neutrophils express GFP under the myeloperoxidase promotor. Once unwanted mutations had been eliminated, Tg*(mpx*:GFP)$^{i114}$; *cxcr1*$^{+/-}$ and Tg(*mpx*:GFP)$^{i114}$; *cxcr2*$^{+/-}$ heterozygote lines were incrossed to generate Tg(*mpx*:GFP)$^{i114}$; *cxcr1*$^{-/-}$*(cxcr1*$^{-/-}$ hereafter) and Tg(*mpx*:GFP)$^{i114}$; *cxcr2*$^{-/-}$ (*cxcr2*$^{-/-}$ hereafter) homozygote lines with GFP positive neutrophils that could be easily visualised during live-imaging.

**Developmental neutrophil distribution in *cxcr1*$^{-/-}$ and *cxcr2*$^{-/-}$ is comparable to WT**

Prior to conducting any neutrophil migration experiments in these knockout lines, it was first important to assess whether the *cxcr1*$^{-/-}$ and *cxcr2*$^{-/-}$ mutations had developmental implications in terms of neutrophil number and distribution. To assess developmental differences in my knockout lines, fluorescent microscopy images of whole 3dpf WT, *cxcr1*$^{-/-}$ and *cxcr2*$^{-/-}$ larvae were acquired and the number of neutrophils in the whole larva and the CHT were counted (Imaging and counts conducted by Hazel Walker) (Fig. 4.3a). Cell counts revealed that *cxcr1*$^{-/-}$ and WT larvae had comparable number of neutrophils across whole larvae (Fig. 4.3b). However, *cxcr1*$^{-/-}$ larvae had fewer neutrophils in the CHT compared to WT, though this did not quite reach significance (Fig.

4.3c). Whilst *cxcr2*$^{-/-}$ larvae had slightly more neutrophils overall compared to WT, this did not quite reach significance (Fig 4.3d). The number of neutrophils in the CHT of *cxcr2*$^{-/-}$ larvae was comparable to WT (Fig 4.3e). Thus, whilst slight developmental differences were observed in both knockout lines, none reached statistical significance.

**Cxcr1$^{-/-}$ neutrophils show a defect in recruitment and are more dispersed at the wound**

I used high resolution spinning disk microscopy to image neutrophil migration to wounds in real time. For these live-imaging experiments, I used a ventral fin wound assay which, as discussed in the previous chapter, is particularly amenable to live-tracking of neutrophil migration behaviour (Fig 4.4a). I first compared neutrophil migration to ventral fin wounds in WT and *cxcr1*$^{-/-}$ larvae. Following wounding, WT neutrophils exited the CHT and migrated directionally to the wound. At the target site WT neutrophils displayed a balanced response with some cells stopping and focalising at the wound margin and others showing a level of dispersal (Fig 4.4b left panel). In the case of *cxcr1*$^{-/-}$ larvae, neutrophils showed reduced recruitment and cluster size (Fig 4.4b, middle panel, c-d), suggesting a role for Cxcr1 in forward migration. For a more in depth analysis which could distinguish chemotaxis from reverse migration, 'whole' neutrophil trajectories were split into 'forward' and 'reverse' trajectories respectively (Fig 4.5). 'Forward' neutrophil trajectories included all those prior to neutrophil arrival at the 'occupied wound area' (owa), assigned as the area occupied by clustering neutrophils. 'Reverse' neutrophil trajectories included only those after neutrophils depart the owa. Both forward- and reverse- trajectories were taken 50 μm from the owa margin. Analysis of 'entire' cell trajectories revealed that neutrophils in *cxcr1*$^{-/-}$ larvae had lower straightness compared to those of WT neutrophils (Fig 4.6a). Furthermore, analysis of 'forward' trajectories revealed that *cxcr1*$^{-/-}$ and WT neutrophils were comparable in terms of overall speed and directional speed (Fig 4.6b-c). Taken together, these results suggest that *cxcr1*$^{-/-}$ neutrophils show no defect in directional sensing. Reverse migration was quantified by measuring the total number of reverse tracks over the total number of forward tracks. Quantification using the 'net reverse traffic' metric revealed no difference in reverse migration of WT and *cxcr1*$^{-/-}$ neutrophils (Fig 4.6d).

**Cxcr2$^{-/-}$ neutrophils show defective dispersal**

Next, I assessed neutrophil migration to ventral fin wounds in *cxcr2*$^{-/-}$ larvae. Live-imaging revealed that *cxcr2*$^{-/-}$ neutrophils formed concentrated and persistent clusters at the wound margin, with cells displaying next to no motility or exploration at all (Fig 4.4b right panel). Quantification revealed that *cxcr2*$^{-/-}$ neutrophils showed no defect in early recruitment to the ventral fin (Fig 4.4 c) and had similar cluster sizes to WT neutrophils (Fig 4.4d). Furthermore, analysis of 'whole' trajectories showed similar track straightness to WT (Fig. 4.6a). Analysis of 'forward' trajectories revealed no defect in directional sensing but did show that *cxcr2*$^{-/-}$ neutrophils are significantly slower at all distances measured and independent of orientation, suggesting a general role for Cxcr2 in promoting motility (Fig. 4.6b and c). As suspected, analysis of 'reverse' trajectories showed that *cxcr2*$^{-/-}$ neutrophils display reduced net reverse traffic, reflective of reduced dispersal from the wound (Fig. 4.6d). Taken together, these results suggest that Cxcr2 powers neutrophil motility and promotes dispersal.

**Cxcr2 promotes resolution**

To assess the impact of the *cxcr2*$^{-/-}$ mutation on resolution, we (myself and C.K) transected the tails of 3dpf WT, *cxcr1*$^{-/-}$ and *cxcr2*$^{-/-}$ larvae and fixed injured larvae at 24 hpw, a time point at which the response should have largely resolved. Neutrophil accumulation was visualised using Sudan Black staining, a lipid stain which labels the granules of neutrophils enabling them to be counted (Fig. 4.7a) (neutrophil counts conducted by C.K). Neutrophil counts revealed that *cxcr1*$^{-/-}$ larvae had less neutrophils present at the wound 24hpw compared to WT larvae, suggesting efficient resolution of the response (Fig. 4.7b). In contrast, *cxcr2*$^{-/-}$ larvae showed significantly enhanced neutrophil accumulation at 24 hpw when compared to WT larvae (Fig. 4.7b). Taken together, the results from live-imaging and fixed cell analysis suggest that Cxcr2 sustains neutrophil motility, and that this motility is crucial for timely resolution of the response.

**Both Cxcr1 and Cxcr2 play a role in initial recruitment**

Live-imaging of *cxcr2*$^{-/-}$ neutrophils at a ventral fin wound had revealed no defect in *cxcr2*$^{-/-}$ neutrophil accumulation at early time points. However, analysis of cell speeds had revealed that *cxcr2*$^{-/-}$ neutrophils were slower overall suggesting some level of contribution in signalling during forward migration. It remained possible that the highly-related receptor Cxcr1 could functionally compensate in the absence of Cxcr2 and that any such compensation could mask

potential *cxcr2*$^{-/-}$ forward migration defects. To directly test whether both Cxcr1 and Cxcr2 play a role in forward migration I sought to target both receptors simultaneously and assess effects on neutrophil behaviour. However, it was not possible to generate double knockouts via fish crossing given that the Cxcr1 and Cxcr2 genes lie in tandem on the same chromosome. Therefore, I instead targeted both receptors by injecting a previously validated morpholino against Cxcr2 into *cxcr1*$^{-/-}$ larvae. Morpholino-injected *cxcr1*$^{-/-}$ larvae showed a significant defect in neutrophil mobilisation to ventral fin wounds compared with *cxcr1*$^{-/-}$ larvae (Fig. 4.8a-c). This suggests that Cxcr2 also contributes to forward migration but that it is compensated by Cxcr1. Furthermore, trajectory analysis of the few neutrophils that were mobilised revealed that neutrophils in morpholino-injected larvae displayed no directional bias on speed and exhibited reduced speed during forward traffic (Fig. 4.8d-e). Importantly, injection of the Cxcr2 morpholino reduced the overall accumulation of neutrophils in tail fin wounds in *cxcr1*$^{-/-}$ but not in *cxcr2*$^{-/-}$ larvae, confirming its specificity of action (Fig. 4.9). Thus, Cxcr1 and Cxcr2 show a level of redundancy at early stages of the response but have differential non-redundant roles in clustering and dispersal at wound sites.

**Cxcr1 is important for Cxcl8a mediated chemotaxis**

To investigate which ligands are responsible for the *cxcr1*$^{-/-}$ and *cxcr2*$^{-/-}$ phenotypes observed, I used Cxcl8a-secreting transplants to assess the specificity of Cxcr1 and Cxcr2 for the chemokine. For this, I transplanted Cxcl8a-secreting HEK293T cells into 3 dpf WT, *cxcr1*$^{-/-}$ and *cxcr2*$^{-/-}$ larvae and analysed neutrophil migration behaviour at the transplant (Fig.4.10a). Wildtype neutrophils successfully accumulated at the transplant, forming interactions with the chemokine secreting HEK293T cells (Fig.4.10b). Quantification of the percentage of cells 'on target' revealed that *cxcr1*$^{-/-}$ neutrophils had a defect in accumulation compared to WT cells (Fig 4.10c), supporting the idea that Cxcr1 is important for Cxcl8a mediated chemotaxis. Whilst accumulation was found to be slightly enhanced in *cxcr2*$^{-/-}$ neutrophils, this did not reach statistical significance. Thus, from these results the role of Cxcr2/Cxcl8a binding in neutrophil recruitment remains less clear.

**Cxcr1 sequesters Cxcl8a**

I next considered non-cell autonomous implications of Cxcr1 trafficking. To address this I assessed intracellular accumulation of Cxcl8a in WT and *cxcr1*$^{-/-}$ neutrophils. For this, I repeated the above transplant experiment (transplanting Cxcl8a-mcherry secreting HEK293 cells, into WT and

*cxcr1*$^{-/-}$ larvae) but imaged at a higher magnification such that intracellular accumulation of fluorescent chemokine could be visualised (Fig. 4.11a). Interestingly, accumulation of fluorescently labelled Cxcl8a could be seen in WT neutrophils at the transplant (Fig. 4.11 b, upper panels). In contrast, no fluorescently labelled chemokine was visible inside *cxcr1*$^{-/-}$ neutrophils (Fig. 4.11 b, lower panels). Quantification of the levels of Cxcl8a-mcherry inside neutrophils (performed by A.G) confirmed Cxcr1 specific internalisation of the chemokine (Fig. 4.11 c). Furthermore, this assay provided an indirect confirmation of endogenous Cxcr1 internalisation in response to Cxcl8a. This is particularly useful as currently there are no available antibodies to enable visualisation of endogenous Cxcr1 and Cxcr2 receptor levels in zebrafish.

**Cxcr1 mediated sequestration can significantly affect extracellular chemokine levels**

Having shown that Cxcr1 internalisation sequesters Cxcl8a, I next asked whether cxcr1 internalisation can significantly affect the external chemokine gradient. This is an interesting question given that any such modification of the external chemokine gradient could affect behaviour of other locally migrating cells. An ideal experiment would be to assess Cxcl8a levels at wounds in WT and *cxcr1*$^{-/-}$ larvae. However, there are currently no available antibodies to enable visualisation of endogenous Cxcl8a gradients *in vivo*. As an alternative approach, I tested whether the levels of exogenous Cxcl8a can be significantly affected by Cxcr1 internalisation through expression in gastrulating embryos. I expressed Cxcl8a-eCFP in gastrulating embryos, with or without Cxcr1 receptor. In the absence of the receptor, Cxcl8a-CFP accumulated in the extracellular space as expected (Fig 4.12, left panel). When the receptor was co-injected, the chemokine was extensively internalised and the extracellular levels were significantly reduced (Fig. 4.12, right panel). This suggests that Cxcr1 internalisation can significantly affect Cxcl8a levels, though the extent at which this plays a role *in vivo* remains unknown.

**Preliminary data suggests that *cxcr1*$^{-/-}$ neutrophils show no marked cell-autonomous differences**

To further investigate cell autonomous vs non-cell autonomous effects of Cxcr1 internalisation I used a 'parabiosis' technique which enables two distinct populations of neutrophils to be compared in the same tissue. Parabiosis is a recently developed method in which two genetically distinct zebrafish blastulae are surgically fused such that they develop to be conjoined[133]. Importantly, parabiotic larvae can develop to share their circulation enabling blood cells from the two genetic

lineages to distribute between the fused larvae. This strategy therefore enables behavioural responses of genetically distinct immune cells experiencing the same signals to be directly compared *in vivo*.

I utilised a parabiosis technique to compare WT and *cxcr1*$^{-/-}$ neutrophil migration to the same inflammatory stimulus. I used differential fluorescence of *cxcr1*$^{-/-}$ and WT neutrophils to identify the two genetically distinct cells in the same larvae. Neutrophils in the *cxcr1*$^{-/-}$ line (*cxcr1*$^{-/-}$/Tg(*mpx*:GFP) fluoresce green. To visualise WT neutrophils that have endogenous Cxcr1 receptors, I therefore utilised a Tg(*lyz*:Dsred)$^{nz50}$ line[151] in which neutrophils fluoresce red. My aim was to conduct a wound in the WT larvae which would have WT tissue with a mixture of WT and *cxcr1*$^{-/-}$ neutrophils. However, in parabiotic larvae that share the circulation it is common for the blood cells to distribute evenly throughout the two con-joined larvae. As such, following fusion, it is not possible to use the colour of the neutrophils to identify which of the two fish has WT body tissue and which has *cxcr1*$^{-/-}$ tissue. To overcome this issue, I crossed a Tg(*lyz*:Dsred)$^{nz50}$ to a Tg(*ath5*:gap-GFP)[132] transgenic line in which GFP is expressed in the retina. The fluorescent retina acted as a marker and enabled identification of the WT fish post-fusion. To generate the parabiotic larvae, I performed a small surgical wound in Tg(*lyz*:Dsred)$^{nz50}$/ Tg(*ath5*:gap-GFP) and *cxcr1*$^{-/-}$ embryos between the 256-cell stage and 30% epiboly and fused the embryos at the wounded sites (Fig. 4.13 a-b). I conducted a laser wound in the WT (as identified by the green retina) head region of successfully joined 3 dpf parabiotic larvae and imaged WT and *cxcr1*$^{-/-}$ neutrophil responses to the wound (Fig. 4.13 c). An in-depth analysis was not conducted due to time constraints, but there were no clear phenotypic differences between the two neutrophil populations by visual inspection.

# 4. Discussion

**Summary of results**

The work presented in this chapter focused on understanding the functional contribution of Cxcr1 and Cxcr2 to neutrophil migration behaviour at wounds through use of receptor knockout lines. Live-imaging of neutrophil responses to ventral fin wounds in receptor knockout lines revealed that Cxcr1 and Cxcr2 show a level of redundancy at early stages of the response with both receptors contributing to forward migration. However, the two receptors have differential non-redundant roles thereafter with Cxcr1 promoting focalisation and Cxcr2 driving dispersal which promotes resolution of the response.

**Disclaimer**

Here I would like to note that another lab, also investigating the functional role of Cxcr1 and Cxcr2 through receptor knockouts, published their work during the time frame of my PhD. Given that much of my receptor knockout work was completed prior to their publication there is a degree of overlap in the results presented in this chapter and those published by Powell et al. Accordingly, the Powell el al study is referred to throughout this discussion. It is important to highlight that receptor dynamics were not addressed in the Powell et al. study and the mechanisms underlying their published knockout phenotypes remain unknown.

**Roles for Cxcr1 and Cxcr2 in neutrophil homeostasis/development**

Prior to conducting neutrophil migration assays in knockout larvae, I first determined whether the mutations affected the developmental distribution of neutrophils in WT, *cxcr1*$^{-/-}$ and *cxcr2*$^{-/-}$ larvae. This was an important consideration, as any differences in starting cell number could affect the interpretation of results in subsequent analyses. Previous studies have reported slight differences in neutrophil number in Cxcr1 and Cxcr2 knockdowns[124,152,153]. A study by Deng et al. 2013 found the number of neutrophils in the head mesenchyme of WT, Cxcr1-MO and Cxcr2-MO injected larvae to be comparable[124]. However, when quantification was restricted to the CHT region, the number of neutrophils in the CHT was found to be significantly lower in Cxcr1-MO injected larvae (approximately 33% less than WT). The number of neutrophils in the CHT of Cxcr2-MO injected larvae was higher than WT but this did not reach significance[124]. Powell et al. reported no difference in the total number of neutrophils in *cxcr1*$^{-/-}$ but found a slight increase (20%) in total

number in their TALEN-based *cxcr2*$^{-/-}$ line[152]. Thus, slight differences in neutrophil development and distribution have been reported in Cxcr1 and Cxcr2 deficient lines. Given that Deng et al. had reported differences specific to the CHT, the quantification was also split in my study and neutrophil counts were assessed both across the whole larvae and in the CHT region specifically. Neutrophil counts in fixed larvae revealed no significant difference in the CHT or in the total number of neutrophils across WT, *cxcr1*$^{-/-}$ and *cxcr2*$^{-/-}$ larvae. However, it is worth noting that there was a trend for *cxcr1*$^{-/-}$ larvae to have fewer neutrophils in the CHT, a trend which was also noticeable during live-imaging experiments. Indeed, during quantification it was difficult to distinguish neutrophils from one another at the magnification used and thus using a higher magnification would be accurate. Nonetheless, the small differences in starting cell density are insufficient to account for the differences in cell migration observed in this study.

**Cxcr1 promotes accumulation**

In my study, live-imaging of *cxcr1*$^{-/-}$ neutrophils revealed a defect in accumulation at ventral fin wounds at 1-2hpw. This is consistent with data published by Powell et al. assessing *cxcr1*$^{-/-}$ neutrophil migration to tail transections using Sudan Black staining in fixed larvae. In their study, *cxcr1*$^{-/-}$ larvae showed a defect in neutrophil accumulation with less neutrophils present in the fin at 1-6 hpw. Thus, both studies agree that Cxcr1 has a role in promoting neutrophil accumulation early in the response.

**Cxcr2 has a specific role in reverse migration**

In my study, fixed cell analysis of neutrophil responses in *cxcr2*$^{-/-}$ larvae 24 hpw revealed increased neutrophil accumulation compared to WT larvae. This result is consistent with Powell et al. who also reported enhanced accumulation of *cxcr2*$^{-/-}$ neutrophils in stained fixed-larvae at later time points. Therefore, both studies agree that Cxcr2 promotes resolution of the response. Through live-imaging of *cxcr2*$^{-/-}$ neutrophils at wound sites, both my study and that of Powell et al. show that Cxcr2 promotes resolution by driving reverse migration. However, the analytical approaches used to reach this shared conclusion were different. To track reverse migration, Powell et al. utilised a technique in which *cxcr2*$^{-/-}$ neutrophils expressed the photo-convertible protein, Dendra. Photoconversion of dendra-expressing neutrophils that have arrived at the wound facilitates subsequent tracking of these specific cells and thus serves as a method to track reverse migration. In my study, an alternative computational approach was used to track reverse migration (conducted

by A.G). Here, neutrophil trajectories were split into 'forward' and 'reverse' tracks. 'Forward' neutrophil trajectories included all those prior to neutrophil arrival at the 'occupied wound area' (owa), whilst 'reverse' neutrophil trajectories include only those after neutrophils depart the owa. Thus photo-conversion of dendra and subsequent tracking can be considered analogous to the 'reverse' trajectory analysis conducted in this project. Importantly, both approaches reached the same conclusion acting to validate the computational approach used here to score reverse migration without need of photo-activation. Furthermore, this validated the use of this approach for the analysis of reverse migration in future experiments that are presented in subsequent chapters of this thesis.

**Cxcr1 and Cxcr2 both contribute to forward traffic**

Whilst the data presented in my study revealed that *cxcr2*$^{-/-}$ neutrophils had no defect in directional sensing, they were slower at all distances suggesting a general role for Cxcr2 in promoting motility throughout the response. Interestingly, when I injected a Cxcr2-targeting MO into *cxcr1*$^{-/-}$ larvae, neutrophils showed a defect in recruitment when compared to *cxcr1*$^{-/-}$ neutrophils. This suggests that as well as having a role in reverse migration, Cxcr2 also contributes to forward migration. Thus, the two receptors are, at least to some degree, redundant with regards to driving forward migration but Cxcr1 can compensate for Cxcr2 in its absence. These results are in line with previous studies, where use of a chemical inhibitor (SB225002) of human CXCR2 also revealed a role for Cxcr2 in recruitment to wounds[123]. In these studies, fewer neutrophils were recruited to SB225002 treated tail wounds. It is worth noting that it remains unclear whether SB225002 is specific to Cxcr2 in zebrafish or whether Cxcr1 is also inhibited[154].

**Ligands responsible for Cxcr1$^{-/-}$ and Cxcr2$^{-/-}$ phenotypes**

To investigate which ligands are responsible for the *cxcr1*$^{-/-}$ and *cxcr2*$^{-/-}$ phenotypes observed, I used Cxcl8a-secreting transplants to assess the specificity of Cxcr1 and Cxcr2 for the chemokine. Neutrophils in *cxcr1*$^{-/-}$ larvae showed a defect in the percentage of cells 'on target' at Cxcl8a-secreting transplants providing further evidence that Cxcr1 binds Cxcl8a. Given that there was no difference in the number of cells on target in WT and *cxcr2*$^{-/-}$ larvae, it remains less clear whether Cxcr2 is specific to Cxcl8a. A complication in the interpretation of migratory behaviours when using the above Cxcl8a-secreting transplant assay is that neutrophils are imaged responding to a

chronic chemokine gradient instead of an acute gradient. This is because larvae are imaged one day post transplantation to allow for the resolution of any inflammatory response to the process of transplantation itself. Given the HEK293T cells constantly secrete chemokine, the shape, reach and physiological relevance of the gradient is unclear. To further address this question in knockout larvae, it would be interesting to knockdown Cxcl8a by injection of morpholino and assess *cxcr1*$^{-/-}$ and *cxcr2*$^{-/-}$ neutrophil responses at ventral fin wounds. Whilst my studies in *cxcr2*$^{-/-}$ larvae did not confirm specificity for Cxcl8a, the knockout phenotype did confirm that the ligand for Cxcr2 is present at the wound site. This is an important point given that, from the data presented in the previous chapter, it remained unclear whether Cxcr2 is sustained at the membrane in response to its ligand or whether it is sustained because the ligand is not present. Thus, Cxcr2 is relatively sustained in response to its ligand present at wound sites.

**Endogenous neutrophil Cxcr1 sequesters Cxcl8a**

Having shown that Cxcr1 exhibits extensive internalisation in response to Cxcl8a, I next asked whether internalisation led to concurrent sequestration of the bound chemokine. Through transplantation of Cxcl8a-mcherry secreting HEK293T cells I show that neutrophils internalise the chemokine and that, more specifically, this is dependent on Cxcr1. Through expression of Cxcr1 in gastrulating embryos I showed that Cxcr1 internalisation can significantly affect extracellular chemokine levels. Thus Cxcr1-driven Cxcl8a consumption could play a role in the decay of the chemoattractant signal, promoting resolution of the response or it may have other implications[155]. In other systems, receptor internalisation-mediated chemokine consumption has been shown to pattern extracellular gradients and affect the migration of cells experiencing the modified gradient. For example, a group of receptors known as ‘atypical chemokine receptors’ bind and internalise chemokine, modifying external chemokine levels and regulating the responses of other GPCRs that bind the same ligand. The formation of functional physiological gradients of CCL21 in the murine lymph node was found to be dependent on the expression of the atypical receptor CCRL1 (also known as ACKR4) which also binds CCL21[145]. Receptor internalisation and associated chemokine sequestration has also been linked to the migration behaviour of the lateral line primordium during development. Here it was shown that internalisation of Cxcr7 shapes the Cxcl12 gradient and drives Cxcr4 mediated migration of the primordium[128]. It would be interesting to confirm to what extent WT and *cxcr1*$^{-/-}$ neutrophils differentially affect endogenous Cxcl8a gradients *in vivo* and to further investigate how this functionally affects neutrophil responses. Owing to a lack of Cxcl8a

antibodies, I was not able to test this during my project. Future studies could aim to address this by injecting recombinant Cxcl8a protein into WT and *cxcr1*$^{-/-}$ larvae and testing (by western blot) how the levels of Cxcl8a change over time.

**Chemokine sequestration in *cxcr1*$^{-/-}$ neutrophils confirms internalisation of endogenous receptor**

In the previous chapter I investigated how exogenously expressed Cxcr1-FT and Cxcr2-FT respond to physiological gradients *in vivo*. The results I presented showed that exogenously expressed Cxcr1-FT exhibits extensive internalisation. However, it could be argued that this may not fully reflect the behaviour of the endogenous receptor. For example, endogenous membrane levels could be affected by transcriptional or translational regulation and these regulatory sequences were not included in my construct. However, monitoring endogenous Cxcr1 and Cxcr2 levels is not a trivial task given that there are currently no knock-in fluorescent reporter lines and no available antibodies for either of these zebrafish receptors. In this chapter I addressed this question using the *cxcr1*$^{-/-}$ line. I transplanted Cxcl8a-secreting HEK293T cells into WT and *cxcr1*$^{-/-}$ and used intracellular sequestration of chemokine as an in-direct read-out for endogenous Cxcr1 internalisation. The presence of fluorescently-labelled Cxcl8a within WT but not *cxcr1*$^{-/-}$ neutrophils provided strong evidence for internalisation of endogenous Cxcr1. To further test endogenous Cxcr1 receptor levels, fluorescently-labelled Cxcl8a (recently obtained in our lab) could be used in combination with *cxcr2*$^{-/-}$ neutrophils to indirectly monitor endogenous Cxcr1 levels upon exposure to chemokine *in vitro*. As far as we know, *cxcr2*$^{-/-}$ neutrophils only have one Cxcl8a binding receptor, Cxcr1. This knockout line could therefore be used to study Cxcr1 receptor independently/specifically. Given the results from this study, pre-incubation of *cxcr2*$^{-/-}$ neutrophils with non-labelled chemokine (priming) would be expected to induce Cxcr1 internalisation. Subsequent staining of these cells with fluorescently labelled chemokine (on ice) would enable the change in levels of endogenous Cxcr1 to be indirectly measured via the fluorescently tagged receptor-bound chemokine.

**Approaches to elucidate cell autonomous from non-cell autonomous functions of Cxcr1 and Cxcr2**

To investigate whether the observed *cxcr1*$^{-/-}$ phenotype was due to cell-autonomous effects on neutrophil migration, I performed parabiosis experiments. These experiments in which two larvae

are fused facilitate the direct comparison of genetically distinct cells responding to the same wound. My initial aim was to compare migration of the two cell types at ventral fin wounds however, given that parabiotic larvae tended to develop such that their ventral fin was not accessible for wounding this was not possible. Thus, I instead utilised a laser wound technique targeted to the head region which was consistently accessible across larvae. Transition to the laser wound assay in the head was not ideal given that the ventral fin wound assay is used throughout the rest of this study. It remains unclear how consistent neutrophil responses are across the two assays. Indeed, there appeared to be less recruitment overall to a head laser wound and many of the early recruited cells tended to 'stick' at the laser wound margin which was not the typical response observed in ventral fin wounds. Whilst I did not observe any noticeable difference in migration behaviour, it is worth highlighting that these videos were not quantified and it remains possible that an in-depth trajectory analysis could identify differences between the two cell types. It would be possible and interesting to conduct this experiment using the ventral fin wound assay in suitable parabiotic larvae that develop with access to the ventral fin.

**Validation of *cxcr1*$^{-/-}$ and *cxcr2*$^{-/-}$ lines**

It is often not straightforward to validate protein knockouts in the zebrafish given the lack of target-specific antibodies currently available in this model. Indeed, there are currently no available antibodies targeting Cxcr1 or Cxcr2 in zebrafish. I was therefore unable to directly assess protein levels and confirm protein knockout via western blot in this study. An alternative approach to validate protein knockout could be to assess WT transcript levels. For example, RT-PCR could be performed in WT and receptor knockout fish using primers that bind to the truncated region of the transcript. Here, PCR product would be predicted to be present in WT fish but not in receptor knockout fish. A lack of WT transcript in knockout fish would provide indirect evidence for the presence of the mutant truncated transcript. It remains unclear as to whether the mutant transcript is degraded via the nonsense mediated RNA decay surveillance pathway[156] or whether the mutant transcript is translated, either into a functional or non-functional truncated protein. It is worth noting that data presented later in this thesis (Chapter 5, Fig 5.2) suggests that a significantly less severe truncation of the Cxcr1 C-terminus (Cxcr1-trunc mutant truncated at amino acid 330/364) results in translation of a protein that is unable to be integrated into the membrane, strongly suggesting that the more substantial truncations in the knockout mutants would, if successfully translated, result in non-integrated and thus non-functional receptors. It is important to highlight

that from my data presented in this chapter, I do show that there is strong phenotypic support for *cxcr1*$^{-/-}$ and *cxcr2*$^{-/-}$ being true null mutant lines.

# 4. Figures

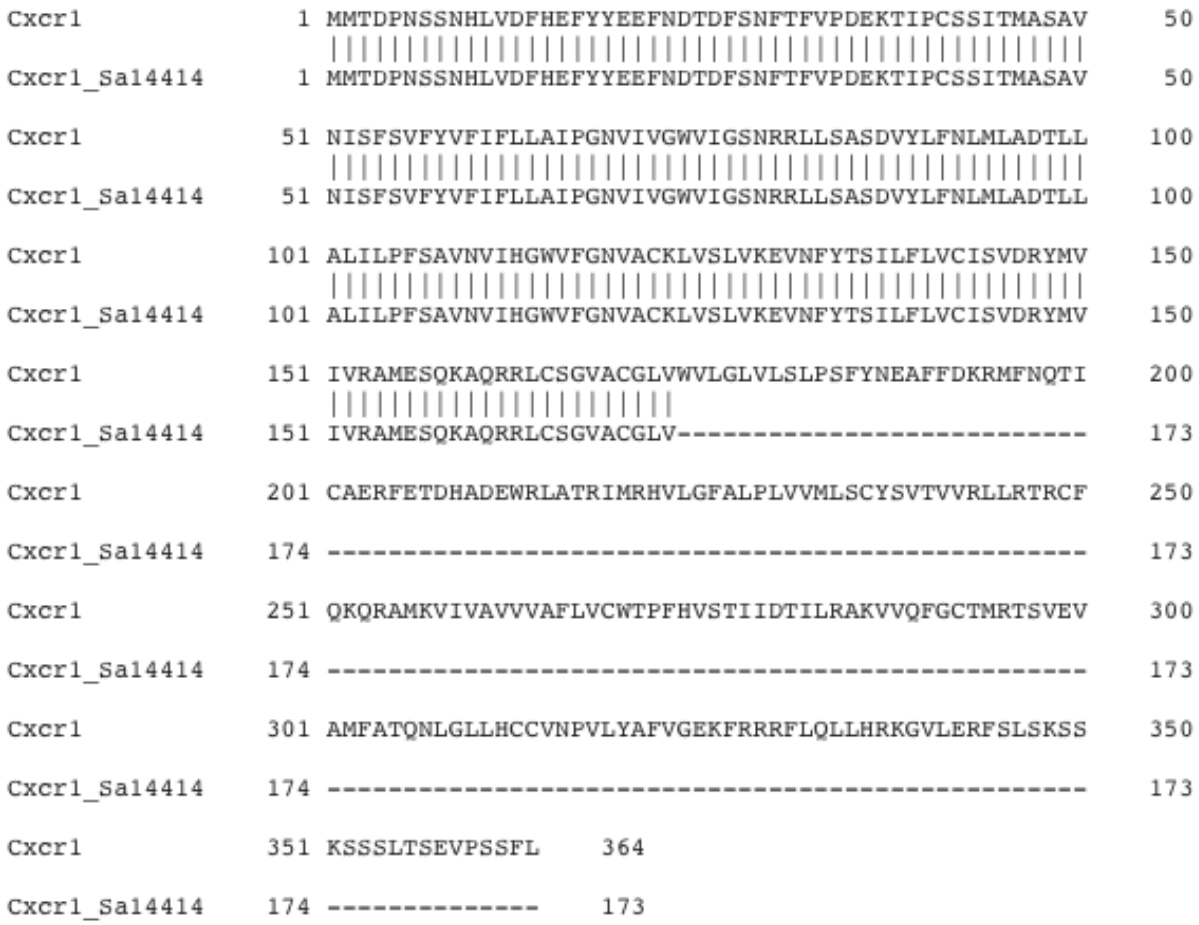


**Figure. 4.1. Nucleotide alignment of wildtype *cxcr1* and the *cxcr1* mutant allele (*cxcr1*$^{Sa14414}$).** Sequences aligned using Basic Local Alignment Search Tool (BLAST).


**Figure 4.2. Nucleotide alignment of wildtype *cxcr2* and the *cxcr2* mutant allele (*cxcr2*$^{sa6118}$).** Sequences aligned using Basic Local Alignment Search Tool (BLAST).

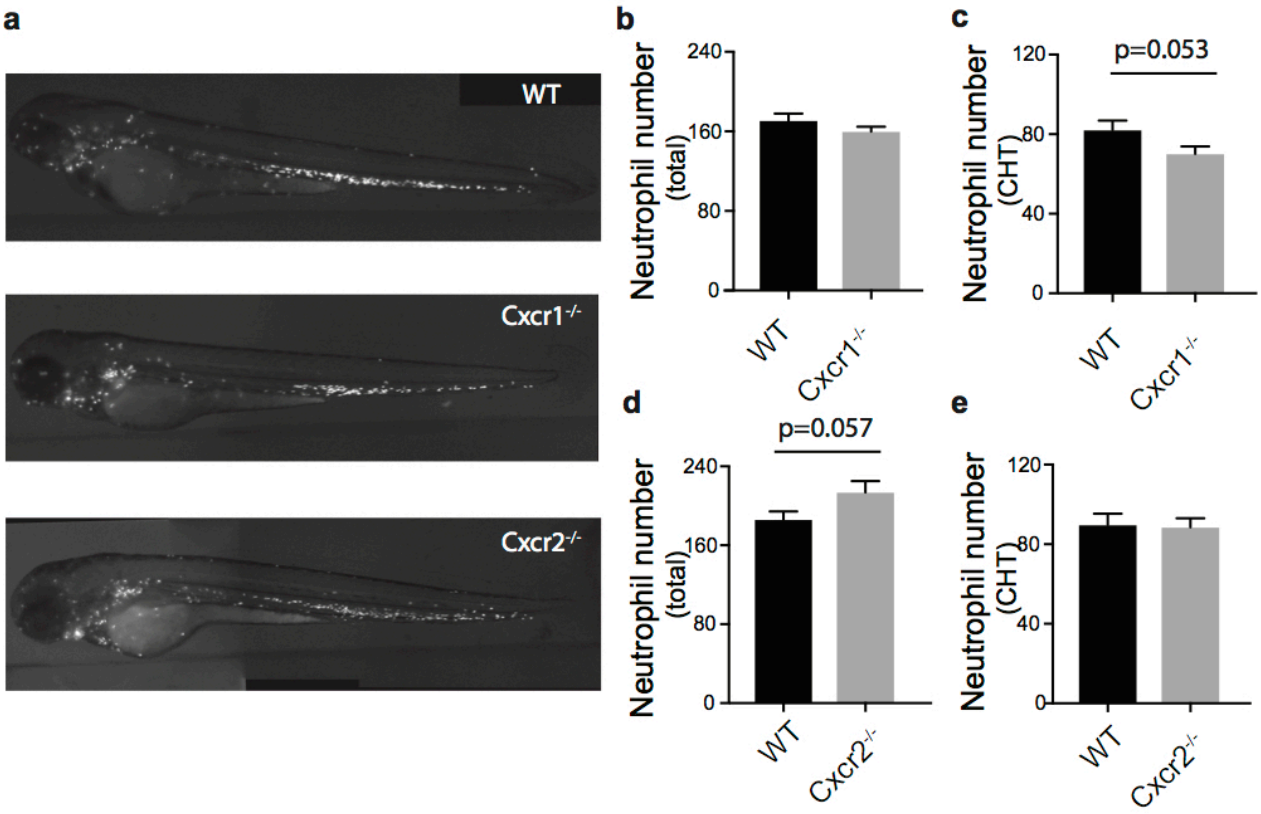


**Figure 4.3. Neutrophil distribution and neutrophil counts in wild type, *cxcr1*$^{-/-}$ and *cxcr2*$^{-/-}$ Tg(*mpx*:GFP)$^{i114}$ larvae.** a) Fluorescent microscopy images of non-challenged 3dpf wild-type/ Tg(*mpx:*GFP)$^{i114}$ (top), *cxcr1*$^{-/-}$/Tg(*mpx:*GFP)$^{i114}$ (middle) and *cxcr2*$^{-/-}$/Tg(*mpx:*GFP)$^{i114}$ (lower) larvae. Acquired by H.W. b) Number of neutrophils in whole wild-type and *cxcr1*$^{-/-}$ larvae. c) Number of neutrophils in CHT of WT and *cxcr1*$^{-/-}$ larvae. d) Number of neutrophils in whole WT and *cxcr2*$^{-/-}$ larvae. e) Number of neutrophils in CHT of WT and *cxcr2*$^{-/-}$ larvae. Unpaired t test (b-e). n=18 wild type, n=31 *cxcr1*$^{-/-}$ (b,c) and n=21 wildtype n=21 *cxcr2*$^{-/-}$ (d,e). Error bar represents SEM. Neutrophil counts by H.W.

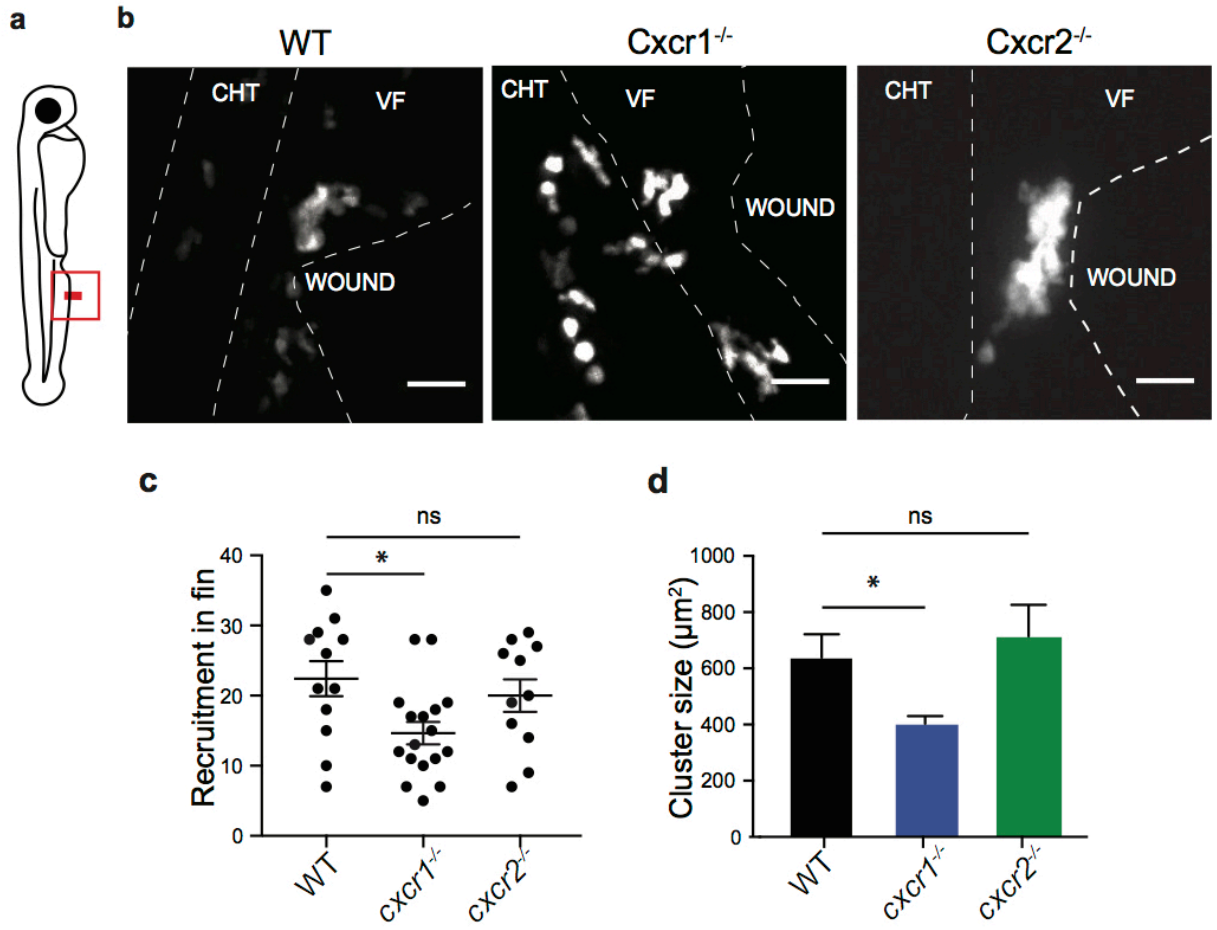


**Figure 4.4. Differential contributions of Cxcr1 and Cxcr2 in neutrophil migration at wounds** a) Schematic of larva indicating area wounded (red line) and area imaged (red box). b) Confocal projection images showing distribution of neutrophils at the wound in WT/Tg(mpx:GFP) (left), *cxcr1*$^{-/-}$ /Tg(*mpx*:GFP) (middle) or *cxcr2*$^{-/-}$/Tg(*mpx*:GFP) (right) larvae at 2 hpw. CHT=caudal hematopoietic tissue. VF= ventral fin. Dashed line shows outline of ventral fin and CHT. Scale bar=25µm. c) Number of recruited neutrophils at 2hpw, within a square area of 200µm length around the wound. One-way ANOVA with Tukey's multiple comparisons test. n=12 (WT), n=17 (*cxcr1*$^{-/-}$) and n=11 (*cxcr2*$^{-/-}$) larvae. Larvae shown in panel a are represented with a red dot in these plots. d) Average neutrophil cluster size per larva. n=12 (WT), n=17 (*cxcr1*$^{-/-}$) and n=11 (*cxcr2*$^{-/-}$) larvae. Kruskal-Wallis test with Dunn's multiple comparisons test. Quantification (c,d) by A.G.

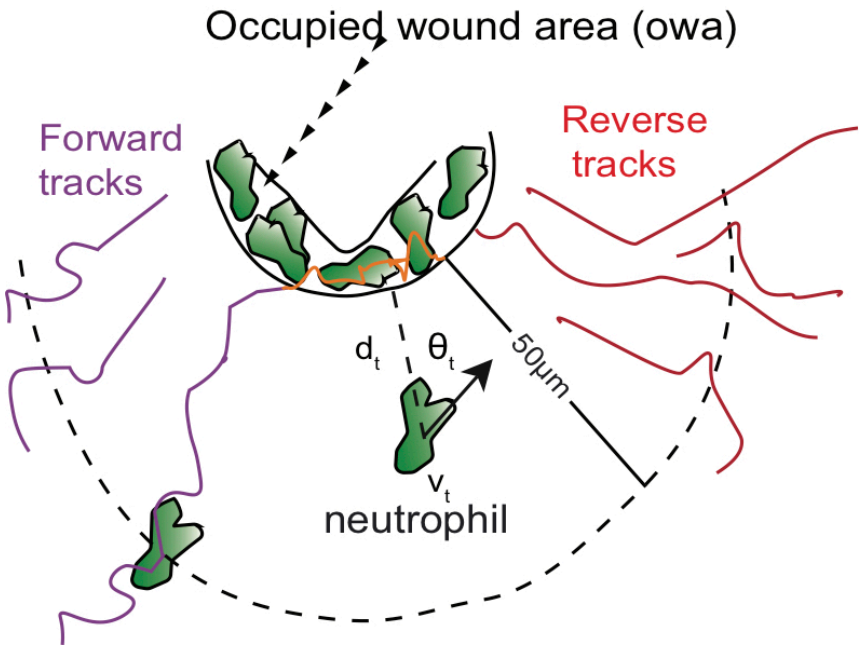


**Figure 4.5. Forward and reverse trajectory analysis**. Schematic depicting trajectory parameters measured. Wound-occupied area (woa) is the area of the neutrophil cluster. Forward (purple) and reverse (red) segments of cell trajectories are defined as the path of neutrophils prior to entering and after entering leaving the woa respectively. The angle θ is defined as the angle of the neutrophil vector in relation to the closest point of the woa. dt, vt and θt refer to distance, velocity, and cosineθ over time respectively.

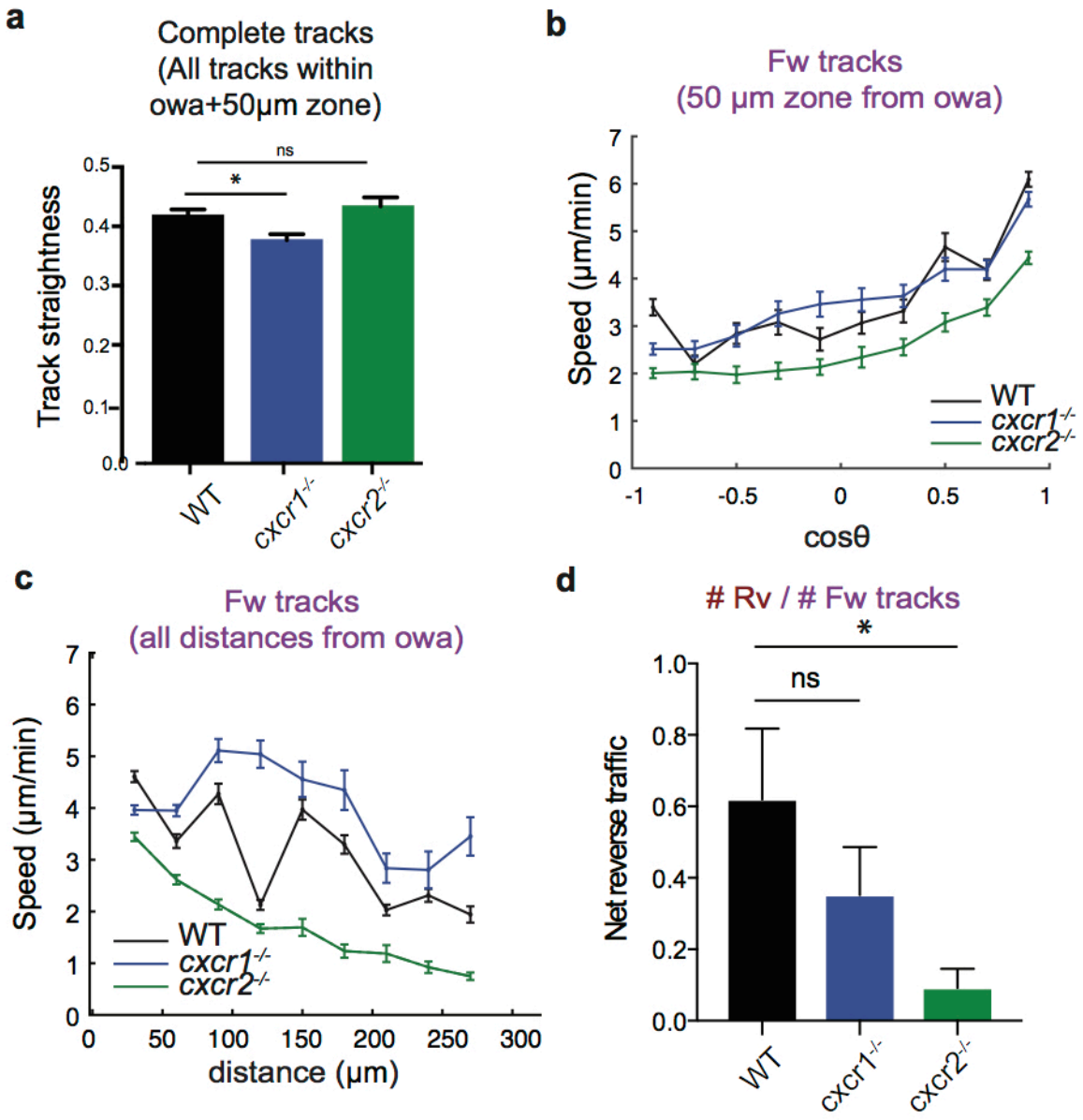


**Figure 4.6. Cxcr2 promotes motility and reverse migration** a) Neutrophil track straightness. Track data within the owa and an area extending 50 µm beyond. n=680 tracks (WT), n=603 tracks (*cxcr1*$^{-/-}$) and n=319 tracks (*cxcr2*$^{-/-}$) larvae. Kruskal-Wallis test with Dunn's multiple comparisons test. b) Neutrophil speed in relation to cosine of the angle θ from the owa. Track data within a zone of 0-50 µm from the owa are shown. n=131-2423 steps per bin (WT), n=11-3008 steps per bin (*cxcr1*$^{-/-}$), n=88-2823 steps per bin (*cxcr2*$^{-/-}$) larvae. c) Neutrophil speed in relation to distance from the owa. Average speeds per cell step per distance bin are n=133-1227 steps per bin (WT), n=231-1436 steps per bin (*cxcr1*$^{-/-}$), n=202-1382 steps per bin (*cxcr2*$^{-/-}$) larvae. d) Neutrophil traffic as measured by number of reverse tracks over number of forward tracks. For all panels error bars represent standard error of either pooled cell means across n=12 wild-type larvae, n=17 cxcr1$^{-/-}$ larvae from 6 and 10 imaging sessions respectively. Cells were analysed for two hours from the start of the movie. Quantificaton by A.G.

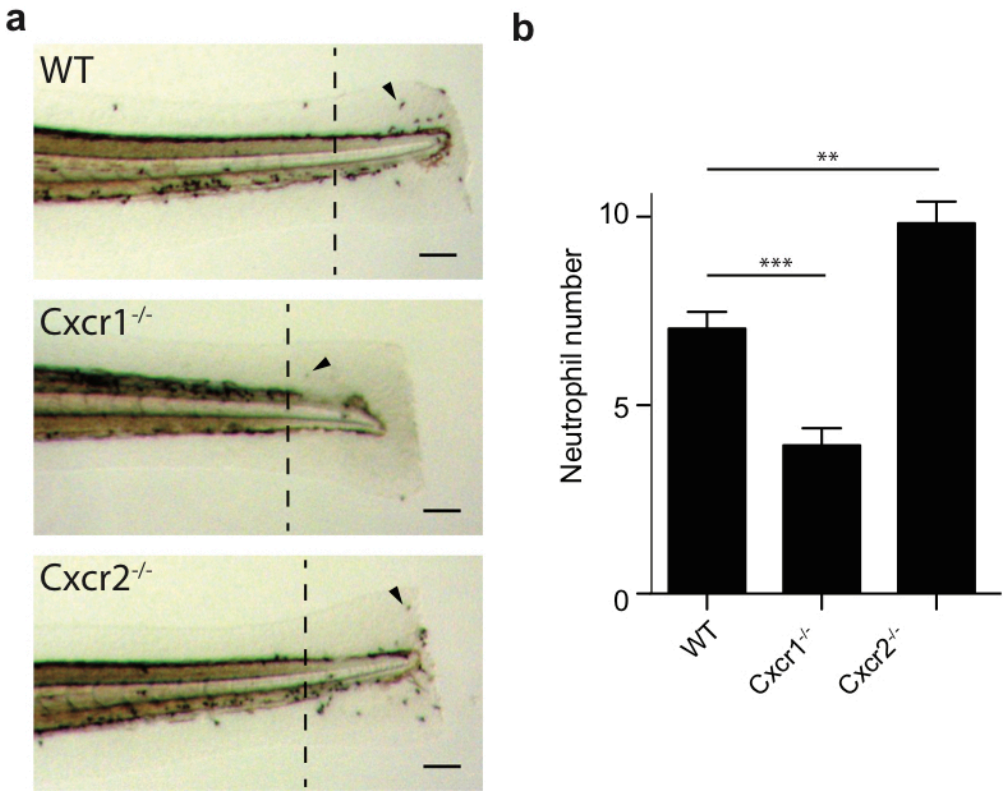


**Fig 4.7. Cxcr1 knockdown facilitates resolution whilst Cxcr2 knockdown compromises resolution of inflammation.** A) Bright field images of fixed, sudan black-stained embryos at 24h post tail fin wound. Arrows point to examples of neutrophils. Neutrophil number within the proximal ventral, dorsal and tail fin were counted. For consistency, neutrophils were counted within a distance corresponding to about 250-300µm from the end of the notochord (dashed line). b) Quantification of neutrophil number. Error bars represent standard error of the mean (SEM). Kruskal-Wallis test with Dunns multiple comparison test. n=95 for WT/Tg(*mpx*:gfp), n=69 for Cxcr1 $^{-/-}$/mpx:gfp and n=104 for *cxcr2*$^{-/-}$/Tg(*mpx*:gfp). Pooled from 4 experiments. Neutrophil staining and counts performed by myself and C.K.

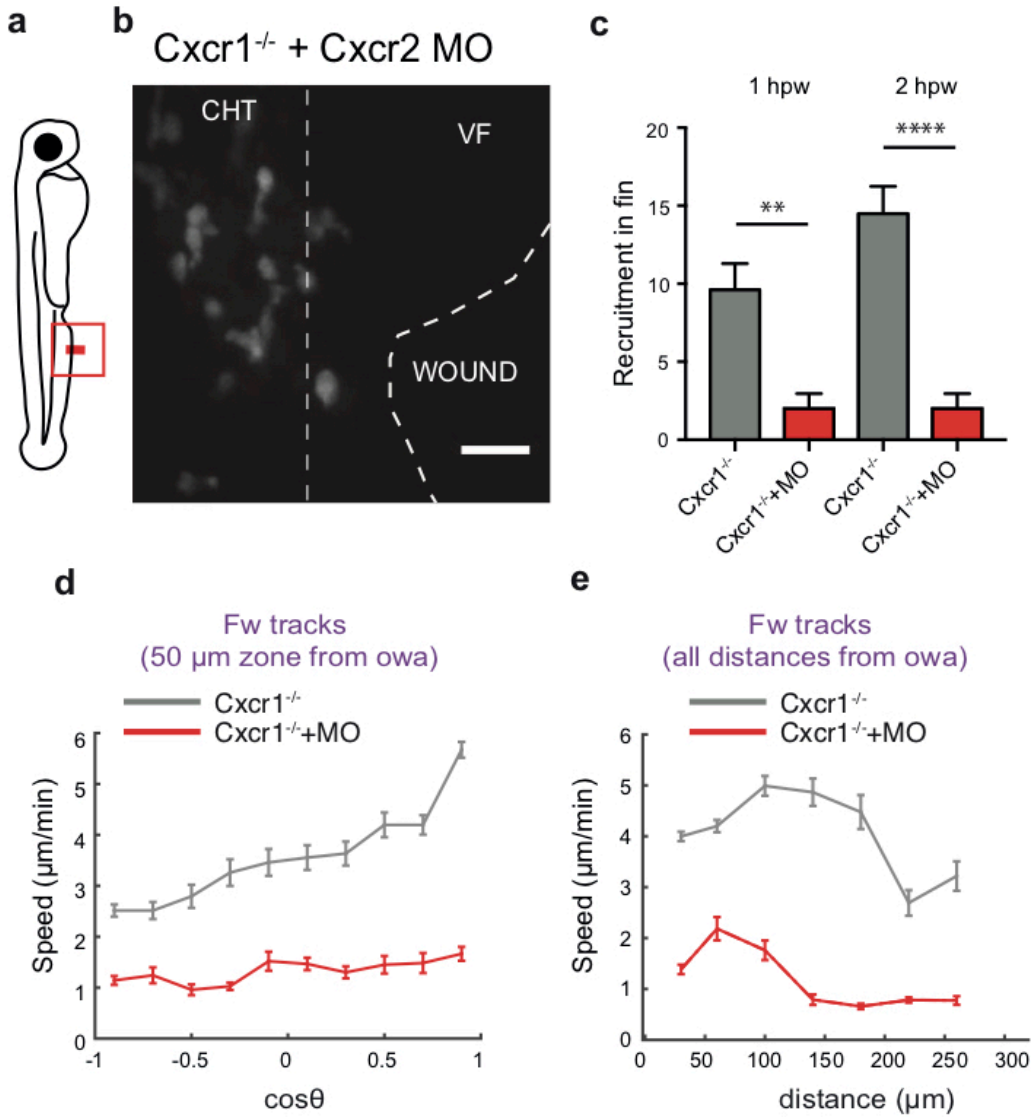


**Figure 4.8. Cxcr2 morpholino knockdown in *cxcr1*$^{-/-}$ larvae inhibits recruitment to wound**. a) Schematic showing region wounded (red line) and imaged (red box). b) Confocal projection image of neutrophil recruitment to a ventral fin wound at 1hrpw in Cxcr2 morpholino injected Cxcr1$^{-/-}$ larvae. CHT=caudal hematopoietic tissue. VF=ventral fin. Scale bar 25um. c) Neutrophil recruitment to the ventral fin at 1hpw and 2hpw within a sample square field of 200µm length around the wound. n=17 (*cxcr1*$^{-/-}$) and n=8 (*cxcr1*$^{-/-}$ + MO) larvae, from 10 and 3 imaging sessions respectively. Two-tailed Mann-Whitney test d) Neutrophil speed in relation to cosine of angle θ (cosθ). Average speeds per cell per cosθ bin shown. n=231-1436 steps per bin (*cxcr1*$^{-/-}$) and n=24-213 steps per bin (*cxcr1*$^{-/-}$ + MO) larvae. Track data within a zone of 0-50 µm from the owa are shown. e) Neutrophil speed in relation to distance from wound. Average speeds per cell per distance are shown. n=19-2922 steps per bin (*cxcr1*$^{-/-}$) and n=41-603 steps per bin (*cxcr1*$^{-/-}$ + MO) larvae. c,d) Data are from 17 (*cxcr1*$^{-/-}$) and 8 (*cxcr1*$^{-/-}$ + MO) larvae from 10 and 3 imaging sessions respectively. Quantification (b-e) by A.G.

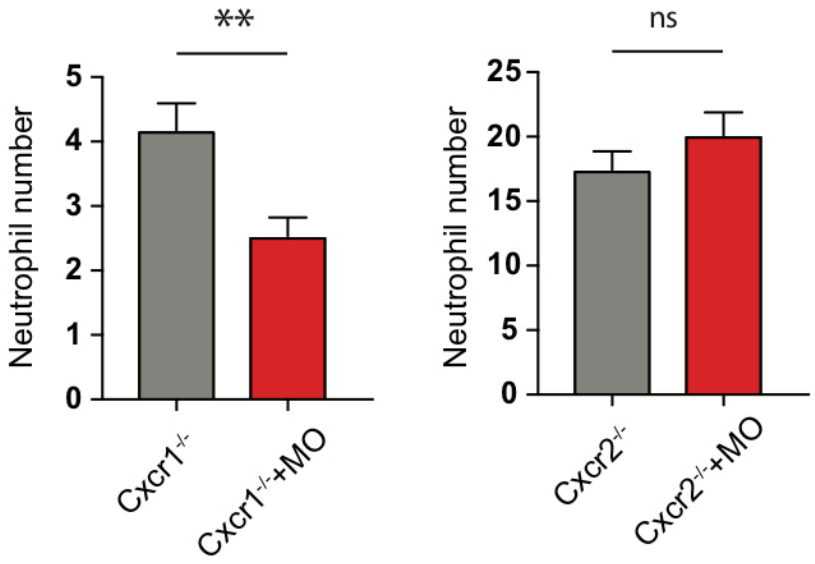


**Figure 4.9. Cxcr2 morpholino specifically targets Cxcr2**. Quantification of neutrophil number at tail wound of fixed, sudan black stained 3dpf larvae at 4 hours post-wound. Mann Whitney test. Error bars represent standard error of the mean from n=57 *cxcr1*$^{-/-}$, n=69 morpholino injected *cxcr1*$^{-/-}$ larvae, n=64 *cxcr2*$^{-/-}$ larvae and n=68 morpholino-injected *cxcr2*$^{-/-}$ larvae.

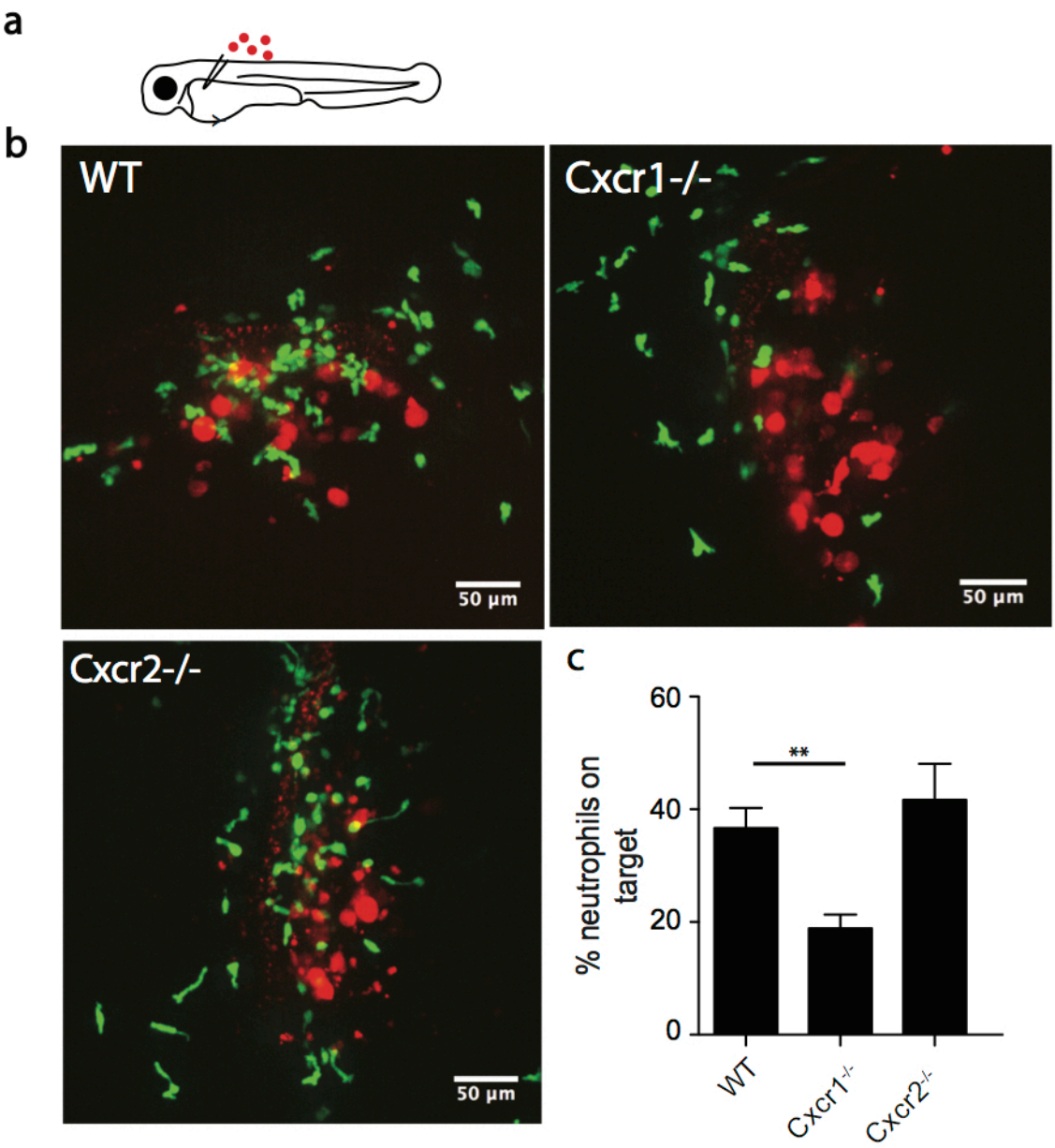


**Figure 4.10. *cxcr1*$^{-/-}$ neutrophils show defective accumulation at Cxcl8a secreting transplant**. a) Schematic of larva depicting area of transplantation of Cxcl8a- mCherry secreted cells. Confocal projections of neutrophils (green) in WT (mpx:gfp) or *cxcr1*$^{-/-}$ Tg(*mpx*:gfp) or *cxcr2*$^{-/-}$/Tg(*mpx*:gfp) larvae, transplanted with Cxcl8a-mCherry-expressing cells (red). Scale bar, 50µm. c) Quantification of percentage of neutrophils in contact with chemokine-expressing cells ('on target'). n=12,10,5 embryos for WT, *cxcr1*$^{-/-}$ and *cxcr2*$^{-/-}$ acquired in 3, 3 and 2 imaging sessions respectively. ANOVA with Bonferroni multiple comparison test.

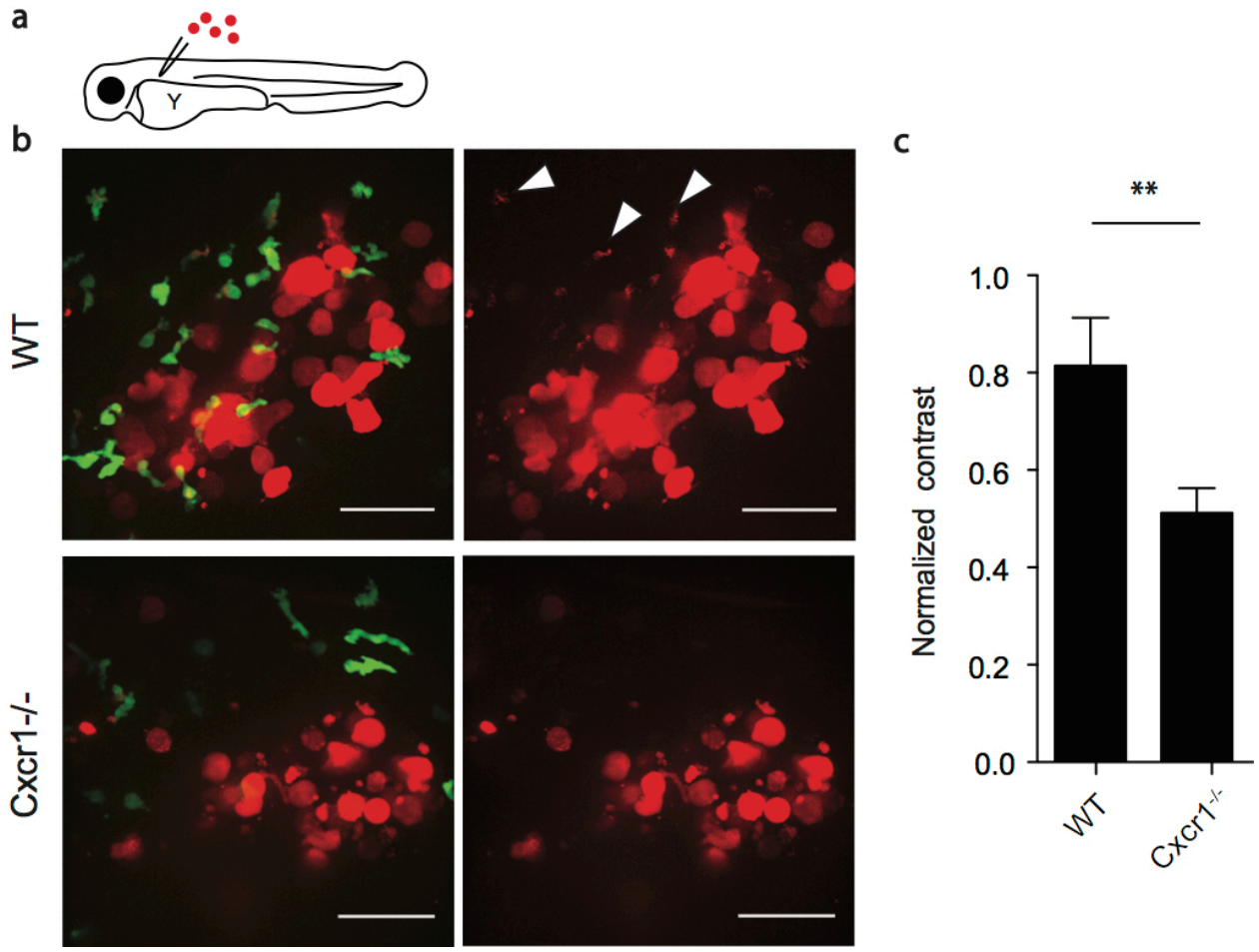


**Figure 4.11. Cxcr1 consumes extracellular Cxcl8a**. a) Schematic of larva indicating the area of transplantation of Cxcl8a-secreting cells. b) Confocal projections of wild-type (mpx:gfp) or *cxcr1*$^{-/-}$ /Tg(*mpx*:gfp) responding to Cxcl8a-secreting cells. Arrows point to internalised chemokine in GFP+ neutrophils. Scale bar, 50µm. c) Quantification of levels of Cxcl8a-mCherry inside neutrophils. Pixel contrast within segmented neutrophils normalised to mean intensity of transplant in the same image. Levels in the *cxcr1*$^{-/-}$ condition correspond to background signal detection by the segmentation algorithm. n=33 cells from 3 embryos for *cxcr1*$^{-/-}$, n=29 from for 2 embryos for WT, from 2 imaging sessions. Unpaired t test. Quantification (c) by A.G.

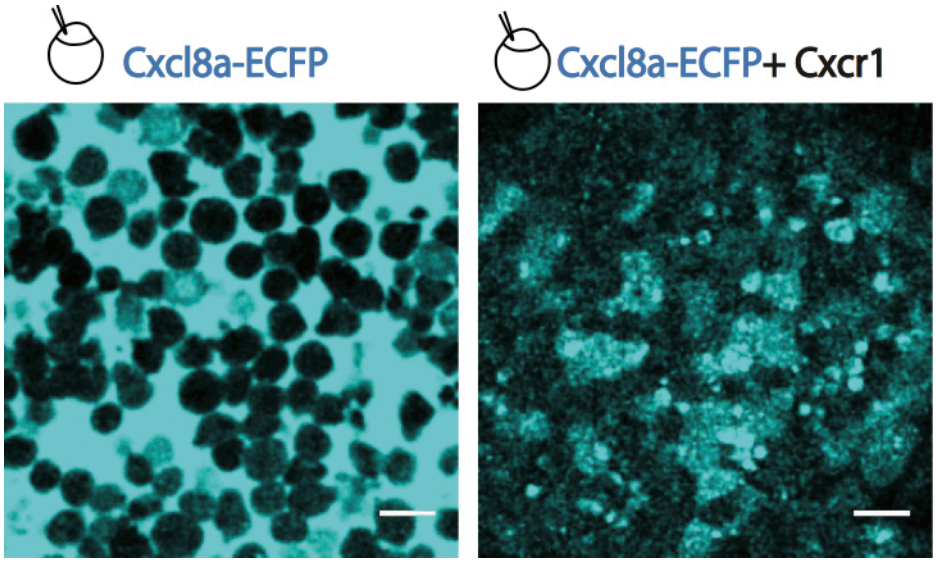


**Fig 4.12. Cxcr1 internalisation can modify external chemokine levels**. 30pg Cxcl8a-ECFP mRNA was injected without (left) or with (right) 100pg Cxcr1 mRNA. Laser scanning confocal slices of gastrulating embryos showing Cxcl8a-ECP tissue distribution. Scale bar, 25μm.

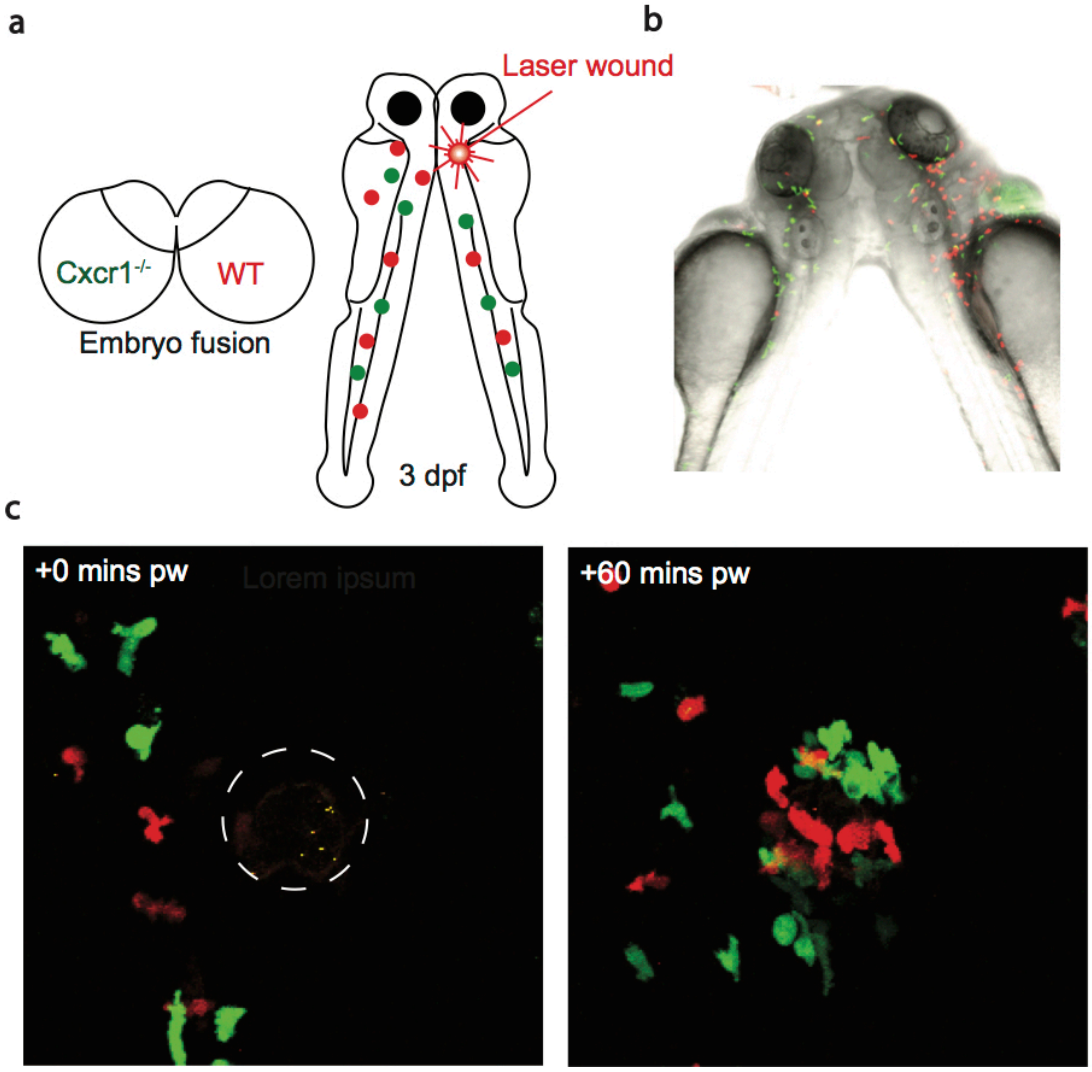


**Figure 4.13. Use of parabiosis approach to investigate cell-autonomous receptor roles.** a) Schematic of parabiosis approach. Fusion was performed at the blastula stage between WT Tg(*Lyz*:Dsred) and *cxcr1*$^{-/-}$/Tg(*mpx*:GFP) larvae b) Confocal image showing an example of a parabiotic fish with both red (wt) and green (*cxcr1*$^{-/-}$) neutrophils at 3 dpf. c) Snapshots from two-photon movie showing wt (red) and *cxcr1*$^{-/-}$ (green) neutrophil responses to a laser wound in a representative parabiotic WT fish. Timepoint following laser wound is indicated in minutes. Dashed circle indicates position of laser wound.

# Chapter 5: Differential trafficking of Cxcr1 and Cxcr2 balances neutrophil clustering and dispersal at wounds

## 5. Introduction

The focus of this chapter was to determine whether the differential trafficking of Cxcr1 and Cxcr2 (internalisation vs sustenance) is responsible for the distinct functional contributions of the two receptors (i.e. clustering versus dispersal). To investigate this, my aim was to manipulate receptor trafficking through the generation of mutant receptors and analyse the effects on cell migration behaviour at target sites.

The role of receptor trafficking in generating specific cell migration behaviours has been studied in other systems. For example, the role of receptor desensitisation has been studied in neutrophil migration in WHIM syndrome, an immunodeficiency disorder characterised by warts, hypogammaglobulinemia (low antibody count), recurrent bacterial infection and myelokathexis (increased number of mature myeloid cells in bone marrow and concurrent peripheral blood neutropenia) [5,157]. In most cases, WHIM syndrome results from mutations in the C-terminus of CXCR4 which leads to the synthesis of a truncated CXCR4 receptor that is unable to be phosphorylated and is not able to desensitise[65]. CXCR4 binds the chemokine CXCL12 (also known as SDF1a), a signalling pathway that is important in regulating homeostatic neutrophil release from the bone marrow. In WHIM syndrome, the defect in receptor desensitisation has been shown to result in persistent CXCR4-CXCL12 signalling[65]. This 'over-engagement' of neutrophils to CXCL12 prevents neutrophils from responding to other sources of alternative attractants that would usually draw them out of the bone marrow. Consequently, neutrophils are retained in the bone marrow and normal homeostasis is disrupted[5]. Thus, in this setting, blocking of receptor desensitisation (through receptor truncation) prevents cells from moving towards other sources of alternative attractants. The behavioural implication of receptor desensitisation has also been studied during developmental processes and has been shown to play an important role in fine-tuning migration of primordial germ cells (PGCs)[158]. PGCs, the progenitors of germline cells, express the receptor Cxcr4b which binds to the chemokine Cxcl12 (Sdf1a). During development, PGCs follow gradients of Cxcl12 and migrate to what will become the gonad where they then differentiate.

Interestingly, when Cxcr4b desensitisation was blocked through truncation of the C-terminal domain, cells were found to overshoot their target and failed to accumulate at the target site. Instead, cells were found to migrate to alternative ectopic sites of Cxcl12 production. In this setting, blocking desensitisation through receptor truncation led to cells overshooting their target. The behavioural impact of desensitisation differs in the examples studied so far. Thus, it is difficult to predict how receptor trafficking might regulate neutrophil migration during inflammatory responses. Indeed, the implication of receptor trafficking on neutrophil inflammatory responses *in vivo* has not been studied.

# 5. Objectives

- Generate mutant receptors and identify those defective in internalisation/desensitisation
- Generate zebrafish transgenic rescue lines in which mutant receptors are expressed specifically in neutrophils
- Conduct live-imaging to investigate behavioural implications of receptor desensitisation on neutrophil migration behaviour at wounds

**Notes on contributions:**

Antonios Georgantzoglou (A.G) conducted most of the image analysis presented in the results section of this chapter. His contribution is noted throughout the text and figure legends. Any contribution to analysis made by Milka Sarris (M.S) is also referred to in the text and figure legends.

# 5. Results

### Generation of Cxcr1 mutant receptors

I generated internalisation-deficient Cxcr1 receptors by targeting mutations to the serine-rich region of the C-terminus (Fig. 5.1). Serine residues in the C-terminus are substrates for GRK phosphorylation and have been shown to regulate receptor internalisation[136159]. I generated multiple different mutant receptors, by PCR, which each carried different mutations in this region. I generated a 'Cxcr1-trunc' mutant in which the Cxcr1 receptor was truncated through deletion of the entire C-terminus (including the serine-rich region). I also generated a more conservative 'Cxcr1-ser' mutant in which only the serine-rich region of the Cxcr1 C-terminus was deleted. I generated a 'Cxcr1-ala' mutant in which all serine residues in the C-terminus were substituted for alanine residues which cannot be phosphorylated. Finally, I generated a chimeric 'Cxcr1-chim' receptor in which the Cxcr1 C-terminus was substituted for that of Cxcr2. Given the receptor trafficking results presented in chapter 3, the Cxcr2 terminus was expected to bear the motifs necessary for membrane sustenance. This was deemed a more physiologically relevant method of enforcing membrane sustenance. Despite the limited used of tagRFP in this system, I retained usage of the FT-cassette when generating mutant receptors. This was to maintain consistency in analysis and to facilitate screening of transgenic embryos based on the brighter signal of tagRFP.

### Effect of receptor mutagenesis on plasma membrane distribution

Following generation of the above mutant receptors, the first step was to determine which, if any, of the mutations resulted in a receptor that is unable to internalise in response to Cxcl8a. To this end, I expressed mutant receptors in zebrafish gastrulating embryos and assessed receptor responses to co-injected Cxcl8a. The complete C-terminus truncation mutation (Cxcr1-trunc) resulted in a receptor that was unable to traffic to the membrane even when expressed in the absence of Cxcl8a (Fig. 5.2). Therefore, these images were not quantified and this mutant receptor was not used in any further experiments. Both the Cxcr1-ser (Fig. 5.3) and Cxcr1-ala mutant receptors (Fig 5.4) appeared membranous (i.e. did not internalise) in the presence of Cxcl8a. Interestingly, above a certain concentration of Cxcl8a (40 pg), Cxcr1-ala receptor expression proved to be lethal, whilst the Cxcr1-ser receptor had no toxic effect at any concentrations tested. This suggested that the Cxcr1-ala receptor retained its ability to signal and, through its enforced membrane sustenance, transmitted excessive signalling that was toxic to the embryo. Given that these results suggested

that Cxcr1-ala retained its ability to signal, I selected this receptor for future experiments. For this reason, Cxcr1-ser expressing embryos were not quantified. Quantification of Cxcr1-ala receptor distribution in gastrulating embryos confirmed that this mutant receptor is sustained in response to Cxcl8a (Fig. 5.5). Due to time restraints, I did not test internalisation of the Cxcr1-chim receptor in gastrulating embryos. Instead, I expressed this receptor, and observed the response to endogenous ligand, directly in neutrophils (see following section).

**Cxcr1-ala and Cxcr1-chim expressed in neutrophils remain membranous in response to endogenous chemokine**

Having identified which of the generated mutant receptors were unable to internalise, the next step was to express the internalisation deficient receptors in neutrophils and confirm that they are not internalised in response to endogenous gradients at wound sites. To this end, I generated new Tg(*lyz*:Cxcr1-FT); *cxcr1*$^{-/-}$, Tg(*lyz*:Cxcr1_ala-FT); *cxcr1*$^{-/-}$, and Tg(*lyz*:Cxcr1_chim-FT); *cxcr1*$^{-/-}$ fish lines in which Cxcr1-wt, Cxcr1-ala or Cxcr1-chim receptors were expressed in neutrophils in a *cxcr1*$^{-/-}$ background. Expressing mutant receptors in a knockout background would exclude any contribution of endogenous Cxcr1 receptors. To assess receptor responses in response to endogenous gradients, I conducted a ventral fin wound in Tg(*lyz*:Cxcr1-FT); *cxcr1*$^{-/-}$, Tg(*lyz*:Cxcr1_ala-FT); *cxcr1*$^{-/-}$, and Tg(*lyz*:Cxcr1_chim-FT); *cxcr1*$^{-/-}$ larvae and analysed receptor responses during neutrophil migration to the target site. As expected, consistent with earlier observations in Tg(*Lyz*:Cxcr1-FT) neutrophils, the Cxcr1-wt receptor was progressively internalised as neutrophils approached the wound site (Fig. 5.6a left panel, and b). Importantly, neither the Cxcr1-ala (Fig. 5.6a middle panel, and b) or Cxcr1-chim (Fig. 5.6 a right panel, and b) mutant receptors were internalised at the target site. This confirmed that when expressed in neutrophils, both Cxcr1-ala and Cxcr1-chim are unable to internalise in response to endogenous gradients present at wound sites. Given that both receptor mutants showed a gain of plasma membrane sustenance it was expected that any shared gain of function behaviors would point to the functional importance of plasma membrane sustenance.

**Cxcr1-WT rescues Cxcr1$^{-/-}$ clustering defect**

I next assessed the behavioural implications of the Cxcr1 internalisation deficient mutant receptors at a ventral fin wound. As a control, I first assessed neutrophil behaviour in Cxcr1-wt rescue larvae. Importantly, when expressed in a *cxcr1*$^{-/-}$ background, the Cxcr1-wt receptor rescued the clustering

defect of *cxcr1*$^{-/-}$ neutrophils, confirming that this defect in focalisation was, at least in part, due to lack of neutrophil expression of Cxcr1 and not due to other factors such as other cell types or the tissue environment (Fig.5.7a-c and Fig. 5.8, left panel).

**Cxcr1-ala show enhanced motility and focalisation**

Interestingly, the behaviour of Cxcr1-ala mutant neutrophils was strikingly different to that of Cxcr1-wt neutrophils. At the wound site, Cxcr1-ala neutrophils formed focalised 'tornado-like' swarms forming unusually large and motile clusters where cells circled around each other (Fig. 5.8, middle panel). Quantification confirmed increased cluster size compared to Cxcr1-wt (Fig. 5.9a) and a gain of function with regards to motility, with Cxcr1-ala neutrophils showing increased speeds both inside the owa as well as throughout forward migration to the owa (Fig 5.9b-d). Quantification of 'net reverse traffic', confirmed that Cxcr1-ala mutant neutrophils showed less reverse interstitial migration representative of their over-attentive engagement with the wound (Fig. 5.9e).

**Cxcr1-chim show enhanced motility and dispersal**

I next assessed the behavioural implication of the Cxcr1-chim mutation on neutrophil migration behaviour at ventral fin wounds. As for Cxcr1-ala neutrophils, Cxcr1-chim neutrophils were visibly quicker than Cxcr1-wt cells. However, in contrast to Cxcr1-ala, Cxcr1-chim neutrophils showed enhanced dispersal compared to cxcr1-wt neutrophils (Fig. 5.8, right panel). Quantification (by A.G) confirmed that Cxcr1-chim neutrophils showed a gain of function with regards to motility, with neutrophils showing increased speeds both inside the owa (Fig. 5.9a) as well as throughout forward migration to the owa (Fig 5.9b-c). Cxcr1-chim neutrophils showed less directionality, indicative of a more random-like migration behaviour (Fig. 5.9d). Quantification of overall 'cell traffic' confirmed that Cxcr1-chim neutrophils showed increased reverse migration, reflective of their bidirectional and dispersive behaviour (Fig. 5.9e).

**Generation of Cxcr2 mutant receptors**

Following generation of the Cxcr1 mutants I generated analogous Cxcr2 mutant receptors. I generated a Cxcr2-ala mutant receptor in which all serine residues in the C–terminus were replaced with alanine residues and I also generated a Cxcr2-chim receptor in which the C-terminus of Cxcr2 was substituted for that of Cxcr1 (Fig. 5.10). The Cxcr2-chim receptor was expected to possess the

ligand binding characteristics of Cxcr2 but bear the C-terminus amino acid residues (from Cxcr1) necessary for internalisation/desensitisation. Due to time restraints Cxcr2-mutant constructs were not expressed in gastrulating embryos but were instead directly expressed in neutrophils under the Lyz promoter. I generated new Tg(*lyz*:Cxcr2-FT); *cxcr2*$^{-/-}$, Tg(*lyz*:Cxcr2_ala-FT); *cxcr2*$^{-/-}$, and Tg(*lyz*:Cxcr2_chim-FT); *cxcr2*$^{-/-}$ rescue lines in which Cxcr2-wt, Cxcr2-ala and Cxcr2-chim receptors were expressed in a *cxcr2*$^{-/-}$ background to exclude any contribution of endogenous Cxcr2.

**Cxcr2-wt and Cxcr2-ala are sustained at the membrane in response to endogenous wound gradients whilst Cxcr2-chim is internalised**

I conducted ventral fin wounds in Tg(*lyz*:Cxcr2-FT); *cxcr2*$^{-/-}$, Tg(*lyz*:Cxcr2_ala-FT); *cxcr2*$^{-/-}$, and Tg(*lyz*:Cxcr2_chim-FT); *cxcr2*$^{-/-}$ larvae and assessed receptor trafficking dynamics in response to endogenous gradients generated at wound sites. As expected, Cxcr2-wt remained predominantly membranous at the wound site (Fig 5.11a, left panel and b). Cxcr2-ala also had a membranous distribution (Fig. 5.11a, middle panel and b). In contrast, Cxcr2-chim showed a gain in internalisation at wound sites confirming that it is the Cxcr1 C-terminus that confers internalisation (Fig 5.11a, right panel and b).

**Cxcr2-WT and Cxcr2-ala rescue *cxcr2*$^{-/-}$ dispersal defect whereas Cxcr2-chim does not**

Importantly, the Cxcr2-wt construct rescued both the slow forward motility defect and the dispersal defect observed in *cxcr2*$^{-/-}$ larvae (Fig. 5.12a-b). This confirmed that neutrophil specific expression of Cxcr2 promotes dispersal. I next assessed the implication of the Cxcr2-chim mutation on neutrophil migration behaviour at ventral fin wounds. Like Cxcr1-wt, the Cxcr2-chim construct rescued the slow forward motility defect of *cxcr2*$^{-/-}$ neutrophils (Fig. 5.12a). Interestingly, Cxcr2-chim neutrophils migrated to the wound but, concurrent with receptor internalisation, suddenly stopped and appeared less motile at the wound. Quantification of net reverse traffic confirmed that Cxcr2-chim neutrophils were less dispersive (Fig 5.12b). Thus, in contrast to the Cxcr2-wt receptor, the Cxcr2-chim receptor was unable to rescue the dispersal defect of cxcr2$^{-/-}$ neutrophils. This shows that sustained residence of Cxcr2 at the plasma membrane is required for Cxcr2-mediated dispersal. The Cxcr2-ala construct also rescued the slow forward motility defect of *cxcr2*$^{-/-}$ neutrophils. Cxcr2-ala neutrophil migration behaviour at wound sites was comparable to that of Cxcr2-WT neutrophils with quantification of net reverse traffic revealing no significant

difference between the two neutrophil populations (Fig. 5.12b). Thus, mutating the serine residues in the Cxcr2 terminus did not confer the same behavioural phenotype as mutating serine residues in the Cxcr1 C- terminus (Cxcr1-ala). This may suggest that desensitisation of Cxcr2 plays a more negligible role in generating specific migration behaviours at wound sites.

**Exploring differential signalling of Cxcr1 and Cxcr2**

Cxcr1-ala and Cxcr1-chim neutrophils showed a qualitative difference in behaviour, being focalised and dispersed respectively. I therefore reasoned that a possible explanation for the phenotypes of Cxcr1-ala and Cxcr1-chimera could be differential signalling. For example, it is possible that the Cxcr1 alanine mutations merely block desensitisation and that the transplantation of Cxcr2 C-tail changes both the signalling and the trafficking. A key component of chemokine receptor signalling is the associated trimeric G protein complex (consisting of Gα, Gβ and Gγ subunits) which transduces the external signal to intracellular signalling molecules. Eukaryote genomes have multiple genes that encode several different types of Gα, Gβ and Gγ proteins. For example, there are four main Gα protein subclasses, $G\alpha_{(i/o)}$, $G\alpha_{(q)}$, $G\alpha_{(s)}$, $G\alpha_{(12/13)}$, which can activate distinct signalling cascades. While many chemoattractant receptors couple to Gi, Gq coupling has been reported for some receptors in leukocytes, for example in dendritic cells and neutrophils[160]. To investigate potential differences in Gα protein coupling between Cxcr1 and Cxcr2, the amino acid sequence was inputted into an algorithm (performed by Milka Sarris) that predicts G protein coupling partners (ie. $G\alpha_i$, $G\alpha_q$, $G\alpha_s$, etc.). Interestingly, Cxcr1 and Cxcr2 were predicted to have differential Gα coupling. Whilst Cxcr2 was predicted to couple to Gi, as is common for chemokine receptors, Cxcr1 was predicted to couple to $G\alpha_q$. To investigate Cxcr1 receptor coupling to $G\alpha_q$ subunits, I used two $G\alpha_q$ pharmacological inhibitors, YM-254890 and FR900359, to assess whether they could inhibit the focalised and highly motile behaviour seen in Cxcr1-ala mutants. However, quantification of speed, directional sensing and cluster size revealed no difference between DMSO and $G\alpha_q$ inhibitor-treated Cxcr1-alanine neutrophils (Fig. 5.13).

# 5. Discussion

**Summary of results**

The results presented in this chapter focused on understanding the role of Cxcr1 and Cxcr2 receptor trafficking in generating specific neutrophil migration behaviours (focalisation vs bi-directional movement) during wound responses. I addressed this through generation of desensitisation-deficient (Cxcr1-ala, Cxcr2-ala) and chimeric (Cxcr1-chim, Cxcr2-chim) mutant receptors. Interestingly, Cxcr1-ala and Cxcr1-chim neutrophils had qualitatively different, contrasting behaviours with Cxcr1-ala neutrophils showing enhanced focalisation whilst Cxcr1-chim neutrophils showed enhanced bidirectional motility. The excess focalisation observed in Cxcr1-ala neutrophils suggests that Cxcr1 desensitisation is essential to prevent an overly focalised response. Internalisation of Cxcr2-chim receptor and the concurrent defect in dispersal showed that Cxcr2 sustenance is required for dispersal.

**Cxcr1 desensitisation is required for dispersal**

Cxcr1-ala neutrophils displayed strikingly enhanced focalisation suggesting that Cxcr1 receptor internalisation is required for neutrophil dispersal. It is tempting to speculate that Cxcr1 signalling acts as a molecular sign-post, keeping cells highly directed and targeted towards the source. Indeed, during live-imaging neutrophils were often seen to make U-turns when migrating away from the wound and were quickly drawn back to the target. Interestingly, even when the Cxcr1-ala receptor was expressed in a *cxcr1*$^{+/-}$ heterozygote background (data not shown) neutrophils still exhibited a highly motile and focalised swarming behaviour. Thus, even in the presence of endogenous Cxcr1 receptor, which is capable of internalisation, the non-desensitising Cxcr1-ala receptor provides adequate excess signal to generate the swarming phenotype.

**Sustained Cxcr2 residence at the plasma membrane is required for dispersal**

I showed that Cxcr2-wt is largely sustained at the membrane in response to endogenous ligands present at wound sites. When the C-terminus of Cxcr2 was substituted with that of Cxcr1 the receptor internalised at the wound site. This suggests that the Cxcr1 terminus carries the residues necessary for internalisation in response to endogenous ligands present at the wound site. Importantly, neutrophils expressing Cxcr2-chim showed reduced reverse migration, suggesting that sustenance of Cxcr2 is required for dispersal. It remains unclear whether the endogenous ligand

responsible for Cxcr2-chim internalisation is Cxcl8a or another ligand. To verify this, a possible future experiment would be to suppress the expression of Cxcl8a (e.g. via morpholino) or other candidate ligands and assess the effect on Cxcr2-chim internalisation.

**Blocking desensitisation of Cxcr1 is not sufficient to mediate dispersal, in contrast to cytoplasmic domain swapping with Cxcr2**

Enforced membrane sustenance of Cxcr1-ala resulted in enhanced focalisation whilst enforced sustenance of Cxcr1-chim resulted in an overly dispersive behaviour. Given that both mutant receptors are sustained at the membrane, it seems unlikely that membrane sustenance alone accounts for this qualitative difference. One possibility is that the C-terminus of Cxcr2 used in the Cxcr1-chim receptor confers different signalling properties to that of Cxcr1 and that this results in a qualitatively different dispersive migration behaviour. I therefore reasoned that a possible explanation for the phenotypes of Cxcr1-ala and Cxcr1-chimera could be differential G protein coupling conferred by the different C-tails. For example, Cxcr1 and Cxcr2 could have different G protein and down-stream signalling effectors. While the Cxcr1 alanine mutations merely block desensitisation, the transplantation of the Cxcr2 C-tail changes both the G protein-binding and the trafficking. Interestingly, based on their amino acid sequence Cxcr1 and Cxcr2 were predicted to couple to Gq and Gi respectively. In my study, pharmacological inhibition of Gq signalling by YM-254890 and FR900359 had no observable effect on Cxcr1-ala migration behaviour. However, it is unclear whether this drug is able to inhibit all zebrafish Gq proteins expressed in neutrophils. Indeed, ongoing work from collaborators indicates that the drug does not inhibit all neutrophil Gqs. Therefore, more systematic work is required to characterise Cxcr1 and Cxcr2 signalling profiles and their roles in focalisation versus dispersal. Ongoing work in the lab aims to genetically inhibit the Gq proteins expressed in zebrafish neutrophils that are not targeted by FR900359, via CRISPR gene editing technology.

# 5. Figures

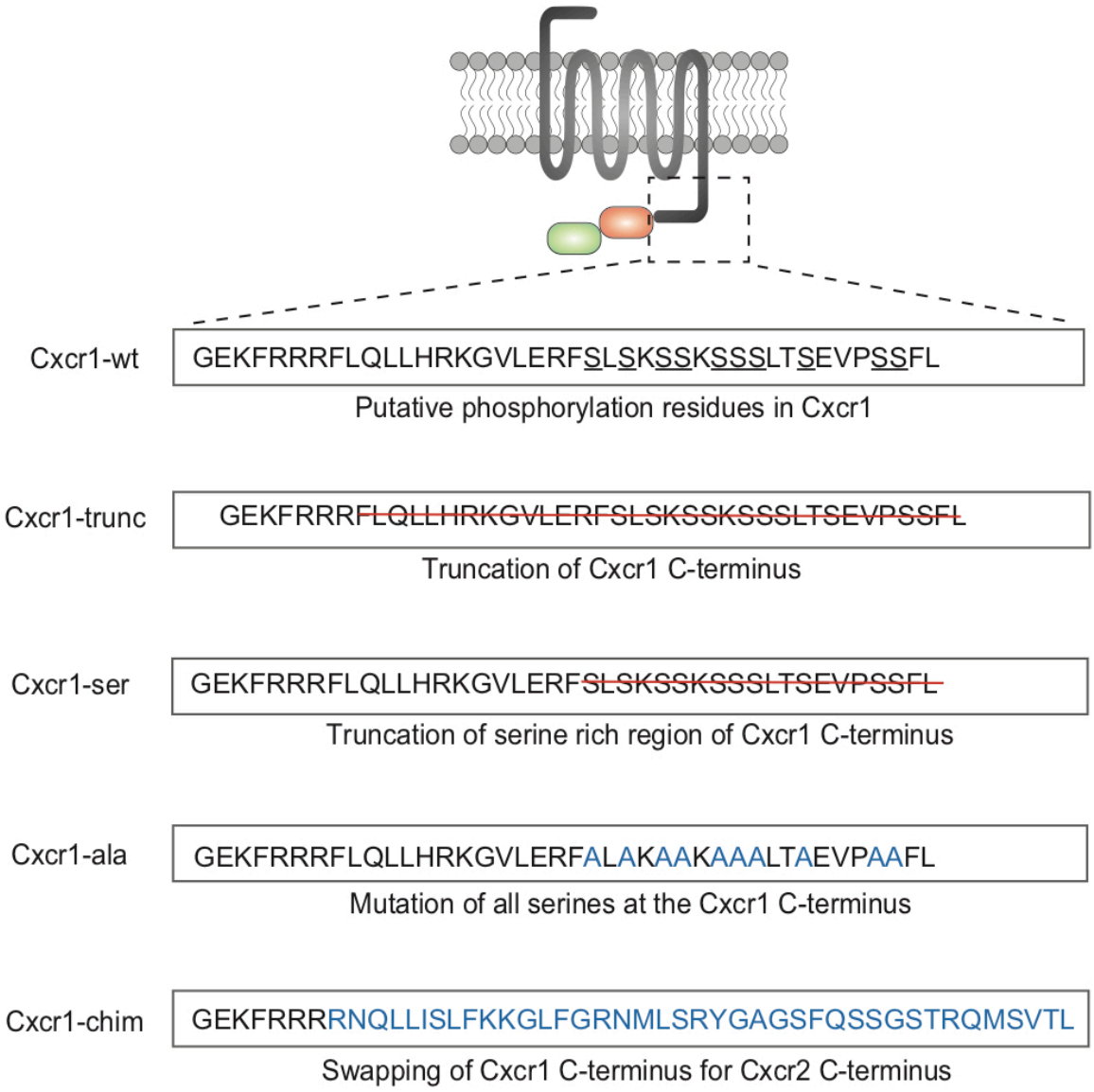


**Figure 5.1. Mutagenesis of Cxcr1 C-terminus.** Schematic showing Cxcr1 mutagenesis approach. Amino acid sequence of Cxcr1-wt C-terminus is shown with candidate phosphorylation (serine) residues underlined. Cxcr1-trunc mutant with truncated C-terminus, truncated region crossed out with red line. Cxcr1-ser with truncated serine rich region crossed out with red line. Cxcr1-ala mutant receptor with all serines substituted for alanines, substitutions indicated in blue. Cxcr1-chim receptor has C-terminus of Cxcr1 replaced by that of Cxcr2, substituted region indicated in blue.

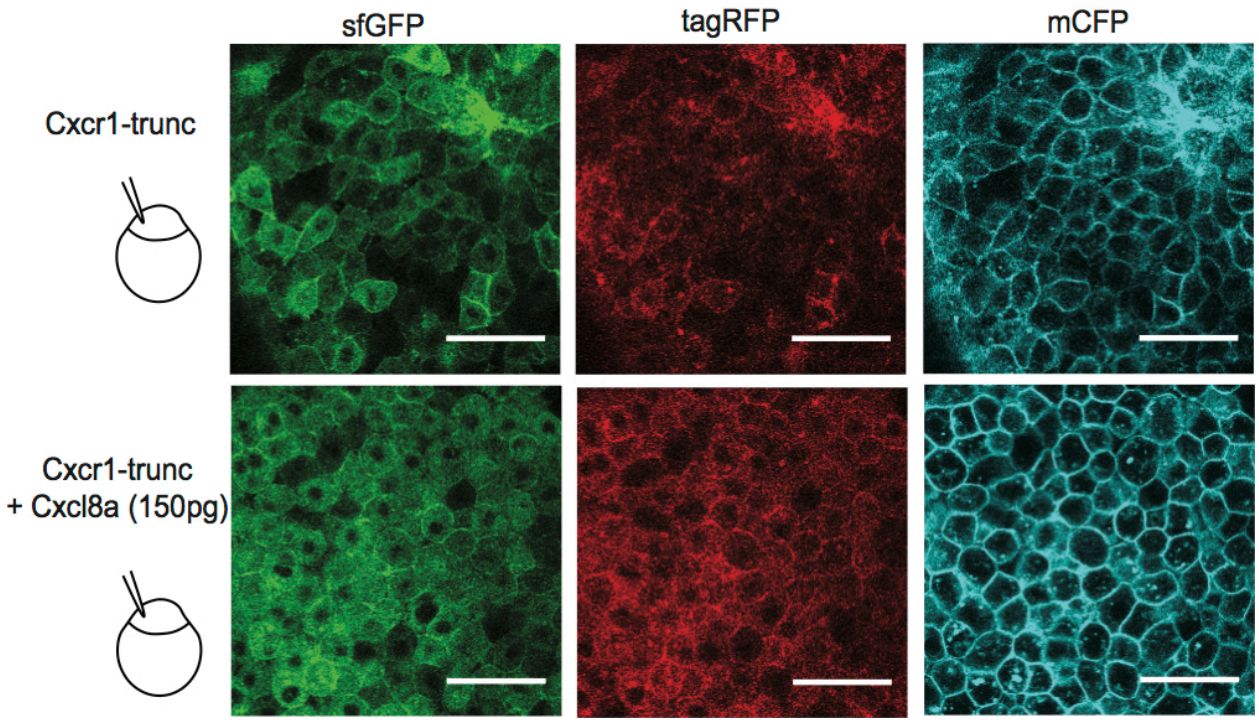


**Figure 5.2. Cxcr1-trunc expression in gastrulating embryos.** 100pg of Cxcr1-trunc mRNA was injected into in one-cell stage zebrafish embryos either in the absence or presence of 150pg Cxcl8a mRNA. A control membrane marker (cyan) was co-injected in all cases. Laser scanning confocal slices of gastrulating embryos expressing Cxcr1-trunc without (top panels) or with Cxcl8a (lower panels). sfGFP and tagRFP receptors are shown in separate channels. Control membrane marker is shown in the blue channel. Representative images from 4 embryos from 1 imaging session (Cxcr1-trunc), and from 6 embryos from 1 imaging session (Cxcr1-trunc +Cxcl8a). Scale bar, 50 μm.

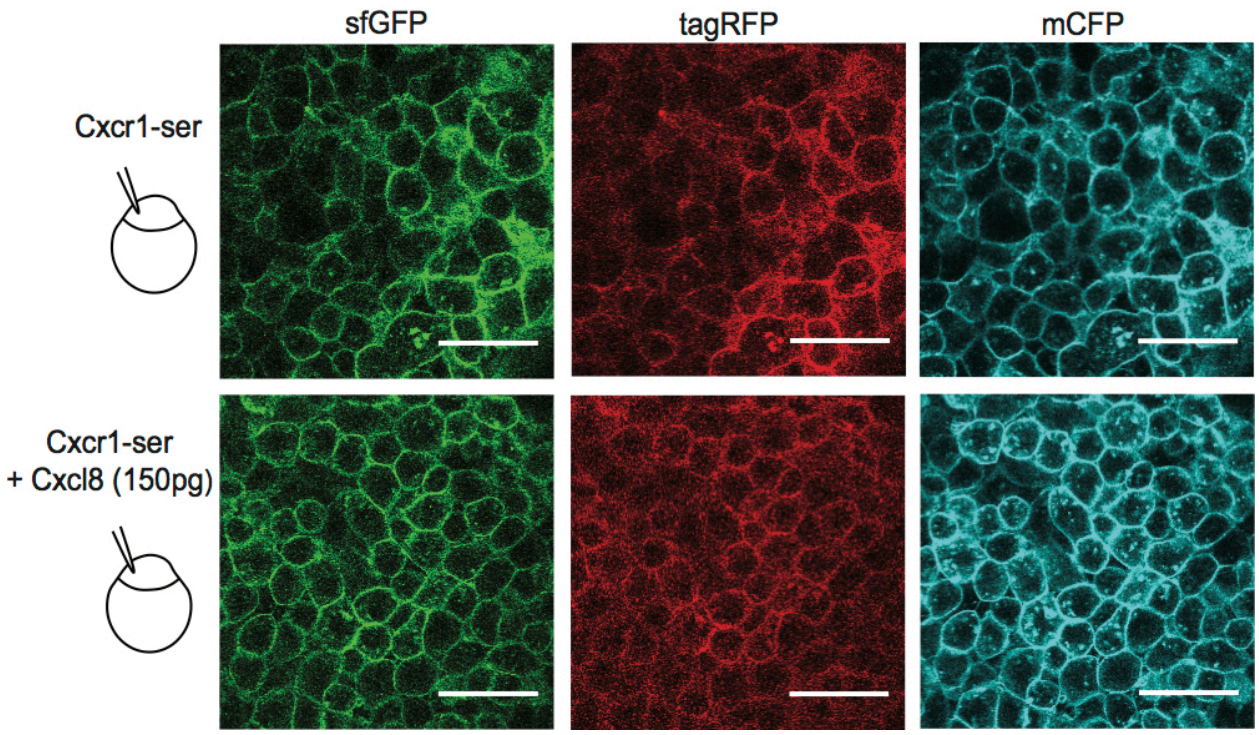


**Figure 5.3. Cxcr1-ser is not internalised in response to Cxcl8a.** 100pg of Cxcr1-ser mRNA was injected into in one-cell stage zebrafish embryos either in the absence or presence of 150pg Cxcl8a mRNA. A control membrane marker (cyan) was co-injected in all cases. Laser scanning confocal slices of gastrulating embryos expressing Cxcr1-ser without (top panels) or with Cxcl8a (lower panels). Green and red receptors are shown in separate channels. Control membrane marker is shown in the blue channel. Representative images from 16 embryos from 3 imaging experiments (Cxcr1-ser), and 14 embryos from 3 experiments (Cxcr1-ser + Cxcl8a). Scale bar, 50 μm.

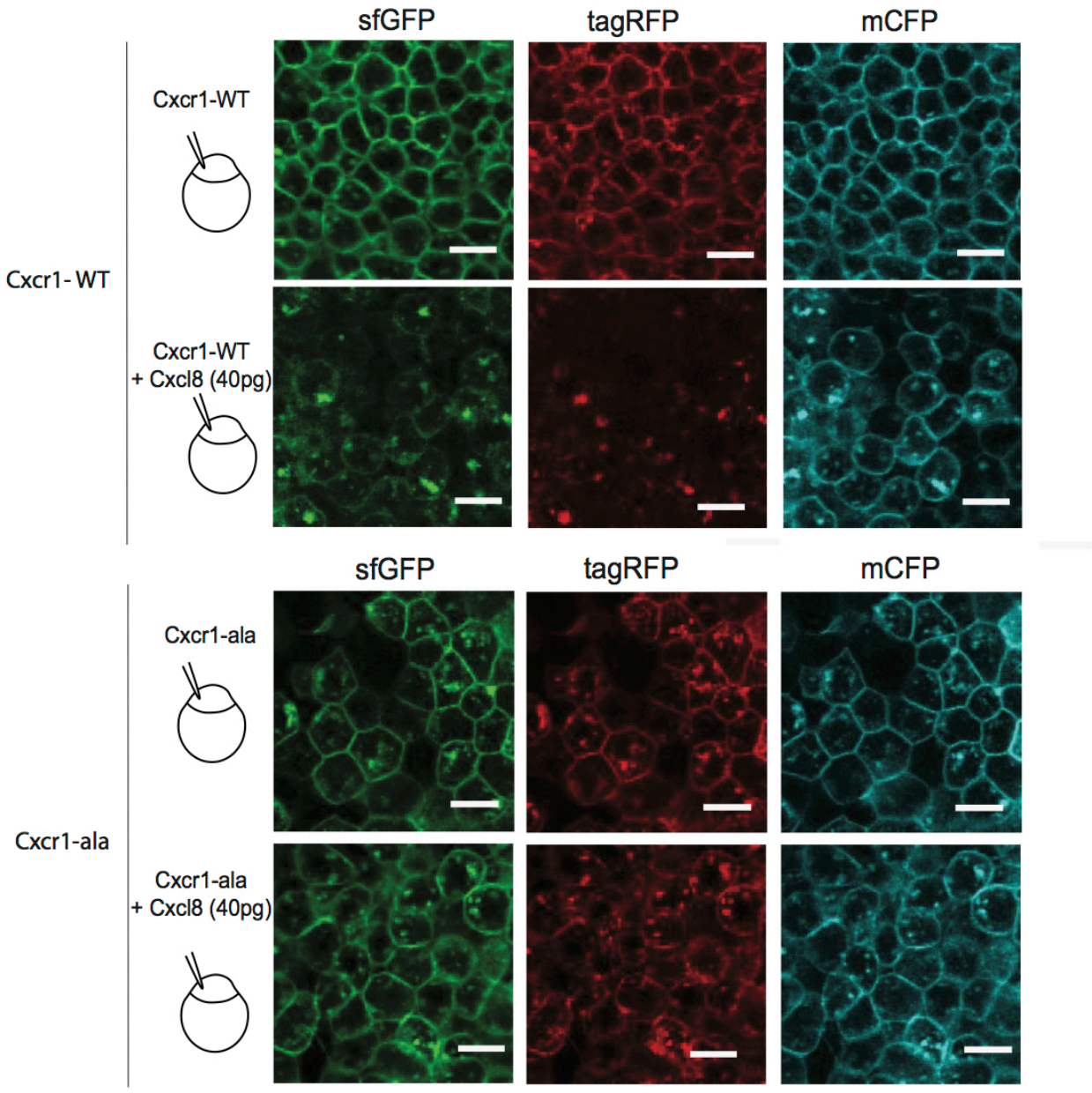


**Figure 5.4. Cxcr1-ala is not internalised in response to Cxcl8a.** 100pg of Cxcr1-WT or Cxcr1-ala mRNA was injected with or without 40pg Cxcl8a mRNA in one-cell stage embryos. a) Laser scanning confocal slices of gastrulating embryos expressing Cxcr1-WT in the absence and presence of Cxcl8a. b) Laser scanning confocal slices of gastrulating embryos expressing Cxcr1-ala receptor in the absence and presence of Cxcl8a. sfGFP and tagRFP receptors are shown in separate channels. Control membrane marker is shown in the blue channel. Scale bar, 20µm.

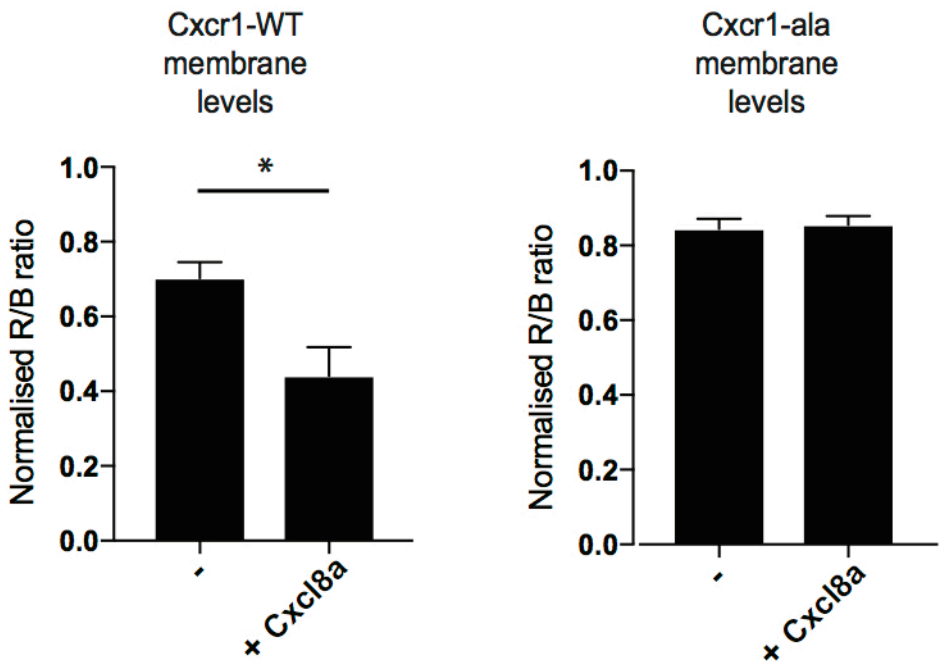


**Figure 5.5. Cxcr1-ala remains membranous in response to Cxcl8a.** Quantification of wild type Cxcr1-wt and Cxcr1-ala membrane expression as a function of a control membrane marker (mCFP). Ratio of red over blue fluorescence (R/B) at the cell membrane is shown. Ratios at the cell membrane were normalised to corresponding mean intensity ratios in the whole image. Mann Whitney test, n=12 embryos for Cxcr1 from nine imaging sessions, n=4 embryos for Cxcr1+Cxcl8a from two imaging sessions, n=6 embryos for Cxcr1-ala from two imaging sessions, n=9 embryos for Cxcr1+Cxcl8a from two imaging sessions. Quantification by M.S.

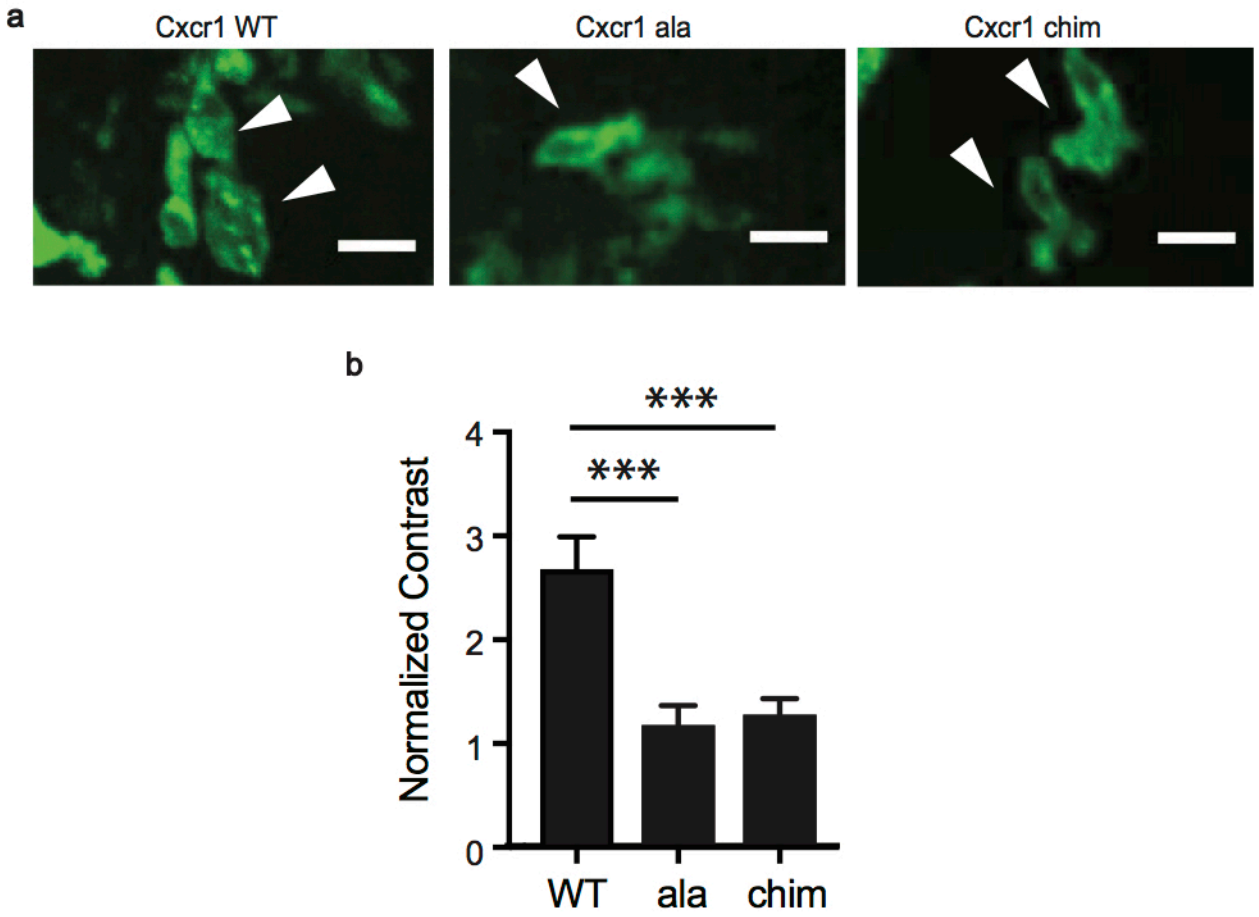


**Figure 5.6. Cxcr1-wt is internalised at wound sites, whilst Cxcr1-ala and Cxcr1-chim remain membranous** a) Confocal images showing Cxcr1-wt (left), Cxcr1-chim (middle) and Cxcr1-ala (right) receptor distribution in neutrophils at wounds, Scale bar, 15µm b) Quantification of contrast in *cxcr1*$^{-/-}$ or *cxcr1*$^{-/+}$ neutrophils rescued by the different Cxcr1-FT receptor variants. n=23 cells (WT) from 7 larvae, n=26 cells (Cxcr1-ala) from 6 larvae, n=19 cells (Cxcr1-chim) from 5 larvae. Kruskal-Wallis test with Dunn's multiple comparison test. Error bars represent S.E.M across cells. Quantification (b) by A.G.

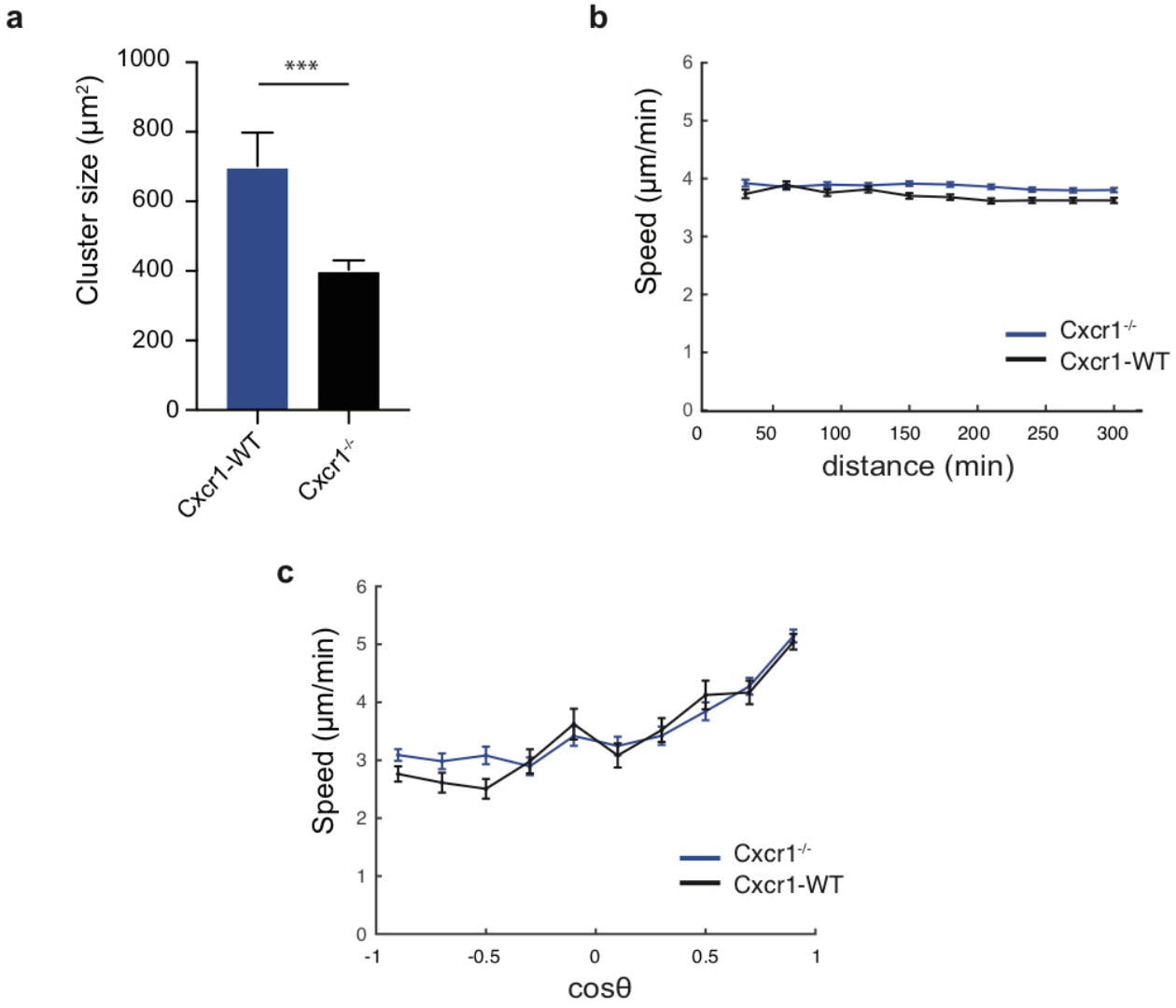


**Figure 5.7. Neutrophil expression of Cxcr1-FT rescues Cxcr1$^{-/-}$ clustering defect** a) Average neutrophil neutrophil cluster size per larva throughout the first 2 hpw. Mann Whitney test. b) Neutrophil speed in relation to distance from wound. Average speeds per cell per distance bin are shown. c) Neutrophil speed in relation to cosine of angle θ. Average speeds per cell per cosθ bin are shown. Error bars represent standard error of either pooled cell means (b-c) or embryo means (a) across n=17 cxcr1$^{-/-}$ larvae and n=9 Tg(lyz:cxcr1-FT)/cxcr1$^{-/-}$ from 12 and 4 imaging sessions respectively. Quantification by A.G.

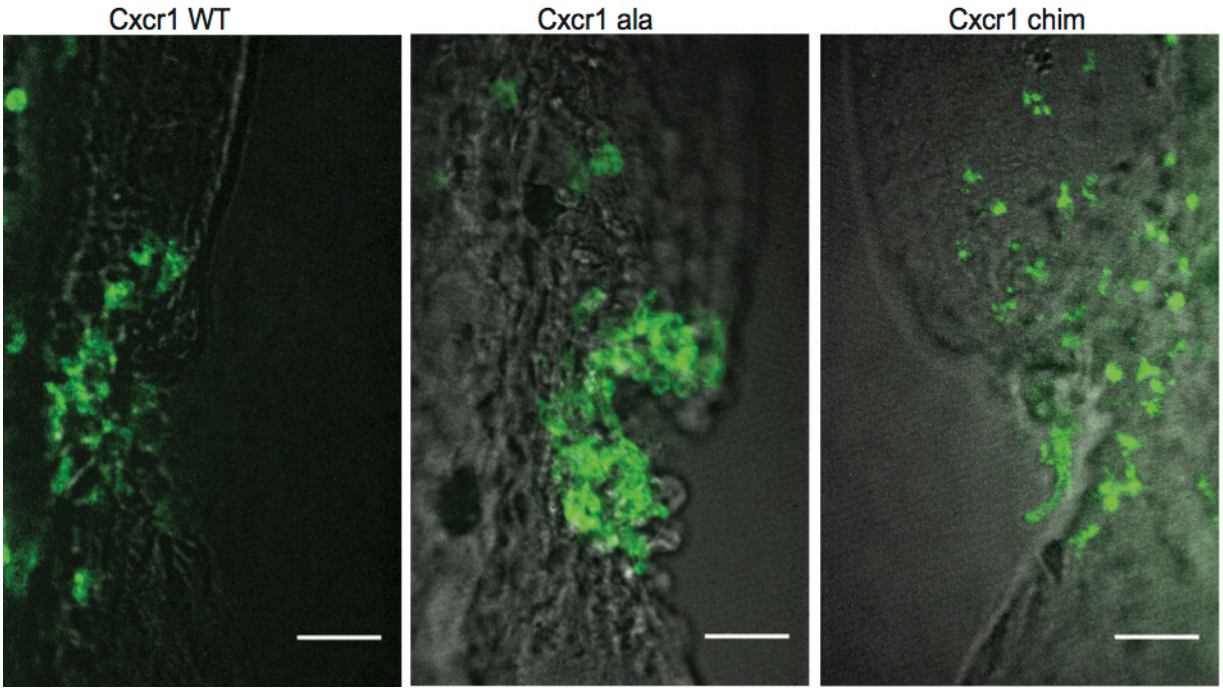


**Figure 5.8**. **Cxcr1-ala neutrophils form focalised clusters whilst Cxcr1-chim neutrophils are dispersed.** Confocal images showing distribution of Cxcr1-wt (left), Cxcr1-ala (middle) and Cxcr1-chim (right) neutrophils (green) at a ventral fin wound, approximately 2hrpw. Due to bleaching issues during imaging, the distribution of Cxcr1-chim (right) neutrophils is shown via the tgRFP fluorophore of the fluorescent timer, not sfGFP, but is shown here pseudo-coloured as green. Scale bar, 30μm.

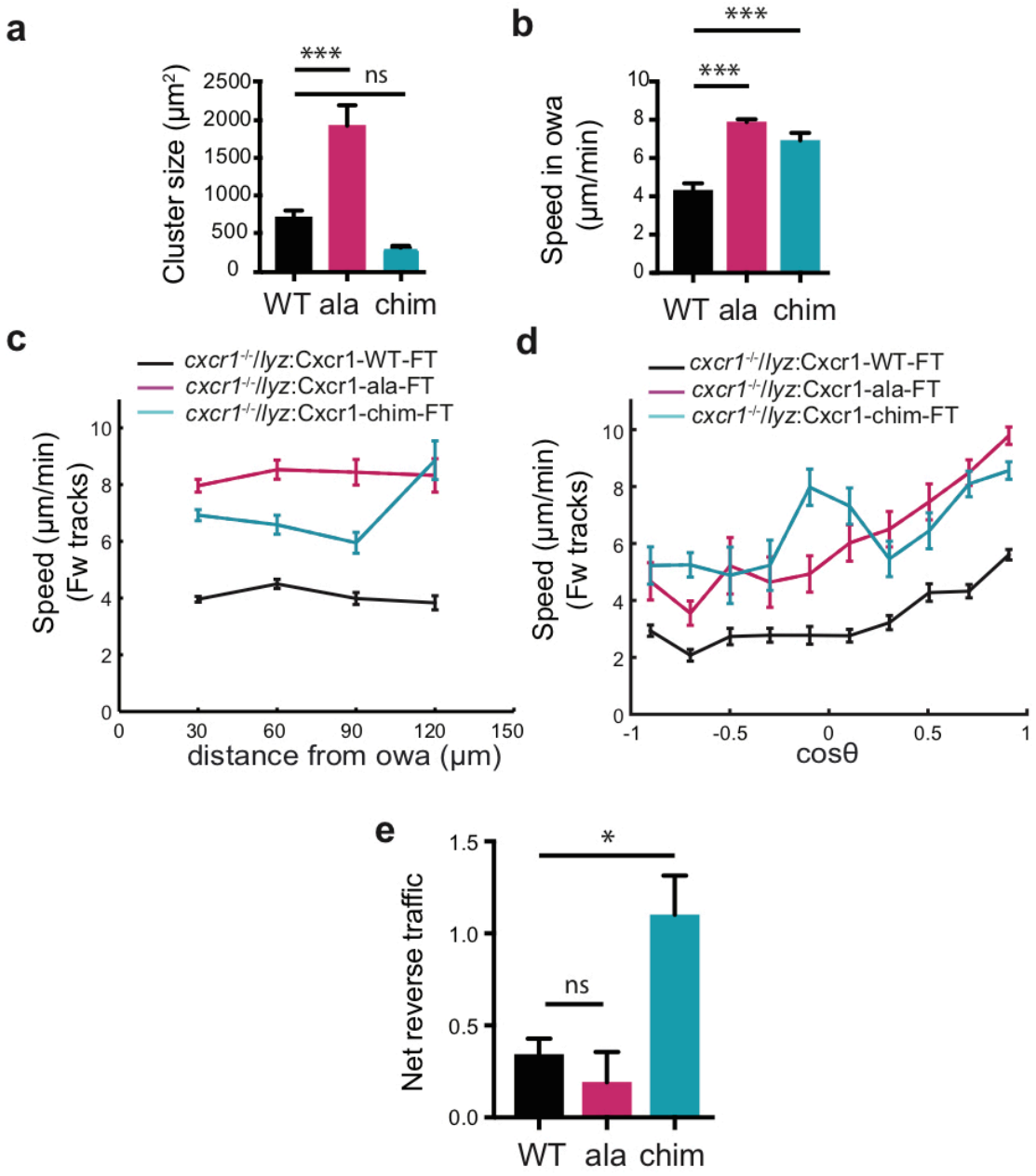


**Figure 5.9**. **Cxcr1-ala neutrophils form focalised clusters whilst Cxcr1-chim neutrophils are dispersed.** a) Quantification of neutrophil cluster size, n=8 (WT), n=6 (ala) and n=4 (chim) larvae from 3 imaging sessions per condition. One-way ANOVA test with Tukey's multiple comparisons test. b) Quantification of speed within the owa. n=9 (WT), n=6 (ala) and n=7 (chim) larvae. One-way ANOVA test with Tukey's multiple comparisons test. c) Quantification of speed within the owa. N=.test. c) Neutrophil speed in relation to distance from the owa. Average speeds per cell step per distance bin are shown. n=316-1942 steps per bin (WT), n=105-706 steps per bin (ala), n=83-896 steps per bin (chim). d) Neutrophil speed in relation to cosine of angle θ. Average speeds per cell per cosθ bin are shown. n=128-849 steps per bin (WT), n 22-445 steps per bin (ala), n=44-417 steps per bin (chim). e) Net reverse traffic. n=9 (WT), n=6 (ala) and N=7 (chim) larvae. Kruskal-Wallis test with Dunn's multiple comparisons test. Quantification by A.G.

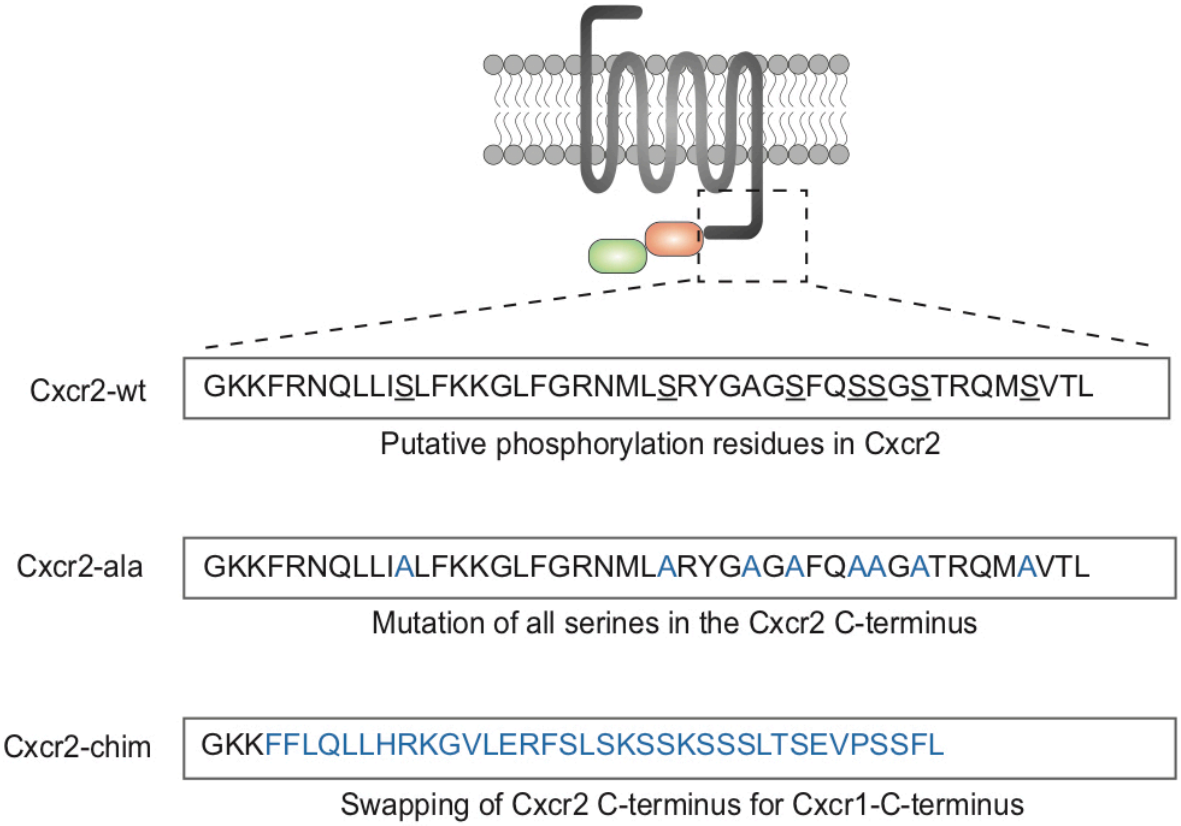


**Figure 5.10. Mutagenesis of Cxcr2.** Schematic showing Cxcr2 mutagenesis approach. From top to bottom: Amino acid sequence of Cxcr2-WT C-terminus is shown with candidate phosphorylation targets (serines) underlined. Cxcr2-ala mutant with all serine residues substituted for alanine residues, shown in blue. Cxcr2-chimera receptor has C-terminus of Cxcr2 replaced by that of Cxcr1, substituted region indicated in blue.

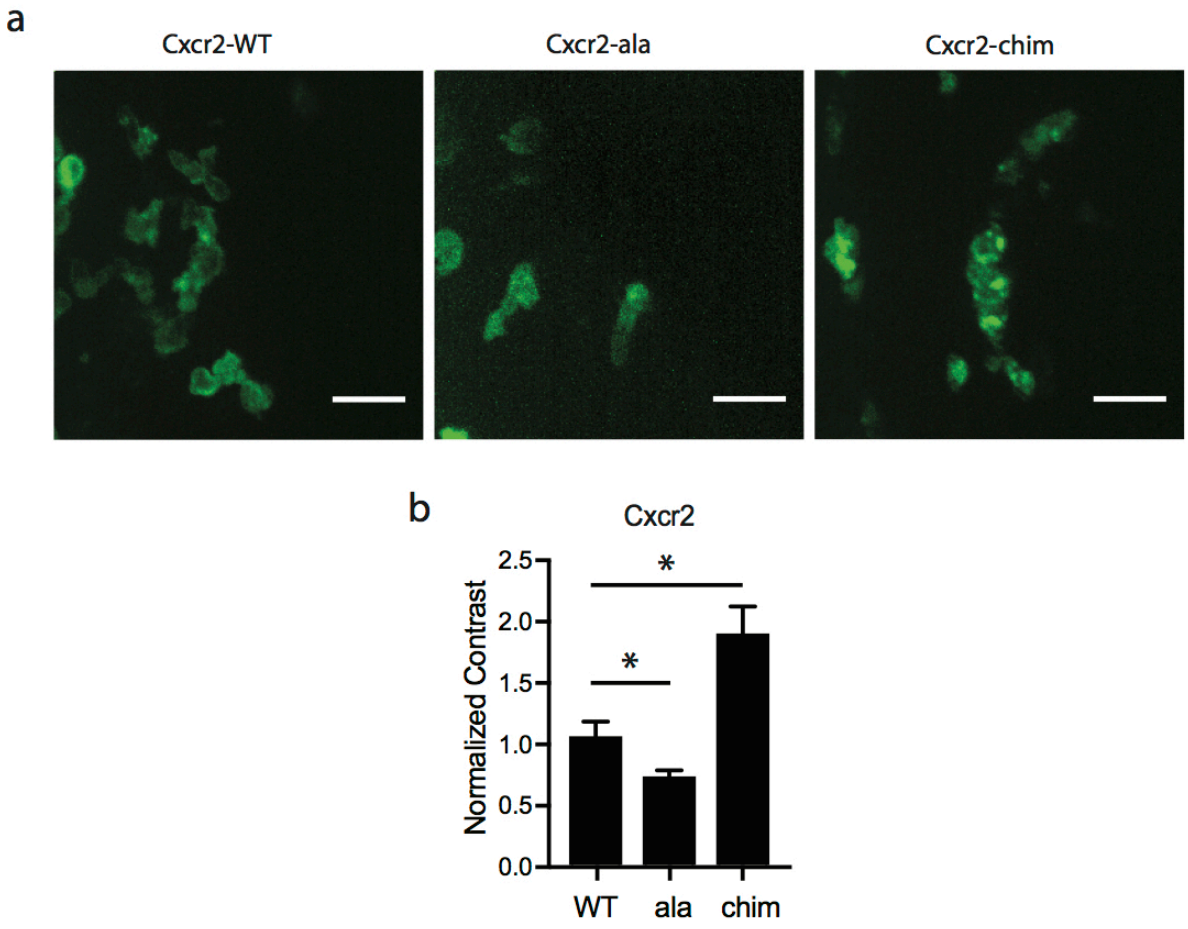


**Figure 5.11. Cxcr2-WT and Cxcr2-ala are sustained at the cell membrane, whilst Cxcr2-chim is internalised.** Confocal images of receptor distribution in Cxcr2KO-WT rescue (left), Cxcr2KO-ala (middle) and Cxcr2KO-chim (right) responding to a ventral fin wound. Scale bar, 20µm. b) Quantification of contrast in *cxcr2*$^{-/-}$ neutrophils rescued by the different Cxcr2-FT receptor variants. n=33 cells (WT) from 5 larvae, n=18 cells (ala) from 5 larvae, n=33 cells (chim) from 8 larvae. Data are from independent larvae in 3-5 imaging sessions. Kruskal-Wallis test with Dunn's multiple comparisons test. Error bars represent standard error of means across cells. Quantification by (b) A.G.

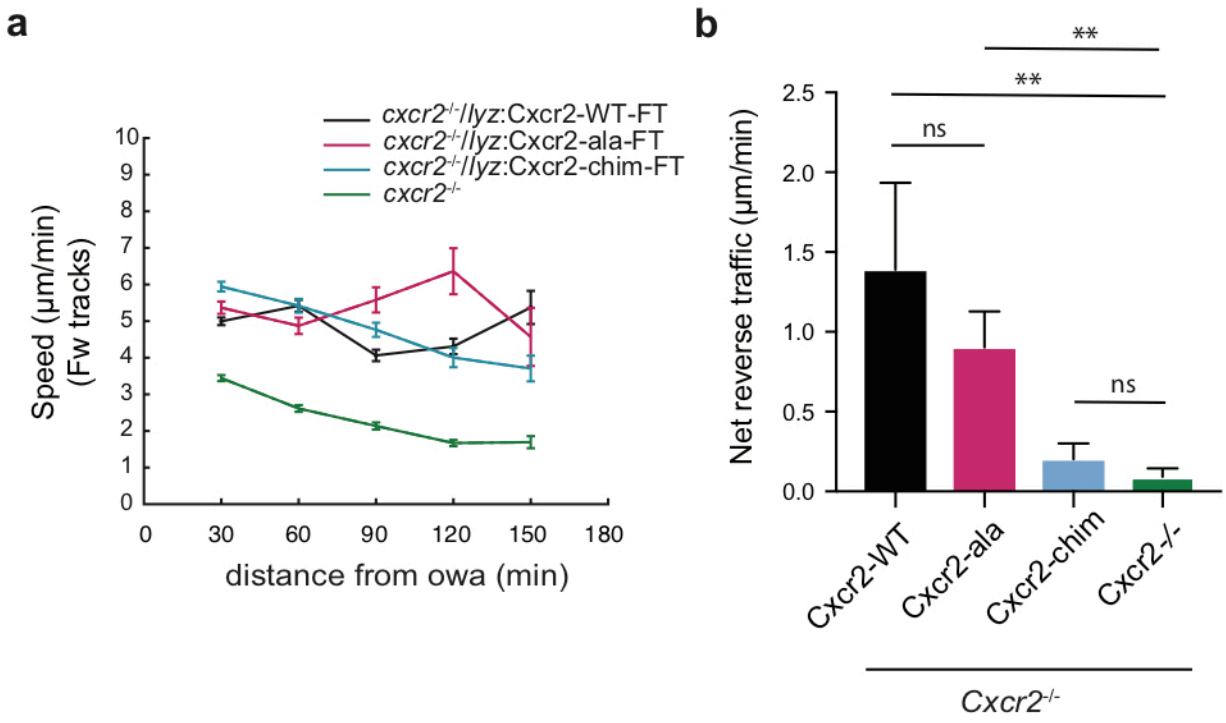


**Figure 5.12. Cxcr2 membrane sustenance is required for dispersal.** a) Neutrophil speed in relation to distance from the owa. Average speeds per cell per distance bin are shown. n=558-2651 steps per bin (WT), n=95-1266 steps per bin (ala), n=494-2000 steps per bin (chim), n=1168-2823 steps per bin for *cxcr2*$^{-/-}$ larvae. b) Net reverse traffic. n=6 (WT), n=9 (ala), n=8 (chim), n=11 larvae for *cxcr2*$^{-/-}$ (-). Kruskal-Wallis test with Dunn's multiple comparisons test. In b and c, data are from 6 (WT), 9 (ala), 8 (chim) and 11 *cxcr2*$^{-/-}$ (-) larvae from 3, 4, 3 and 8 imaging sessions respectively. Cells were analysed from the start of the movie (approximately 15 mpw) up to 2 hpw. Quantification by A.G.

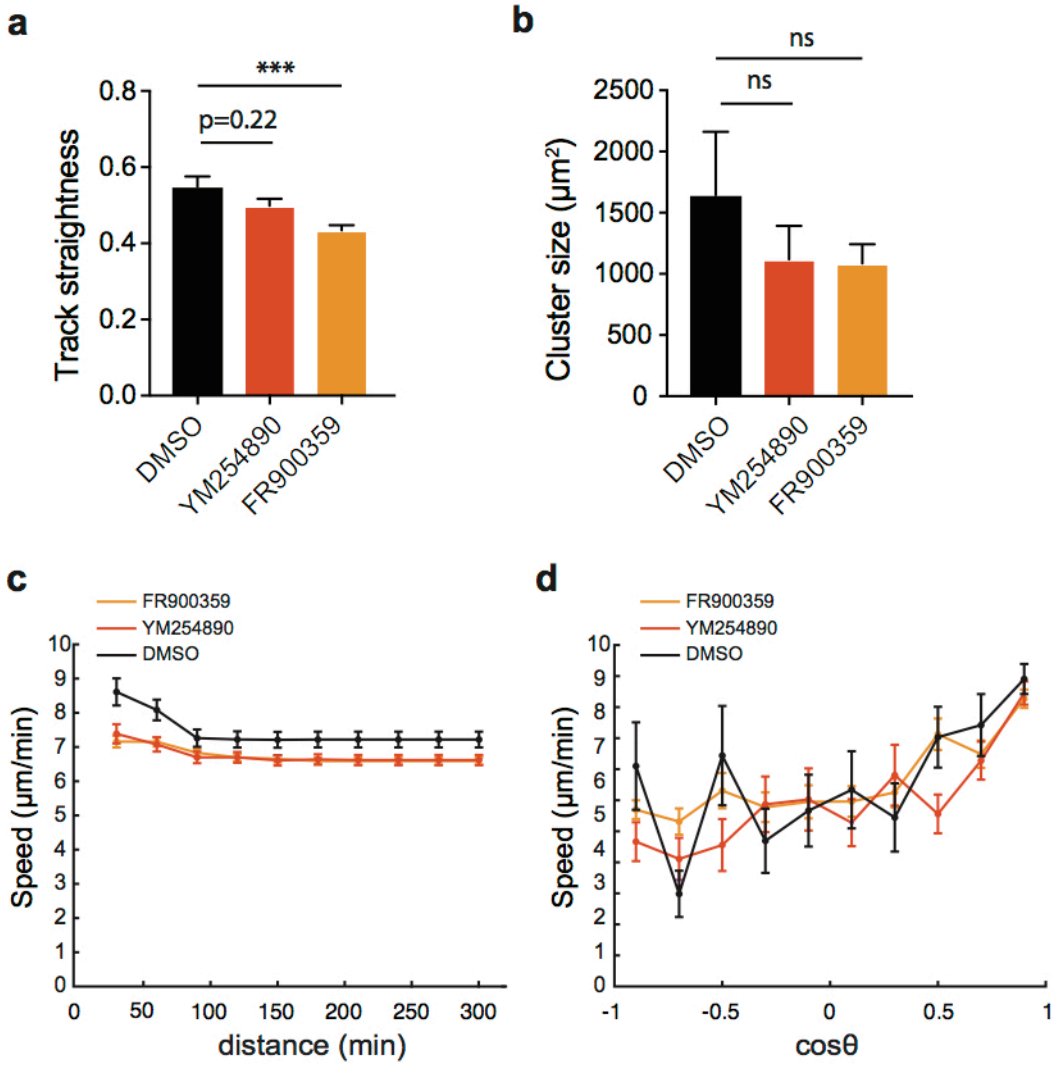


**Figure 5.13. Analysis of neutrophil behaviour in Cxcr1-ala larvae treated with Gq inhibitors.** a) Pre-arrival trajectory straightness. Kruskall-Wallis with Dunn's post-test. n=46 tracks, n=88 tracks, n-217 tracks from 6 DMSO-treated, 7 YM254890-treated and 8 FR900359-treated larvae respectively. b) Average cluster size. One way ANOVA. n=6 DMSO-treated, n=7 YM254890-treated larvae and n=8 FR900359-treated larvae. c) Neutrophil speed in relation to distance from wound (pre-arrival trajectory segment). Average speeds per cell per distance bin are shown. d) Neutrophil speed in relation to cosine of angle θ. Average speeds per cell per cosθ bin are shown (pre-arrival trajectory segment). Error bars represent SEM. Cells were imaged and analysed 1-2 hpw. Quantification by A.G.

# Chapter 6: Concluding remarks and future directions

## Subchapter 6.1: Concluding remarks

The overarching aim of this thesis was to understand how GPCR trafficking in neutrophils influences the interpretation of endogenous chemokine gradients to generate specific migration behaviours at inflammatory sites. Here I used zebrafish Cxcr1 and Cxcr2 as a model system to address this *in vivo*.

In chapter 3, my aim was to dissect the trafficking dynamics of Cxcr1 and Cxcr2 during neutrophil migration *in vivo*. For this, I fluorescently labelled each receptor using a fluorescent timer (FT) approach in which receptors were tagged to a fast maturing sfGFP in tandem with a slower maturing tagRFP. Through expression of FT-receptors in gastrulating embryos I showed that Cxcr1 internalises in response to Cxcl8a whilst Cxcr2 is relatively sustained. To test receptor trafficking in neutrophils, I generated new Tg(*lyz*:Cxcr1-FT) and Tg(*lyz*:Cxcr2-FT) transgenic lines in which the FT-receptors are specifically expressed in neutrophils. Live-imaging of neutrophil responses in Tg(*lyz*:Cxcr1-FT) and Tg(*lyz*:Cxcr2-FT) larvae revealed that under steady state conditions neutrophils show rapid constitutive turnover of the two receptors. My study reveals that whilst sfGFP is a suitable marker to resolve receptor dynamics in neutrophils, tagRFP is not given its maturation time is greater than the residence time at the plasma membrane. Thus, selection of appropriate fluorophores is an important consideration for future studies investigating receptor dynamics in immune cells. Live-imaging of neutrophil responses to wounds in Tg(*lyz*:Cxcr1-FT) and Tg(*lyz*:Cxcr2-FT) larvae revealed that the two receptors show differential trafficking dynamics in response to endogenous gradients. Cxcr1 was progressively internalised as neutrophils migrated to the wound site whilst Cxcr2 was sustained on the cell membrane throughout the response. To my knowledge, this study is the first to observe receptor trafficking in neutrophils *in vivo*. Quantification of Cxcr1 internalisation was used to indirectly report endogenous gradients and this could be used in other systems where direct visualisation of the gradient is difficult.

Having shown that Cxcr1 and Cxcr2 display differential trafficking in response to endogenous gradients at wound sites, my next aim and the focus of chapter 4 was to determine whether Cxcr1 and Cxcr2 have differential functional contributions to neutrophil interstitial migration at

inflammatory sites. For this, I generated Cxcr1 and Cxcr2 receptor knockout lines and analysed neutrophil responses to ventral fin wounds. Live-imaging and quantitative detailed trajectory analysis showed that Cxcr1 plays a role in forward migration and promotes focalisation at the wound site whilst Cxcr2 drives dispersal at wound sites and promotes resolution of the response. Importantly, these differential phenotypes are consistent with a parallel study using independently generated TALEN-based knockout mutants[152], supporting a robustness in these phenotypes. Interestingly, injection of a Cxcr2 targeting morpholino into *cxcr1*$^{-/-}$ larvae provided evidence for both receptors contributing to forward migration. Thus, the receptors are somewhat redundant in forward migration but have non-redundant roles thereafter.

In chapter 5 my aim was to determine whether the differential trafficking dynamics of Cxcr1 and Cxcr2 (internalisation vs sustenance) are responsible for the distinct functional contributions of each receptor to neutrophil migration (clustering vs dispersal). To address this, I manipulated receptor trafficking through generation of mutant Cxcr1 and Cxcr2 receptors. By blocking Cxcr1 desensitisation in neutrophils (Cxcr1-ala), I show that Cxcr1 signalling drives focalisation and it is the progressive internalisation of Cxcr1 that is required to enable neutrophil dispersal at later time points. By enforcing Cxcr2 internalisation (Cxcr2-chim), I show that Cxcr2 sustenance at the plasma membrane accounts for the ability of Cxcr2 to sustain bi-directional motility and promote dispersal. Whilst blocking Cxcr1 desensitisation (Cxcr1-ala) promoted focalisation, enforcing sustenance through cytoplasmic domain swapping with Cxcr2 (Cxcr1-chim) resulted in a qualitatively different, overly dispersive, behaviour. This suggests the C-terminus of Cxcr2 confers different signalling properties to that of Cxcr1.

**Model recapitulating how Cxcr1 and Cxcr2 coordinate neutrophil clustering and dispersal**

The results presented in this thesis can be brought together to generate a model of how Cxcr1 and Cxcr2 coordinate clustering and dispersal at wound sites (Fig 6.1). During initial chemotaxis towards the wound, Cxcr1 and Cxcr2 both contribute to forward migration and can compensate for each other. Thus, during the early recruitment phase the two receptors are, at least to some extent, functionally redundant. However, at the target site Cxcr1 and Cxcr2 make differential functional contributions to neutrophil behaviour. Cxcr1 acts to focalize the cells but is progressively internalised to give way to Cxcr2 signalling. Cxcr2 is sustained at the cell surface throughout the response and drives bidirectional motility in the wounded tissue which facilitates departure from

the site at later stages of the response.

In conclusion, I show that the differential trafficking of Cxcr1 and Cxcr2 in response to endogenous ligands facilitates the transition from neutrophil clustering to reverse migration and resolution. Given that many chemoattractant receptors are GPCRs, similar mechanisms may regulate the migration behaviour of other cell types.

# Subchapter 6.2: Future directions

### Ligand preferences of Cxcr1 and Cxcr2

In this study, I assessed Cxcr1 and Cxcr2 trafficking patterns in response to *in vivo* gradients generated at wound sites. However, the ligand preferences of Cxcr1 and Cxcr2 remain unclear. Through expression in gastrulating embryos, I have shown that Cxcr1 internalises in response to Cxcl8a whilst Cxcr2 remains predominantly membranous. Through neutrophil specific expression of the receptors I have shown that Cxcr1 is extensively internalised whilst Cxcr2 is relatively sustained. Thus, Cxcr1 internalisation at wounds provided strong evidence for Cxcr1/Cxcl8a signalling. In addition, injection of a Cxcl8a morpholino blocked Cxcr1 internalisation, further supporting that Cxcr1 binds Cxcl8a at the wound *in vivo*. However, my studies did not provide evidence for Cxcr2/Cxcl8a signalling. Given that Cxcr2 remains predominantly membranous in response to endogenous ligands *in vivo*, it is unclear whether Cxcr2 binds to Cxcl8a and is sustained or whether it instead binds an alternative endogenous ligand present at the wound and is sustained. It is worth commenting that in gastrulating embryos I saw no internalisation of Cxcr2 in response to co-injected Cxcl8a and whilst Cxcr2 was relatively sustained in neutrophils a degree of internalisation was visible when using a higher magnification. This could indicate that Cxcr2 binds to another non-Cxcl8a ligand. Importantly, I do provide evidence that a Cxcr2 ligand is present at the wound given the phenotype observed in *cxcr2*$^{-/-}$ is rescued by expression of the WT receptor. Thus, the ligand preferences of Cxcr1 and Cxcr2 remain to be clarified. There are two CXCL8 homologues expressed in zebrafish, Cxcl8a and Cxcl8b. Both chemokines have been shown to be up-regulated during inflammatory responses but differential expression has been reported depending on the inflammatory setting[121,119,124,117,72]. It remains unknown whether both chemokines are upregulated in the ventral fin wound and to what degree. It would be interesting to confirm via RT-PCR whether both Cxcl8a and Cxcl8b are upregulated at ventral fin wounds and to also determine the kinetics of expression. Receptor responses to Cxcl8b could be assessed through expression in gastrulating embryos as was done for Cxcr1/Cxcr2 and Cxcl8a in this study. It remains unclear whether Cxcr1 is specific to Cxcl8a or also internalises to Cxcl8b. Given that Cxcr2 showed no internalisation to Cxcl8a in gastrulating embryos it would be particularly interesting to determine whether Cxcr2 internalises in response to Cxcl8b. As mentioned previously, injection of a Cxcl8a targeting morpholino blocked Cxcr1 internalisation, providing strong evidence that Cxcr1 binds Cxcl8a at the wound *in vivo*. This approach could be extended to

test receptor ligand preferences of each receptor for Cxcl8a and Cxcl8b in neutrophils *in vivo*. For example, if Cxcr1 is specific for Cxcl8a, injection of a Cxcl8b targeting morpholino would not be expected to affect receptor internalisation. Given that Cxcr2 shows little internalisation in response to endogenous ligands, the Cxcr2-chimeric transgenic line, in which Cxcr2 internalisation is forced through the Cxcr1 c-terminus, could prove particularly useful in addressing this question. For example, if injection of a Cxcl8a or Cxcl8b targeting morpholino blocked internalisation of the Cxcr2-chim receptor, this would support the idea that Cxcr2 binds Cxcl8a or Cxcl8b respectively. In addition to this approach, we have recently collaborated with another lab with the aim of clarifying the ligand preferences of Cxcr1 and Cxcr2. This ongoing work uses Dynamic Mass Redistribution (DMR) assays in HEK293T cells transfected with Cxcr1 or Cxcr2 and exposed to recombinant Cxcl8a or supernatant from Cxcl8b-transfected HEK293T cells to assess signalling responses in response to each ligand. It is important to highlight that, regardless of the ligand preferences of Cxcr1 and Cxcr2, the conclusions regarding the role of receptor trafficking in neutrophil migration at wounds presented in this thesis stand. These receptor trafficking responses and cell migration behaviours in response to endogenous ligands hold true regardless of whether the receptors bind to Cxcl8a, Cxcl8b or any other ligand.

**Further elucidation of Cxcr1 and Cxcr2 trafficking patterns**

To my knowledge my study is the first to visualize and link receptor trafficking patterns with neutrophil migration behaviour *in vivo*. Whilst internalisation vs membrane sustenance formed the focus of this project, further elucidation of additional trafficking steps would improve our understanding of how these receptors contribute to neutrophil migration. For example, it remains unclear whether either receptor demonstrates recycling. Receptor recycling could play an important role in promoting re-sensitivity to ligand. Given that Cxcr1 remained extensively internalised throughout the response at wound sites, it seems unlikely that this receptor is rapidly recycled. For Cxcr2 it is less clear and would be an interesting point to address in future studies. It is possible that Cxcr2 appears to show little internalisation in neutrophils because it is rapidly recycled back to the membrane. My intention at the start of the project was to utilise the fluorescent timer approach to add temporal resolution that would enable me to determine whether a receptor was being recycled. However, due to the unforeseen rate of constitutive turn over I was unable to elucidate this point. Receptor recycling could be investigated by testing whether Cxcr2 co-localises with recycling markers such as Rab4 or Rab11, small GTPases associated with recycling

endosomes[161162]. A dominant negative Rab11transgenic zebrafish line[163] could be used to assess the effects of Cxcr2 recycling on neutrophil migration behaviour at wound sites. If Cxcr2 is rapidly recycling, here it would be predicted that Rab11 dominant negative neutrophils would display a less dispersive phenotype.

**Further elucidation of cxcr1 and cxcr2 receptor biochemistry**

Whilst this study focused on understanding how receptor trafficking influences neutrophil migration behaviour, further elucidation of Cxcr1 and Cxcr2 receptor biochemistry would enhance our understanding of how these receptors functionally contribute to migration. For example, the affinity of Cxcr1 and Cxcr2 for their cognate ligands was not addressed here. Different receptor/ligand binding affinities could play an important role in generating the migration behaviours observed at wound sites. Such protein interactions can be tested using binding assays with fluorescent chemokine[164]. The differences in migration pattern between Cxcr1-ala and Cxcr1-chim observed in this study suggested that the C-terminus of Cxcr2 confers different signalling properties to that of Cxcr1. Ongoing work with collaborators aims to test this by assessing receptor coupling to Gi or Gq subunits through application of pharmacological treatments (pertussis toxin and FR900359 respectively). It remains unknown whether Cxcr1 and Cxcr2 can dimerise. Indeed, many GPCRs can oligomerise to form homodimers or heterodimers and this can affect signalling responses[165,166]. It remains unclear whether Cxcr1 and Cxcr2 can oligomerise and what functional consequence this would confer. GPCR oligomerisation can be studied using FRET-based analysis where dimerisation is shown by fluorescent resonance energy transfer between fluorophores[167].

**Presentation state of the endogenous chemokine gradient**

*In vivo* studies by Sarris et al. have shown that Cxcl8a establishes tissue-bound or 'haptotactic' gradients by binding extracellular components called heparin sulphate proteoglycans (HSPGs)[72]. Such interactions were found to be required both for directing neutrophils towards the source and for restricting motility at the source. It remains unknown whether Cxcl8b forms interactions with HSPGs. Chemokine presentation state has also been linked to specific migration behaviours in *in vitro* systems. In a study by Schumman et al., soluble CCL19 gradients were shown to drive directional, non-adhesive, migration of (murine) dendritic cells whereas, immobilised CCL21 gradients drove haptokinesis (random migration) and triggered adhesion[168]. Interestingly, when incubated with CCL21, dendritic cells were shown to truncate the anchoring residues of

immobilised CCL21 rendering it soluble. It would be interesting to investigate whether the presentation state of Cxcl8a/b gradients influences receptor trafficking patterns. Receptor responses to soluble and immobilised chemokine could be addressed using HEK293 transplants secreting immobilised Cxcl8a (Cxcl8-DM) that is incapable of binding HSPGs[72]. An alternative experiment would be to locally inject heparinase III at the wound site and assess receptor internalisation and behaviour. Endogenous gradients could also be studied through use of CRISPR technology to generate transgenic knock-in lines expressing fluorescently labelled soluble or immobilised chemokine in the endogenous locus. It would be interesting to test whether neutrophils themselves can modify the ligand. This could be tested by performing western blot analysis of fluorescently labelled Cxcl8a before and after incubation with WT and *cxcr1*$^{-/-}$ neutrophils. The presence of additional smaller Cxcl8a fragments would be indicative of neutrophil specific modification of the chemokine.

**The role of neutrophil priming on the decision of chemotaxis versus chemokinesis and a link with desensitisation**

The chemokine CXCL8 can induce both directed migration and random migration in human neutrophils *in vitro*. Human neutrophils were shown to migrate both away and toward a gradient of CXCL8 in a microfluidic device[169]. Neutrophils migrating towards the gradient showed increased persistence and increased speed when compared to those migrating away. This suggests that in some settings CXCL8 can induce both chemotaxis and chemokinesis, though the mechanisms driving these differential responses to the same ligand remained unclear. A later study by Powell et al. indicated a role for neutrophil priming in such behavioural differences[152]. Here, as expected, naïve non-primed neutrophils exposed to a uniform concentration of CXCL8 exhibited non-directional chemokinesis and when exposed to a CXCL8 gradient they exhibited highly directional chemotaxis. Interestingly however, when neutrophils were pre-exposed to a uniform concentration of CXCL8 and then subsequently exposed to a CXCL8 gradient, neutrophils instead displayed chemokinesis. Here, the degree of chemokinesis was significantly enhanced compared to that of cells treated with a uniform concentration of CXCL8, with cells exhibiting increased velocity and distance. This suggests that the pre-exposure to chemokine somehow primed the cells to drive chemokinesis upon subsequent exposure to a gradient, though the mechanisms of such priming remain unclear. My results using zebrafish neutrophils could support the idea that such

priming may occur by receptor desensitisation. In this model, it would be predicted that in zebrafish neutrophils pre-exposure to chemokine would induce Cxcr1 internalisation, leaving predominantly Cxcr2 to signal, which drives dispersal. *In vitro* assessment of the migration behaviour of ligand-primed vs non-primed zebrafish neutrophils in Cxcl8a/b gradients could provide a link between receptor trafficking and the priming effects observed in human neutrophils.

# 6. Figures

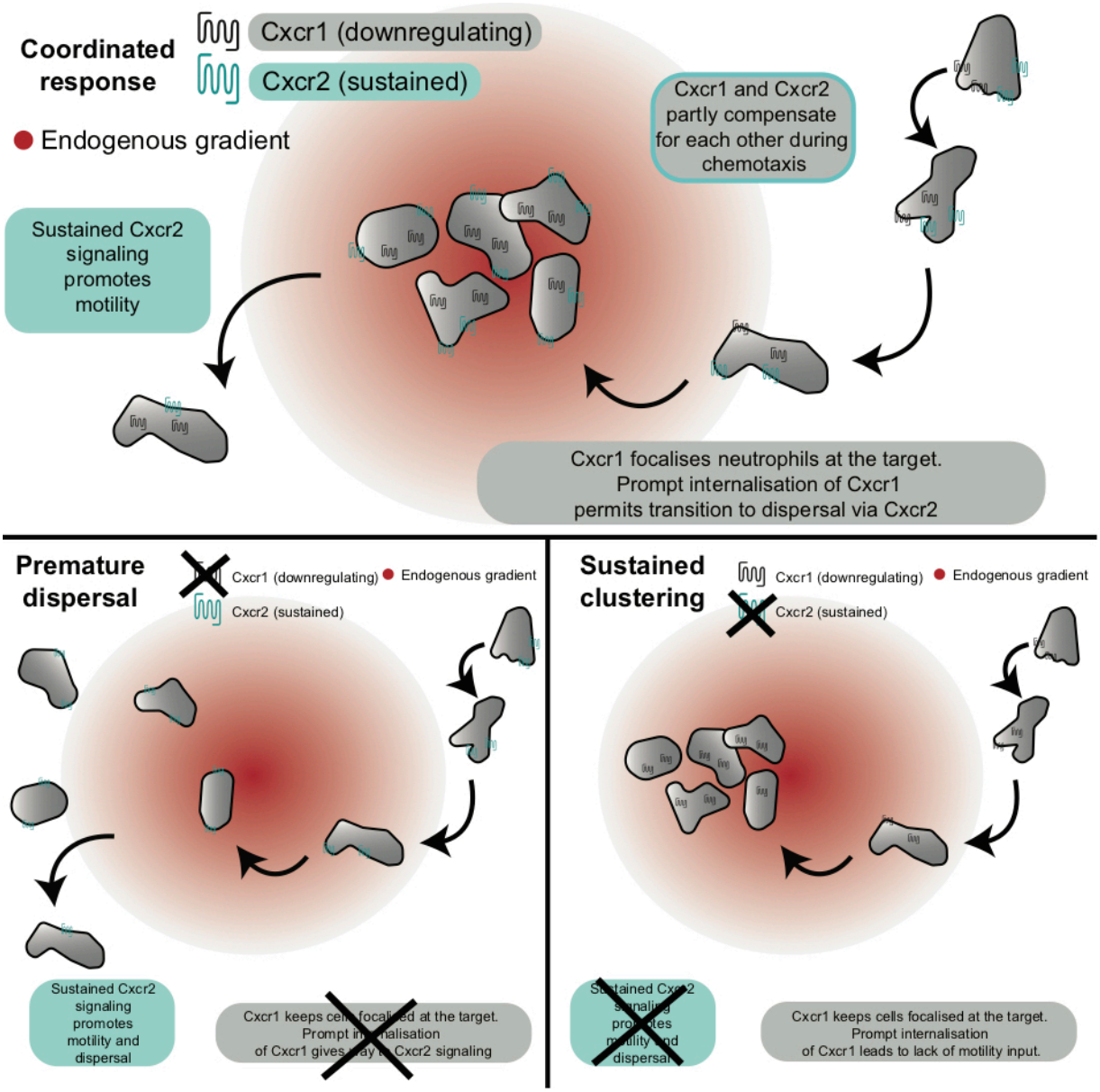


**Figure 6.1. Model recapitulating how Cxcr1 and Cxcr2 coordinate neutrophil clustering and dispersal.** (Top) Cxcr1 and Cxcr2 can partly compensate for each other during initial chemotaxis to the wounded tissue. At wound sites Cxcr1 focalizes the cells but this contribution is transient due to rapid Cxcr1 internalisation. Conversely, Cxcr2 is sustained at the cell surface throughout the response and drives bidirectional motility in the wounded tissue, promoting dispersal. This facilitates exploration and departure from the site. (Bottom Left) In the absence of the down-regulating receptor (Cxcr1 loss of function) neutrophils show a transient gain in dispersal and enhanced motility. (Bottom Right) In the absence of Cxcr2 (Cxcr2 loss of function), reduced motility/chemokinesis input leads to prolonged clustering.

# Bibliography


1. Kolaczkowska, E. & Kubes, P. Neutrophil recruitment and function in health and inflammation. *Nat. Rev. Immunol.* **13,** 159–175 (2013).
2. Lawrence, S. M., Corriden, R. & Nizet, V. The Ontogeny of a Neutrophil: Mechanisms of Granulopoiesis and Homeostasis. *Microbiol Mol Biol Rev* **82,** (2018).
3. Dancey, J. T., Deubelbeiss, K. A., Harker, L. A. & Finch, C. A. Neutrophil kinetics in man. *J. Clin. Invest.* **58,** 705–715 (1976).
4. Summers, C., Rankin, S. M., Condliffe, A. M., Singh, N., Peters, A. M. & Chilvers, E. R. Neutrophil kinetics in health and disease. *Trends Immunol* **31,** 318–324 (2010).
5. Kawai, T. & Malech, H. L. WHIM syndrome: congenital immune deficiency disease. *Curr. Opin. Hematol.* **16,** 20–26 (2009).
6. Nathan, C. & Ding, A. Nonresolving inflammation. *Cell* **140,** 871–882 (2010).
7. Papayannopoulos, V. Neutrophil extracellular traps in immunity and disease. *Nat. Rev. Immunol.* **18,** 134–147 (2018).
8. Singel, K. L. & Segal, B. H. Neutrophils in the tumor microenvironment: trying to heal the wound that cannot heal. *Immunol. Rev.* **273,** 329–343 (2016).
9. Lee, W. L., Harrison, R. E. & Grinstein, S. Phagocytosis by neutrophils. *Microbes Infect.* **5,** 1299–1306 (2003).
10. Nordenfelt, P. & Tapper, H. Phagosome dynamics during phagocytosis by neutrophils. *J. Leukoc. Biol.* **90,** 271–284 (2011).
11. Winterbourn, C. C., Kettle, A. J. & Hampton, M. B. Reactive Oxygen Species and Neutrophil Function. *Annu. Rev. Biochem.* **85,** 765–792 (2016).
12. Nguyen, G. T., Green, E. R. & Mecsas, J. Neutrophils to the ROScue: Mechanisms of NADPH Oxidase Activation and Bacterial Resistance. *Front Cell Infect Microbiol* **7,** 373 (2017).
13. Phan, Q. T., Sipka, T., Gonzalez, C., Levraud, J.-P., Lutfalla, G. & Nguyen-Chi, M. Neutrophils use superoxide to control bacterial infection at a distance. *PLOS Pathogens* **14,** e1007157 (2018).
14. Segal, A. W. The NADPH oxidase and chronic granulomatous disease. *Mol Med Today* **2,** 129–135 (1996).
15. Faurschou, M. & Borregaard, N. Neutrophil granules and secretory vesicles in inflammation. *Microbes and Infection* **5,** 1317–1327 (2003).

16. Lacy, P. Mechanisms of degranulation in neutrophils. *Allergy Asthma Clin Immunol* **2,** 98–108 (2006).
17. Parrow, N. L., Fleming, R. E. & Minnick, M. F. Sequestration and scavenging of iron in infection. *Infect. Immun.* **81,** 3503–3514 (2013).
18. Borregaard, N. & Cowland, J. B. Granules of the human neutrophilic polymorphonuclear leukocyte. *Blood* **89,** 3503–3521 (1997).
19. Brinkmann, V., Reichard, U., Goosmann, C., Fauler, B., Uhlemann, Y., Weiss, D. S., Weinrauch, Y. & Zychlinsky, A. Neutrophil extracellular traps kill bacteria. *Science* **303,** 1532–1535 (2004).
20. McDonald, B., Urrutia, R., Yipp, B. G., Jenne, C. N. & Kubes, P. Intravascular neutrophil extracellular traps capture bacteria from the bloodstream during sepsis. *Cell Host Microbe* **12,** 324–333 (2012).
21. Yu, Y. & Su, K. Neutrophil Extracellular Traps and Systemic Lupus Erythematosus. *J Clin Cell Immunol* **4,** (2013).
22. Jorch, S. K. & Kubes, P. An emerging role for neutrophil extracellular traps in noninfectious disease. *Nat. Med.* **23,** 279–287 (2017).
23. Borregaard, N. Neutrophils, from marrow to microbes. *Immunity* **33,** 657–670 (2010).
24. Wynn, T. A. & Vannella, K. M. Macrophages in Tissue Repair, Regeneration, and Fibrosis. *Immunity* **44,** 450–462 (2016).
25. Oishi, Y. & Manabe, I. Macrophages in inflammation, repair and regeneration. *Int. Immunol.* **30,** 511–528 (2018).
26. Wang, J., Hossain, M., Thanabalasuriar, A., Gunzer, M., Meininger, C. & Kubes, P. Visualizing the function and fate of neutrophils in sterile injury and repair. *Science* **358,** 111–116 (2017).
27. Christoffersson, G., Henriksnäs, J., Johansson, L., Rolny, C., Ahlström, H., Caballero-Corbalan, J., Segersvärd, R., Permert, J., Korsgren, O., Carlsson, P.-O. & Phillipson, M. Clinical and experimental pancreatic islet transplantation to striated muscle: establishment of a vascular system similar to that in native islets. *Diabetes* **59,** 2569–2578 (2010).
28. Gong, Y. & Koh, D.-R. Neutrophils promote inflammatory angiogenesis via release of preformed VEGF in an in vivo corneal model. *Cell Tissue Res* **339,** 437–448 (2010).
29. Ramanathan, S. & Jagannathan, N. Tumor associated macrophage: a review on the phenotypes, traits and functions. *Iran J Cancer Prev* **7,** 1–8 (2014).

30. Tazzyman, S., Lewis, C. E. & Murdoch, C. Neutrophils: key mediators of tumour angiogenesis. *Int J Exp Pathol* **90,** 222–231 (2009).
31. Murdoch, C., Muthana, M., Coffelt, S. B. & Lewis, C. E. The role of myeloid cells in the promotion of tumour angiogenesis. *Nat. Rev. Cancer* **8,** 618–631 (2008).
32. Houghton, A. M. The paradox of tumor-associated neutrophils: fueling tumor growth with cytotoxic substances. *Cell Cycle* **9,** 1732–1737 (2010).
33. Giese, M. A., Hind, L. E. & Huttenlocher, A. Neutrophil plasticity in the tumor microenvironment. *Blood* **133,** 2159–2167 (2019).
34. Jensen, H. K., Donskov, F., Marcussen, N., Nordsmark, M., Lundbeck, F. & Maase, H. von der. Presence of Intratumoral Neutrophils Is an Independent Prognostic Factor in Localized Renal Cell Carcinoma. *Journal of Clinical Oncology* (2009). doi:10.1200/JCO.2008.18.9498
35. Bellocq, A., Antoine, M., Flahault, A., Philippe, C., Crestani, B., Bernaudin, J. F., Mayaud, C., Milleron, B., Baud, L. & Cadranel, J. Neutrophil alveolitis in bronchioloalveolar carcinoma: induction by tumor-derived interleukin-8 and relation to clinical outcome. *Am J Pathol* **152,** 83–92 (1998).
36. Bekes, E. M., Schweighofer, B., Kupriyanova, T. A., Zajac, E., Ardi, V. C., Quigley, J. P. & Deryugina, E. I. Tumor-recruited neutrophils and neutrophil TIMP-free MMP-9 regulate coordinately the levels of tumor angiogenesis and efficiency of malignant cell intravasation. *Am. J. Pathol.* **179,** 1455–1470 (2011).
37. Nozawa, H., Chiu, C. & Hanahan, D. Infiltrating neutrophils mediate the initial angiogenic switch in a mouse model of multistage carcinogenesis. *Proc. Natl. Acad. Sci. U.S.A.* **103,** 12493–12498 (2006).
38. Mishalian, I., Bayuh, R., Eruslanov, E., Michaeli, J., Levy, L., Zolotarov, L., Singhal, S., Albelda, S. M., Granot, Z. & Fridlender, Z. G. Neutrophils recruit regulatory T-cells into tumors via secretion of CCL17--a new mechanism of impaired antitumor immunity. *Int. J. Cancer* **135,** 1178–1186 (2014).
39. Szczerba, B. M., Castro-Giner, F., Vetter, M., Krol, I., Gkountela, S., Landin, J., Scheidmann, M. C., Donato, C., Scherrer, R., Singer, J., Beisel, C., Kurzeder, C., Heinzelmann-Schwarz, V., Rochlitz, C., Weber, W. P., Beerenwinkel, N. & Aceto, N. Neutrophils escort circulating tumour cells to enable cell cycle progression. *Nature* **566,** 553–557 (2019).

40. Cools-Lartigue, J., Spicer, J., McDonald, B., Gowing, S., Chow, S., Giannias, B., Bourdeau, F., Kubes, P. & Ferri, L. Neutrophil extracellular traps sequester circulating tumor cells and promote metastasis. *J. Clin. Invest.* (2013). doi:10.1172/JCI67484
41. Wu, L., Saxena, S., Awaji, M. & Singh, R. K. Tumor-Associated Neutrophils in Cancer: Going Pro. *Cancers (Basel)* **11,** (2019).
42. Gershkovitz, M., Caspi, Y., Fainsod-Levi, T., Katz, B., Michaeli, J., Khawaled, S., Lev, S., Polyansky, L., Shaul, M. E., Sionov, R. V., Cohen-Daniel, L., Aqeilan, R. I., Shaul, Y. D., Mori, Y., Karni, R., Fridlender, Z. G., Binshtok, A. M. & Granot, Z. TRPM2 Mediates Neutrophil Killing of Disseminated Tumor Cells. *Cancer Res.* **78,** 2680–2690 (2018).
43. van Egmond, M. & Bakema, J. E. Neutrophils as effector cells for antibody-based immunotherapy of cancer. *Semin. Cancer Biol.* **23,** 190–199 (2013).
44. Eruslanov, E. B., Bhojnagarwala, P. S., Quatromoni, J. G., Stephen, T. L., Ranganathan, A., Deshpande, C., Akimova, T., Vachani, A., Litzky, L., Hancock, W. W., Conejo-Garcia, J. R., Feldman, M., Albelda, S. M. & Singhal, S. Tumor-associated neutrophils stimulate T cell responses in early-stage human lung cancer. *J. Clin. Invest.* **124,** 5466–5480 (2014).
45. Beauvillain, C., Delneste, Y., Scotet, M., Peres, A., Gascan, H., Guermonprez, P., Barnaba, V. & Jeannin, P. Neutrophils efficiently cross-prime naive T cells in vivo. *Blood* **110,** 2965–2973 (2007).
46. Sadik, C. D., Kim, N. D. & Luster, A. D. Neutrophils cascading their way to inflammation. *Trends Immunol.* **32,** 452–460 (2011).
47. Pittman, K. & Kubes, P. Damage-associated molecular patterns control neutrophil recruitment. *J Innate Immun* **5,** 315–323 (2013).
48. Zhang, Q., Raoof, M., Chen, Y., Sumi, Y., Sursal, T., Junger, W., Brohi, K., Itagaki, K. & Hauser, C. J. Circulating mitochondrial DAMPs cause inflammatory responses to injury. *Nature* **464,** 104–107 (2010).
49. Guo, R.-F. & Ward, P. A. Role of C5a in inflammatory responses. *Annu. Rev. Immunol.* **23,** 821–852 (2005).
50. Afonso, P. V., Janka-Junttila, M., Lee, Y. J., McCann, C. P., Oliver, C. M., Aamer, K. A., Losert, W., Cicerone, M. T. & Parent, C. A. LTB4 is a signal-relay molecule during neutrophil chemotaxis. *Dev. Cell* **22,** 1079–1091 (2012).
51. Rot, A. & von Andrian, U. H. Chemokines in innate and adaptive host defense: basic chemokinese grammar for immune cells. *Annu. Rev. Immunol.* **22,** 891–928 (2004).

52. Miller, M. C. & Mayo, K. H. Chemokines from a Structural Perspective. *Int J Mol Sci* **18,** (2017).

53. Fredriksson, R., Lagerström, M. C., Lundin, L.-G. & Schiöth, H. B. The G-protein-coupled receptors in the human genome form five main families. Phylogenetic analysis, paralogon groups, and fingerprints. *Mol. Pharmacol.* **63,** 1256–1272 (2003).

54. Hilger, D., Masureel, M. & Kobilka, B. K. Structure and dynamics of GPCR signaling complexes. *Nat. Struct. Mol. Biol.* **25,** 4–12 (2018).

55. Rosenbaum, D. M., Rasmussen, S. G. F. & Kobilka, B. K. The structure and function of G-protein-coupled receptors. *Nature* **459,** 356–363 (2009).

56. Weis, W. I. & Kobilka, B. K. The Molecular Basis of G Protein-Coupled Receptor Activation. *Annu. Rev. Biochem.* **87,** 897–919 (2018).

57. Kamp, M. E., Liu, Y. & Kortholt, A. Function and Regulation of Heterotrimeric G Proteins during Chemotaxis. *Int J Mol Sci* **17,** (2016).

58. Futosi, K., Fodor, S. & Mócsai, A. Neutrophil cell surface receptors and their intracellular signal transduction pathways. *Int. Immunopharmacol.* **17,** 638–650 (2013).

59. de Oliveira, S., Rosowski, E. E. & Huttenlocher, A. Neutrophil migration in infection and wound repair: going forward in reverse. *Nat. Rev. Immunol.* **16,** 378–391 (2016).

60. Gambardella, L. & Vermeren, S. Molecular players in neutrophil chemotaxis--focus on PI3K and small GTPases. *J. Leukoc. Biol.* **94,** 603–612 (2013).

61. Yoo, S. K., Deng, Q., Cavnar, P. J., Wu, Y. I., Hahn, K. M. & Huttenlocher, A. Differential regulation of protrusion and polarity by PI(3)K during neutrophil motility in live zebrafish. *Dev Cell* **18,** 226–236 (2010).

62. Li, Z., Jiang, H., Xie, W., Zhang, Z., Smrcka, A. V. & Wu, D. Roles of PLC-beta2 and -beta3 and PI3Kgamma in chemoattractant-mediated signal transduction. *Science* **287,** 1046–1049 (2000).

63. Martin, C., Burdon, P. C. E., Bridger, G., Gutierrez-Ramos, J. C., Williams, T. J. & Rankin, S. M. Chemokines acting via CXCR2 and CXCR4 control the release of neutrophils from the bone marrow and their return following senescence. *Immunity* **19,** 583–593 (2003).

64. Kruger, P., Saffarzadeh, M., Weber, A. N. R., Rieber, N., Radsak, M., von Bernuth, H., Benarafa, C., Roos, D., Skokowa, J. & Hartl, D. Neutrophils: Between host defence, immune modulation, and tissue injury. *PLoS Pathog.* **11,** e1004651 (2015).

65. Hernandez, P. A., Gorlin, R. J., Lukens, J. N., Taniuchi, S., Bohinjec, J., Francois, F., Klotman, M. E. & Diaz, G. A. Mutations in the chemokine receptor gene CXCR4 are associated with WHIM syndrome, a combined immunodeficiency disease. *Nat. Genet.* **34,** 70–74 (2003).
66. Eash, K. J., Greenbaum, A. M., Gopalan, P. K. & Link, D. C. CXCR2 and CXCR4 antagonistically regulate neutrophil trafficking from murine bone marrow. *J Clin Invest* **120,** 2423–2431 (2010).
67. Muller, W. A. Getting leukocytes to the site of inflammation. *Vet. Pathol.* **50,** 7–22 (2013).
68. Nourshargh, S. & Alon, R. Leukocyte migration into inflamed tissues. *Immunity* **41,** 694–707 (2014).
69. Woodfin, A., Voisin, M.-B., Beyrau, M., Colom, B., Caille, D., Diapouli, F.-M., Nash, G. B., Chavakis, T., Albelda, S. M., Rainger, G. E., Meda, P., Imhof, B. A. & Nourshargh, S. The junctional adhesion molecule JAM-C regulates polarized transendothelial migration of neutrophils in vivo. *Nat. Immunol.* **12,** 761–769 (2011).
70. Nourshargh, S., Hordijk, P. L. & Sixt, M. Breaching multiple barriers: leukocyte motility through venular walls and the interstitium. *Nat. Rev. Mol. Cell Biol.* **11,** 366–378 (2010).
71. Sarris, M. & Sixt, M. Navigating in tissue mazes: chemoattractant interpretation in complex environments. *Curr. Opin. Cell Biol.* **36,** 93–102 (2015).
72. Sarris, M., Masson, J.-B., Maurin, D., Van der Aa, L. M., Boudinot, P., Lortat-Jacob, H. & Herbomel, P. Inflammatory chemokines direct and restrict leukocyte migration within live tissues as glycan-bound gradients. *Curr. Biol.* **22,** 2375–2382 (2012).
73. Yoo, S. K. & Huttenlocher, A. Spatiotemporal photolabeling of neutrophil trafficking during inflammation in live zebrafish. *J. Leukoc. Biol.* **89,** 661–667 (2011).
74. Tan, R. Z. & Chiam, K.-H. A computational model for how cells choose temporal or spatial sensing during chemotaxis. *PLoS Comput. Biol.* **14,** e1005966 (2018).
75. Aranyosi, A. J., Wong, E. A. & Irimia, D. A neutrophil treadmill to decouple spatial and temporal signals during chemotaxis. *Lab Chip* **15,** 549–556 (2015).
76. Macnab, R. M. & Koshland, D. E. The gradient-sensing mechanism in bacterial chemotaxis. *Proc. Natl. Acad. Sci. U.S.A.* **69,** 2509–2512 (1972).
77. Zigmond, S. H. Mechanisms of sensing chemical gradients by polymorphonuclear leukocytes. *Nature* **249,** 450–452 (1974).

78. Servant, G., Weiner, O. D., Herzmark, P., Balla, T., Sedat, J. W. & Bourne, H. R. Polarization of chemoattractant receptor signaling during neutrophil chemotaxis. *Science* **287,** 1037–1040 (2000).

79. Gerisch, G. & Keller, H. U. Chemotactic reorientation of granulocytes stimulated with micropipettes containing fMet-Leu-Phe. *J. Cell. Sci.* **52,** 1–10 (1981).

80. Wang, M.-J., Artemenko, Y., Cai, W.-J., Iglesias, P. A. & Devreotes, P. N. The directional response of chemotactic cells depends on a balance between cytoskeletal architecture and the external gradient. *Cell Rep* **9,** 1110–1121 (2014).

81. Albrecht, E. & Petty, H. R. Cellular memory: Neutrophil orientation reverses during temporally decreasing chemoattractant concentrations. *Proc Natl Acad Sci U S A* **95,** 5039–5044 (1998).

82. Petrie Aronin, C. E., Zhao, Y. M., Yoon, J. S., Morgan, N. Y., Prüstel, T., Germain, R. N. & Meier-Schellersheim, M. Migrating Myeloid Cells Sense Temporal Dynamics of Chemoattractant Concentrations. *Immunity* **47,** 862-874.e3 (2017).

83. Lämmermann, T., Bader, B. L., Monkley, S. J., Worbs, T., Wedlich-Söldner, R., Hirsch, K., Keller, M., Förster, R., Critchley, D. R., Fässler, R. & Sixt, M. Rapid leukocyte migration by integrin-independent flowing and squeezing. *Nature* **453,** 51–55 (2008).

84. Bear, J. E. & Haugh, J. M. Directed migration of mesenchymal cells: where signaling and the cytoskeleton meet. *Curr. Opin. Cell Biol.* **30,** 74–82 (2014).

85. Peters, N. C., Egen, J. G., Secundino, N., Debrabant, A., Kimblin, N., Kamhawi, S., Lawyer, P., Fay, M. P., Germain, R. N. & Sacks, D. In vivo imaging reveals an essential role for neutrophils in leishmaniasis transmitted by sand flies. *Science* **321,** 970–974 (2008).

86. Lämmermann, T., Afonso, P. V., Angermann, B. R., Wang, J. M., Kastenmüller, W., Parent, C. A. & Germain, R. N. Neutrophil swarms require LTB4 and integrins at sites of cell death in vivo. *Nature* **498,** 371–375 (2013).

87. Kienle, K. & Lämmermann, T. Neutrophil swarming: an essential process of the neutrophil tissue response. *Immunol. Rev.* **273,** 76–93 (2016).

88. Lämmermann, T. In the eye of the neutrophil swarm-navigation signals that bring neutrophils together in inflamed and infected tissues. *J. Leukoc. Biol.* **100,** 55–63 (2016).

89. Chtanova, T., Schaeffer, M., Han, S.-J., van Dooren, G. G., Nollmann, M., Herzmark, P., Chan, S. W., Satija, H., Camfield, K., Aaron, H., Striepen, B. & Robey, E. A. Dynamics of neutrophil migration in lymph nodes during infection. *Immunity* **29,** 487–496 (2008).

90. Chtanova, T., Schaeffer, M., Han, S.-J., van Dooren, G. G., Nollmann, M., Herzmark, P., Chan, S. W., Satija, H., Camfield, K., Aaron, H., Striepen, B. & Robey, E. A. Dynamics of neutrophil migration in lymph nodes during infection. *Immunity* **29,** 487–496 (2008).
91. Jasper, A. E., McIver, W. J., Sapey, E. & Walton, G. M. Understanding the role of neutrophils in chronic inflammatory airway disease. *F1000Res* **8,** (2019).
92. Cascão, R., Rosário, H. S., Souto-Carneiro, M. M. & Fonseca, J. E. Neutrophils in rheumatoid arthritis: More than simple final effectors. *Autoimmun Rev* **9,** 531–535 (2010).
93. Savill, J. & Haslett, C. Granulocyte clearance by apoptosis in the resolution of inflammation. *Semin. Cell Biol.* **6,** 385–393 (1995).
94. Fox, S., Leitch, A. E., Duffin, R., Haslett, C. & Rossi, A. G. Neutrophil apoptosis: relevance to the innate immune response and inflammatory disease. *J Innate Immun* **2,** 216–227 (2010).
95. Newman, S. L., Henson, J. E. & Henson, P. M. Phagocytosis of senescent neutrophils by human monocyte-derived macrophages and rabbit inflammatory macrophages. *J. Exp. Med.* **156,** 430–442 (1982).
96. Cox, G., Crossley, J. & Xing, Z. Macrophage engulfment of apoptotic neutrophils contributes to the resolution of acute pulmonary inflammation in vivo. *Am. J. Respir. Cell Mol. Biol.* **12,** 232–237 (1995).
97. Hughes, J., Johnson, R. J., Mooney, A., Hugo, C., Gordon, K. & Savill, J. Neutrophil fate in experimental glomerular capillary injury in the rat. Emigration exceeds in situ clearance by apoptosis. *Am. J. Pathol.* **150,** 223–234 (1997).
98. Buckley, C. D., Ross, E. A., McGettrick, H. M., Osborne, C. E., Haworth, O., Schmutz, C., Stone, P. C. W., Salmon, M., Matharu, N. M., Vohra, R. K., Nash, G. B. & Rainger, G. E. Identification of a phenotypically and functionally distinct population of long-lived neutrophils in a model of reverse endothelial migration. *J. Leukoc. Biol.* **79,** 303–311 (2006).
99. Starnes, T. W. & Huttenlocher, A. Neutrophil reverse migration becomes transparent with zebrafish. *Adv Hematol* **2012,** 398640 (2012).
100. Mathias, J. R., Perrin, B. J., Liu, T.-X., Kanki, J., Look, A. T. & Huttenlocher, A. Resolution of inflammation by retrograde chemotaxis of neutrophils in transgenic zebrafish. *J. Leukoc. Biol.* **80,** 1281–1288 (2006).
101. Ellett, F., Elks, P. M., Robertson, A. L., Ogryzko, N. V. & Renshaw, S. A. Defining the phenotype of neutrophils following reverse migration in zebrafish. *J. Leukoc. Biol.* **98,** 975–981 (2015).

102. Tharp, W. G., Yadav, R., Irimia, D., Upadhyaya, A., Samadani, A., Hurtado, O., Liu, S.-Y., Munisamy, S., Brainard, D. M., Mahon, M. J., Nourshargh, S., van Oudenaarden, A., Toner, M. G. & Poznansky, M. C. Neutrophil chemorepulsion in defined interleukin-8 gradients in vitro and in vivo. *J. Leukoc. Biol.* **79,** 539–554 (2006).

103. Holmes, G. R., Anderson, S. R., Dixon, G., Robertson, A. L., Reyes-Aldasoro, C. C., Billings, S. A., Renshaw, S. A. & Kadirkamanathan, V. Repelled from the wound, or randomly dispersed? Reverse migration behaviour of neutrophils characterized by dynamic modelling. *J R Soc Interface* **9,** 3229–3239 (2012).

104. Holmes, G. R., Dixon, G., Anderson, S. R., Reyes-Aldasoro, C. C., Elks, P. M., Billings, S. A., Whyte, M. K. B., Kadirkamanathan, V. & Renshaw, S. A. Drift-Diffusion Analysis of Neutrophil Migration during Inflammation Resolution in a Zebrafish Model. *Adv Hematol* **2012,** 792163 (2012).

105. Tucker, K. A., Lilly, M. B., Heck, L. & Rado, T. A. Characterization of a new human diploid myeloid leukemia cell line (PLB-985) with granulocytic and monocytic differentiating capacity. *Blood* **70,** 372–378 (1987).

106. Rincón, E., Rocha-Gregg, B. L. & Collins, S. R. A map of gene expression in neutrophil-like cell lines. *BMC Genomics* **19,** 573 (2018).

107. Collins, S. J., Ruscetti, F. W., Gallagher, R. E. & Gallo, R. C. Terminal differentiation of human promyelocytic leukemia cells induced by dimethyl sulfoxide and other polar compounds. *Proc. Natl. Acad. Sci. U.S.A.* **75,** 2458–2462 (1978).

108. Majumdar, R., Tavakoli Tameh, A. & Parent, C. A. Exosomes Mediate LTB4 Release during Neutrophil Chemotaxis. *PLoS Biol.* **14,** e1002336 (2016).

109. Barlic, J., Khandaker, M. H., Mahon, E., Andrews, J., DeVries, M. E., Mitchell, G. B., Rahimpour, R., Tan, C. M., Ferguson, S. S. & Kelvin, D. J. beta-arrestins regulate interleukin-8-induced CXCR1 internalization. *J. Biol. Chem.* **274,** 16287–16294 (1999).

110. Henry, K. M., Loynes, C. A., Whyte, M. K. B. & Renshaw, S. A. Zebrafish as a model for the study of neutrophil biology. *J. Leukoc. Biol.* **94,** 633–642 (2013).

111. Deng, Q. & Huttenlocher, A. Leukocyte migration from a fish eye's view. *J. Cell. Sci.* **125,** 3949–3956 (2012).

112. Lieschke, G. J., Oates, A. C., Crowhurst, M. O., Ward, A. C. & Layton, J. E. Morphologic and functional characterization of granulocytes and macrophages in embryonic and adult zebrafish. *Blood* **98,** 3087–3096 (2001).

113. Colucci-Guyon, E., Tinevez, J.-Y., Renshaw, S. A. & Herbomel, P. Strategies of professional phagocytes in vivo: unlike macrophages, neutrophils engulf only surface-associated microbes. *J. Cell. Sci.* **124,** 3053–3059 (2011).
114. Palić, D., Andreasen, C. B., Ostojić, J., Tell, R. M. & Roth, J. A. Zebrafish (Danio rerio) whole kidney assays to measure neutrophil extracellular trap release and degranulation of primary granules. *J. Immunol. Methods* **319,** 87–97 (2007).
115. Peveri, P., Walz, A., Dewald, B. & Baggiolini, M. A novel neutrophil-activating factor produced by human mononuclear phagocytes. *J. Exp. Med.* **167,** 1547–1559 (1988).
116. van der Aa, L. M., Chadzinska, M., Tijhaar, E., Boudinot, P. & Verburg-van Kemenade, B. M. L. CXCL8 Chemokines in Teleost Fish: Two Lineages with Distinct Expression Profiles during Early Phases of Inflammation. *PLoS One* **5,** (2010).
117. Oehlers, S. H. B., Flores, M. V., Hall, C. J., O'Toole, R., Swift, S., Crosier, K. E. & Crosier, P. S. Expression of zebrafish cxcl8 (interleukin-8) and its receptors during development and in response to immune stimulation. *Dev. Comp. Immunol.* **34,** 352–359 (2010).
118. Madeira, F., Park, Y. M., Lee, J., Buso, N., Gur, T., Madhusoodanan, N., Basutkar, P., Tivey, A. R. N., Potter, S. C., Finn, R. D. & Lopez, R. The EMBL-EBI search and sequence analysis tools APIs in 2019. *Nucleic Acids Res.* **47,** W636–W641 (2019).
119. de Oliveira, S., Reyes-Aldasoro, C. C., Candel, S., Renshaw, S. A., Mulero, V. & Calado, A. Cxcl8 (IL-8) mediates neutrophil recruitment and behavior in the zebrafish inflammatory response. *J. Immunol.* **190,** 4349–4359 (2013).
120. Sarris, M., Masson, J.-B., Maurin, D., Van der Aa, L. M., Boudinot, P., Lortat-Jacob, H. & Herbomel, P. Inflammatory chemokines direct and restrict leukocyte migration within live tissues as glycan-bound gradients. *Curr. Biol.* **22,** 2375–2382 (2012).
121. Powell, D., Lou, M., Barros Becker, F. & Huttenlocher, A. Cxcr1 mediates recruitment of neutrophils and supports proliferation of tumor-initiating astrocytes in vivo. *Sci Rep* **8,** 13285 (2018).
122. de Oliveira, S., Lopez-Muñoz, A., Martínez-Navarro, F. J., Galindo-Villegas, J., Mulero, V. & Calado, Â. Cxcl8-l1 and Cxcl8-l2 are required in the zebrafish defense against Salmonella Typhimurium. *Dev. Comp. Immunol.* **49,** 44–48 (2015).
123. Zuñiga-Traslaviña, C., Bravo, K., Reyes, A. E. & Feijóo, C. G. Cxcl8b and Cxcr2 Regulate Neutrophil Migration through Bloodstream in Zebrafish. *J Immunol Res* **2017,** (2017).

124. Deng, Q., Sarris, M., Bennin, D. A., Green, J. M., Herbomel, P. & Huttenlocher, A. Localized bacterial infection induces systemic activation of neutrophils through Cxcr2 signaling in zebrafish. *J Leukoc Biol* **93,** 761–769 (2013).
125. Westerfield. *The Zebrafish Book: A Guide for the Laboratory Use of Zebrafish (Danio Rerio)*. (University of Oregon Press, 2000).
126. Dooley, C. M., Scahill, C., Fényes, F., Kettleborough, R. N. W., Stemple, D. L. & Busch-Nentwich, E. M. Multi-allelic phenotyping--a systematic approach for the simultaneous analysis of multiple induced mutations. *Methods* **62,** 197–206 (2013).
127. Renshaw, S. A., Loynes, C. A., Trushell, D. M. I., Elworthy, S., Ingham, P. W. & Whyte, M. K. B. A transgenic zebrafish model of neutrophilic inflammation. *Blood* **108,** 3976–3978 (2006).
128. Donà, E., Barry, J. D., Valentin, G., Quirin, C., Khmelinskii, A., Kunze, A., Durdu, S., Newton, L. R., Fernandez-Minan, A., Huber, W., Knop, M. & Gilmour, D. Directional tissue migration through a self-generated chemokine gradient. *Nature* **503,** 285–289 (2013).
129. Yoo, S. K., Lam, P.-Y., Eichelberg, M. R., Zasadil, L., Bement, W. M. & Huttenlocher, A. The role of microtubules in neutrophil polarity and migration in live zebrafish. *J. Cell. Sci.* **125,** 5702–5710 (2012).
130. Kwan, K. M., Fujimoto, E., Grabher, C., Mangum, B. D., Hardy, M. E., Campbell, D. S., Parant, J. M., Yost, H. J., Kanki, J. P. & Chien, C.-B. The Tol2kit: a multisite gateway-based construction kit for Tol2 transposon transgenesis constructs. *Dev. Dyn.* **236,** 3088–3099 (2007).
131. Schrage, R., Schmitz, A.-L., Gaffal, E., Annala, S., Kehraus, S., Wenzel, D., Büllesbach, K. M., Bald, T., Inoue, A., Shinjo, Y., Galandrin, S., Shridhar, N., Hesse, M., Grundmann, M., Merten, N., Charpentier, T. H., Martz, M., Butcher, A. J., Slodczyk, T., Armando, S., Effern, M., Namkung, Y., Jenkins, L., Horn, V., Stößel, A., Dargatz, H., Tietze, D., Imhof, D., Galés, C., Drewke, C., Müller, C. E., Hölzel, M., Milligan, G., Tobin, A. B., Gomeza, J., Dohlman, H. G., Sondek, J., Harden, T. K., Bouvier, M., Laporte, S. A., Aoki, J., Fleischmann, B. K., Mohr, K., König, G. M., Tüting, T. & Kostenis, E. The experimental power of FR900359 to study Gq-regulated biological processes. *Nat Commun* **6,** 10156 (2015).
132. Zolessi, F. R., Poggi, L., Wilkinson, C. J., Chien, C.-B. & Harris, W. A. Polarization and orientation of retinal ganglion cells in vivo. *Neural Dev* **1,** 2 (2006).

133. Demy, D. L., Ranta, Z., Giorgi, J.-M., Gonzalez, M., Herbomel, P. & Kissa, K. Generating parabiotic zebrafish embryos for cell migration and homing studies. *Nat. Methods* **10,** 256–258 (2013).
134. Chan, T. F. & Vese, L. A. Active contours without edges. *IEEE Trans Image Process* **10,** 266–277 (2001).
135. Haralick, R. M., Shanmugam, K. & Dinstein. Textural Features for Image Classification. *IEEE Trans Syst Man Cyber* **IEEE Trans Syst Man Cyber,** 610–621 (1973).
136. Hanyaloglu, A. C. & von Zastrow, M. Regulation of GPCRs by endocytic membrane trafficking and its potential implications. *Annu. Rev. Pharmacol. Toxicol.* **48,** 537–568 (2008).
137. Khmelinskii, A., Keller, P. J., Bartosik, A., Meurer, M., Barry, J. D., Mardin, B. R., Kaufmann, A., Trautmann, S., Wachsmuth, M., Pereira, G., Huber, W., Schiebel, E. & Knop, M. Tandem fluorescent protein timers for in vivo analysis of protein dynamics. *Nat. Biotechnol.* **30,** 708–714 (2012).
138. Kawakami, K. Tol2: a versatile gene transfer vector in vertebrates. *Genome Biol.* **8 Suppl 1,** S7 (2007).
139. Suster, M. L., Kikuta, H., Urasaki, A., Asakawa, K. & Kawakami, K. Transgenesis in zebrafish with the tol2 transposon system. *Methods Mol. Biol.* **561,** 41–63 (2009).
140. Clark, K. J., Urban, M. D., Skuster, K. J. & Ekker, S. C. Transgenic zebrafish using transposable elements. *Methods Cell Biol.* **104,** 137–149 (2011).
141. Murayama, E., Kissa, K., Zapata, A., Mordelet, E., Briolat, V., Lin, H.-F., Handin, R. I. & Herbomel, P. Tracing hematopoietic precursor migration to successive hematopoietic organs during zebrafish development. *Immunity* **25,** 963–975 (2006).
142. Sarris, M., Olekhnovitch, R. & Bousso, P. Manipulating leukocyte interactions in vivo through optogenetic chemokine release. *Blood* **127,** e35-41 (2016).
143. Weber, M., Hauschild, R., Schwarz, J., Moussion, C., de Vries, I., Legler, D. F., Luther, S. A., Bollenbach, T. & Sixt, M. Interstitial dendritic cell guidance by haptotactic chemokine gradients. *Science* **339,** 328–332 (2013).
144. Schwarz, J., Bierbaum, V., Vaahtomeri, K., Hauschild, R., Brown, M., de Vries, I., Leithner, A., Reversat, A., Merrin, J., Tarrant, T., Bollenbach, T. & Sixt, M. Dendritic Cells Interpret Haptotactic Chemokine Gradients in a Manner Governed by Signal-to-Noise Ratio and Dependent on GRK6. *Curr. Biol.* **27,** 1314–1325 (2017).

145. Ulvmar, M. H., Werth, K., Braun, A., Kelay, P., Hub, E., Eller, K., Chan, L., Lucas, B., Novitzky-Basso, I., Nakamura, K., Rülicke, T., Nibbs, R. J. B., Worbs, T., Förster, R. & Rot, A. The atypical chemokine receptor CCRL1 shapes functional CCL21 gradients in lymph nodes. *Nat. Immunol.* **15,** 623–630 (2014).

146. Richardson, R. M., Marjoram, R. J., Barak, L. S. & Snyderman, R. Role of the cytoplasmic tails of CXCR1 and CXCR2 in mediating leukocyte migration, activation, and regulation. *J. Immunol.* **170,** 2904–2911 (2003).

147. Subramanian, B. C., Moissoglu, K. & Parent, C. A. The LTB4-BLT1 axis regulates the polarized trafficking of chemoattractant GPCRs during neutrophil chemotaxis. *J. Cell. Sci.* **131,** (2018).

148. Richardson, R. M., Pridgen, B. C., Haribabu, B., Ali, H. & Snyderman, R. Differential cross-regulation of the human chemokine receptors CXCR1 and CXCR2. Evidence for time-dependent signal generation. *J. Biol. Chem.* **273,** 23830–23836 (1998).

149. Kettleborough, R. N. W., Busch-Nentwich, E. M., Harvey, S. A., Dooley, C. M., de Bruijn, E., van Eeden, F., Sealy, I., White, R. J., Herd, C., Nijman, I. J., Fényes, F., Mehroke, S., Scahill, C., Gibbons, R., Wali, N., Carruthers, S., Hall, A., Yen, J., Cuppen, E. & Stemple, D. L. A systematic genome-wide analysis of zebrafish protein-coding gene function. *Nature* **496,** 494–497 (2013).

150. Hofmann, K. & Stoffel, W. A database of membrane spanning proteins segments. *Biological Chemistry* **374,** 166 (1993).

151. Hall, C., Flores, M. V., Storm, T., Crosier, K. & Crosier, P. The zebrafish lysozyme C promoter drives myeloid-specific expression in transgenic fish. *BMC Dev. Biol.* **7,** 42 (2007).

152. Powell, D., Tauzin, S., Hind, L. E., Deng, Q., Beebe, D. J. & Huttenlocher, A. Chemokine Signaling and the Regulation of Bidirectional Leukocyte Migration in Interstitial Tissues. *Cell Rep* **19,** 1572–1585 (2017).

153. Blaser, B. W., Moore, J. L., Hagedorn, E. J., Li, B., Riquelme, R., Lichtig, A., Yang, S., Zhou, Y., Tamplin, O. J., Binder, V. & Zon, L. I. CXCR1 remodels the vascular niche to promote hematopoietic stem and progenitor cell engraftment. *J. Exp. Med.* **214,** 1011–1027 (2017).

154. White, J. R., Lee, J. M., Young, P. R., Hertzberg, R. P., Jurewicz, A. J., Chaikin, M. A., Widdowson, K., Foley, J. J., Martin, L. D., Griswold, D. E. & Sarau, H. M. Identification of a potent, selective non-peptide CXCR2 antagonist that inhibits interleukin-8-induced neutrophil migration. *J. Biol. Chem.* **273,** 10095–10098 (1998).

155. Bonecchi, R. & Graham, G. J. Atypical Chemokine Receptors and Their Roles in the Resolution of the Inflammatory Response. *Front Immunol* **7,** 224 (2016).
156. Chang, Y.-F., Imam, J. S. & Wilkinson, M. F. The Nonsense-Mediated Decay RNA Surveillance Pathway. *Annu. Rev. Biochem.* **76,** 51–74 (2007).
157. Wetzler, M., Talpaz, M., Kleinerman, E. S., King, A., Huh, Y. O., Gutterman, J. U. & Kurzrock, R. A new familial immunodeficiency disorder characterized by severe neutropenia, a defective marrow release mechanism, and hypogammaglobulinemia. *Am. J. Med.* **89,** 663–672 (1990).
158. Minina, S., Reichman-Fried, M. & Raz, E. Control of receptor internalization, signaling level, and precise arrival at the target in guided cell migration. *Curr. Biol.* **17,** 1164–1172 (2007).
159. Magalhaes, A. C., Dunn, H. & Ferguson, S. S. Regulation of GPCR activity, trafficking and localization by GPCR-interacting proteins. *Br. J. Pharmacol.* **165,** 1717–1736 (2012).
160. Shi, G., Partida-Sánchez, S., Misra, R. S., Tighe, M., Borchers, M. T., Lee, J. J., Simon, M. I. & Lund, F. E. Identification of an alternative Gαq-dependent chemokine receptor signal transduction pathway in dendritic cells and granulocytes. *Journal of Experimental Medicine* **204,** 2705–2718 (2007).
161. Takahashi, S., Kubo, K., Waguri, S., Yabashi, A., Shin, H.-W., Katoh, Y. & Nakayama, K. Rab11 regulates exocytosis of recycling vesicles at the plasma membrane. *J. Cell. Sci.* **125,** 4049–4057 (2012).
162. Grant, B. D. & Donaldson, J. G. Pathways and mechanisms of endocytic recycling. *Nat. Rev. Mol. Cell Biol.* **10,** 597–608 (2009).
163. Clark, B. S., Winter, M., Cohen, A. R. & Link, B. A. Generation of Rab-based transgenic lines for in vivo studies of endosome biology in zebrafish. *Dev. Dyn.* **240,** 2452–2465 (2011).
164. Hunter, S. A. & Cochran, J. R. Cell-Binding Assays for Determining the Affinity of Protein-Protein Interactions: Technologies and Considerations. *Meth. Enzymol.* **580,** 21–44 (2016).
165. Stephens, B. & Handel, T. M. Chemokine receptor oligomerization and allostery. *Prog Mol Biol Transl Sci* **115,** 375–420 (2013).
166. Wilson, S., Wilkinson, G. & Milligan, G. The CXCR1 and CXCR2 receptors form constitutive homo- and heterodimers selectively and with equal apparent affinities. *J. Biol. Chem.* **280,** 28663–28674 (2005).
167. Vischer, H. F., Castro, M. & Pin, J.-P. G Protein-Coupled Receptor Multimers: A Question Still Open Despite the Use of Novel Approaches. *Mol. Pharmacol.* **88,** 561–571 (2015).

168. Schumann, K., Lämmermann, T., Bruckner, M., Legler, D. F., Polleux, J., Spatz, J. P., Schuler, G., Förster, R., Lutz, M. B., Sorokin, L. & Sixt, M. Immobilized chemokine fields and soluble chemokine gradients cooperatively shape migration patterns of dendritic cells. *Immunity* **32,** 703–713 (2010).
169. Boneschansker, L., Yan, J., Wong, E., Briscoe, D. M. & Irimia, D. Microfluidic platform for the quantitative analysis of leukocyte migration signatures. *Nat Commun* **5,** 4787 (2014).